SNE SIMULATION NEWS EUROPE

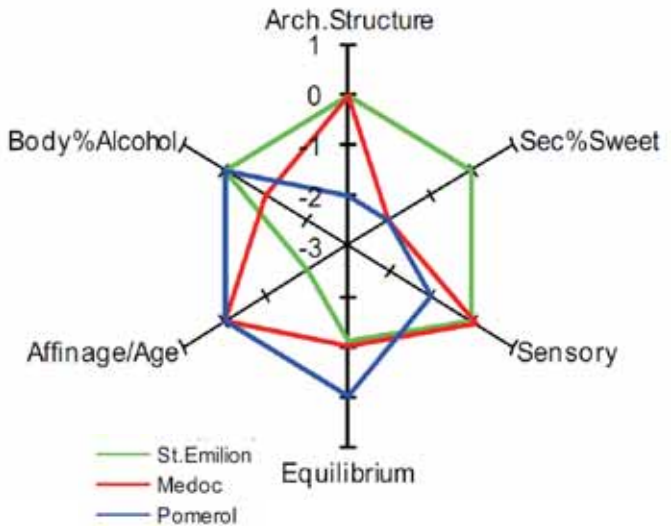

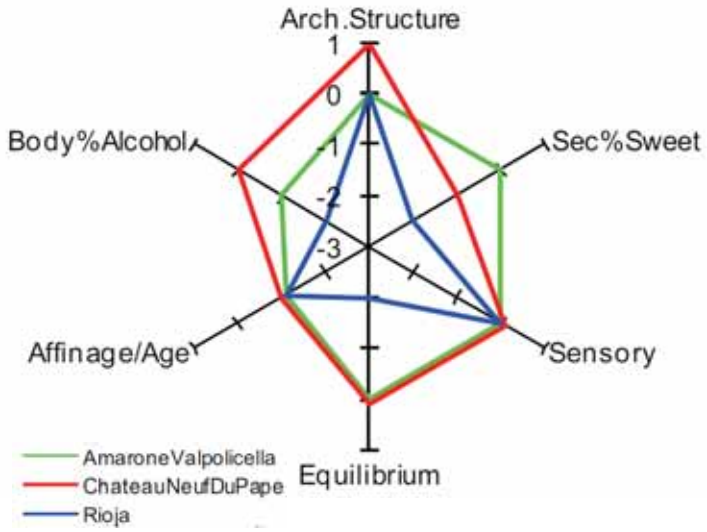

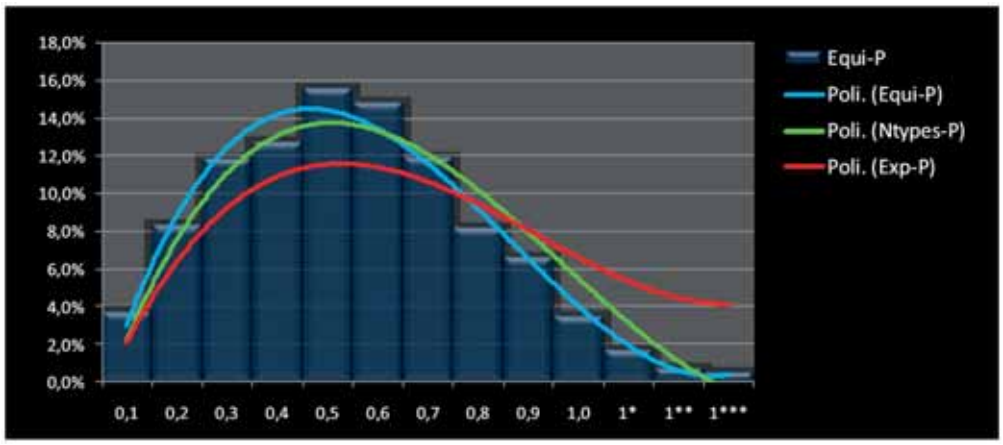

Volume 19 Number 3-4
December 2009

doi: 10.11128/sne.19.34.0994
DOI Reprint ISSN 0929-2268

Print ISSN 2305-9974
Online ISSN 2306-0271

Journal on Developments and Trends in Modelling and Simulation

Membership Journal for Simulation Societies in EUROSIM

ARGESIM

Dear Readers,

This SNE issue SNE 19/3-4 underlines the importance of SNE for the EUROSIM member societies, SNE not only provides in the News Section the possibility for reports and announcements of the EUROSIM member societies, SNE also offers to publish post-conference publications of conferences of EUROSIM societies and of so-called EUROSIM Event Conferences.

In this issue, ASIM and SIMS made use of this possibility and selected publications for SNE from MATHMOD 2009 Vienna (also a EUROSIM Event Conference) and from the annual SIMS Conference 2008. Up to now many contribution were coming from this 'second' contributions source, but from 2010 on this possibility will be fixed with all EUROSIM member societies – and will be open also for future members. But individual submissions of scientific papers are still welcome and are the 'usual' source for publications in SNE

The selection of contributions followed the idea to show the very broad application area of modelling and simulation, and to sketch applications from 'unusual' areas.

One unusual application is discussed in the overview note 'Model-based Development of Self-organizing Earthquake Early Warning Systems', dealing with the 'serious' environment of our life, and another one with the 'luxurious' side of our life – 'A Quantistic Modelling of Wine Evaluation in Oenology – Probability Analysis'- The pictures at right show charts comparing tasted wines belonging to different 'appellations' - the 3 axis represent independent dimensions for wine evaluation. The contents of the other contributions range from biochemical modelling and simulation via trust models and interaction models between producers and customers to room management simulation and underwater vehicle control –as contrast to Valpolicella, Rioja, Medoc, Pomerol, ….

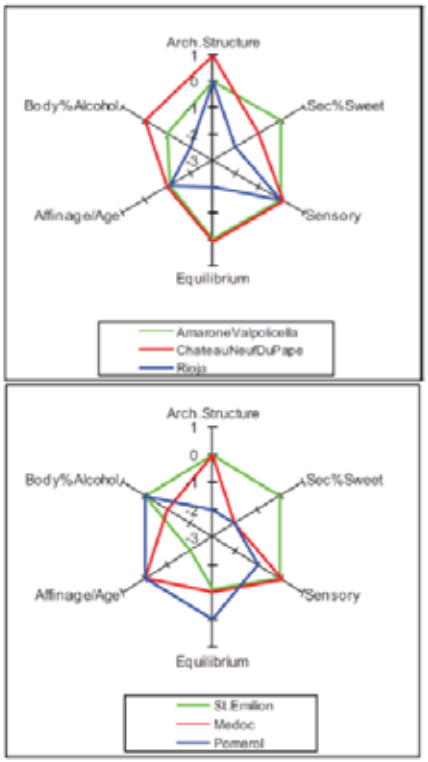

We hope, readers enjoy this 'mixed' the content, and we thank all contributors, the managing editors of the conferences, the members of the editorial boards, and people of our ARGESIM staff for co-operation in producing this SNE issue

Felix Breitenecker, editor-in-chief, eic@sne-journal.org

SNE 19/3-4 in Three Minutes

Impressum, Table of Contents: page 4

ASIM - Buchreihen / ASIM Book Series

Fortschritte in der Simulationstechnik (FS) / Frontiers in Simulation (FS) Proceedings Conferences - Monographs, Proceedings:

I. Troch, F. Breitenecker (eds): *Proceedings MATHMOD 09 - Abstract Volume / Full Papers CD Volume*. Proc. 6th Conference Mathematical Modelling Vienna, February 2009, Vienna; ARGESIM Reports no. 34 & no. 35, ASIM / ARGESIM Vienna, 2009; ISBN 978-3-901608-34-6, ISBN 978-3-901608-35-3

M. Rabe (ed.): *Advances in Simulation for Production and Logistics Applications*. Proc. 13. ASIM-Fachtagung Simulation in Produktion und Logistik, October 2008, Berlin; Fraunhofer IRB-Verlag, Stuttgart, 2008, ISBN 978-3-8167-7798-4.

B. Zupančič, R. Karba, S. Blažič (eds.): *Proceedings EUROSIM 2007 - Abstract Volume / CD Volume*. Proc. 6th EUROSIM Congress on Modelling and Simulation, Sept. 2007, Ljubljana, Slovenia. ARGESIM Report no. 32, ASIM / ARGESIM Vienna, 2007; ISBN 978-3-901608-32-2.

S. Collisi-Böhmer, O. Rose, K. Weiß, S. Wenzel (Hrsg.): *Qualitätskriterien für die Simulation in Produktion und Logistik*. AMB 102, Springer, Heidelberg, 2006; ISBN 3-540-35272-4.

M. Rabe, S. Spiekermann, S. Wenzel (Hrsg.): *Verifikation und Validierung für die Simulation in Produktion und Logistik*. AMB 103, Springer, Heidelberg, 2006; ISBN 3-540-35281-3.

W. Borutzky: *Bond Graphs Methodology for Modelling Multidisciplinary Dynamic Systems*. FS 14, ISBN 3-936150-33-8, 2005.

Fortschrittsberichte Simulation (FB) - ARGESIM Reports (AR) - Special Monographs, PhD Theses, ASIM Workshop Proceedings

D. Leitner: *Simulation of Arterial Blood Flow with the Lattice Boltzmann Method* ARGESIM Report 16, ASIM / ARGESIM Vienna, 2009; ISBN 978-3-901608-66-7.

Th. Löscher: *Optimisation of Scheduling Problems Based on Timed Petri Nets*. ARGESIM Report 15, ASIM / ARGESIM Vienna, 2009; ISBN 978-3-901608-65-0.

R. Fink: *Untersuchungen zur Parallelverarbeitung mit wissenschaftlich-technischen Berechnungsumgebungen*. ARGESIM Report 12, ASIM / ARGESIM Vienna, 2008; ISBN 978-3-901608-62-9.

M. Gyimesi: *Simulation Service Providing als Webservice zur Simulation Diskreter Prozesse*. ARGESIM Report 13, ASIM / ARGESIM Vienna, ISBN 3-901-608-63-X, 2006.

J. Wöckl: *Hybrider Modellbildungszugang für biologische Abwasserreinigungsprozesse*. ARGESIM Report 14, ASIM / ARGESIM Vienna, ISBN 3-901608-64-8, 2006.

H. Ecker: *Suppression of Self-excited Vibrations in Mechanical Systems by Parametric Stiffness Excitation*. ARGESIM Report 11, ISBN 3-901-608-61-3, 2006.

C. Deatcu, P. Dünow, T. Pawletta, S. Pawletta (eds.): Proceedings 4. ASIM-Workshop Wismar 2008 – Modellierung, Regelung und Simulation in Automotive und Prozess-automation. ARGESIM Report 31, ASIM / ARGESIM Vienna, ISBN 978-3-901608-31-5, 2008.

J. Wittmann, H.-P. Bader (Hrsg.): *Simulation in Umwelt- und Geowissenschaften - Workshop Dübendorf 2008*. Shaker Verlag, Aachen 2008, ISBN 978-3-8322-7252-4.

A. Gnauck (Hrsg.): *Modellierung und Simulation von Ökosystemen - Workshop Kölpinsee 2006*. Shaker Verlag, Aachen 2007, AM 107; ISBN 978-3-8322-6058-3.

Available / Verfügbar: ASIM / ARGESIM Publisher Vienna - WWW.ASIM-GI.ORG
SCS Publishing House e.V., Erlangen, WWW.SCS-PUBLISHINGHOUSE.DE
Download ASIM Website WWW.ASIM-GI.ORG (partly; for ASIM members),
Bookstores / Buchhandlung, tw. ermäßigter Bezug für ASIM Mitglieder WWW.ASIM-GI.ORG

Table of Contents

SNE Editorial **Board**

SNE - *Simulation News Europe* (SNE) is advised and supervised by an international editorial board. This board is taking care on peer reviewing and handling of *Technical Notes*, *Education Notes*, *Short Notes*, *Software Notes*, and of *Benchmark Notes* (definitions and solutions). Work of the board is supported by a new SNE Contribution-, Management-, and Reviewing System via the new SNE website. At present, the board is increasing:

Felix Breitenecker, *Felix.Breitenecker@tuwien.ac.at*
Vienna University of Technology, Austria, Editor-in-chief

Peter Breedveld, *P.C.Breedveld@el.utwente.nl*
University of Twenty, Div. Control Engineering, Netherlands

Agostino Bruzzone, *agostino@itim.unige.it*
Universita degli Studi di Genova, Italy

Francois Cellier, *fcellier@inf.ethz.ch*
ETH Zurich, Institute for Computational Science, Switzerland

Vlatko Čerić, *vceric@efzg.hr*
Univ. Zagreb, Fac. of Organization and Informatics, Croatia

Russell Cheng, *rchc@maths.soton.ac.uk*
University of Southampton, Fac. Mathematics/OR Group, UK

Horst Eckerbiochemical modelling and simulation , *Horst.Ecker@tuwien.ac.at*
Vienna University of Technology, Inst. f. Mechanics, Austria

Edmond Hajrizi, *ehajrizi@ubt-uni.net*
University for Business and Technology, Pristina, Kosovo

András Jávor, *javor@eik.bme.hu,*
Budapest Univ. of Technology and Economics, Hungary

Esko Juuso, *esko.juuso@oulu.fi*
Univ. Oulu, Dept. Process/Environmental Engineering, Finland

Rihard Karba, *rihard.karba@fe.uni-lj.si*
University of Ljubljana, Fac. Electrical Engineering, Slovenia

Francesco Longo, *f.longo@unical.it*
Univ. of Calabria, Mechanical Department, Italy

David Murray-Smith, *d.murray-smith@elec.gla.ac.uk*
University of Glasgow, Fac. Electrical Engineering, UK

Thorsten Pawletta, pawel@mb.hs-wismar.de
Univ. Wismar, Dept. Computational Engineering, Germany

Niki Popper, *niki.popper@drahtwarenhandlung.at*
dwh Simulation Services, Vienna, Austria

Thomas Schriber, *schriber@umich.edu*
University of Michigan, Business School, USA

Peter Schwarz, *Peter.Schwarz@eas.iis.fraunhofer.de*
Fraunhofer Foundation-Design Automation Dresden, Germany

Yuri Senichenkov, *sneyb@dcn.infos.ru*
St. Petersburg Technical University, Russia

Sigrid Wenzel, *S.Wenzel@uni-kassel.de*
University Kassel, Inst. f. Production Technique, Germany

SNE Contact. SNE - Editors /ARGESIM
c/o Inst. f. Analysis and Scientific Computation
Vienna University of Technology
Wiedner Hauptstrasse 8-10, 1040 Vienna, AUSTRIA
Tel + 43 - 1- 58801-10115 or 11455, Fax – 42098
office@sne-journal.org; www.sne-journal.org

SNE 19(3-4) Reprint doi: 10.11128/sne.19.34.0994

SNE Simulation News Europe ISSN 1015-8685 (0929-2268).

Scope: Technical Notes and Short Notes on developments in modelling and simulation in various areas /application and theory) and on bechmarks for modelling and simulation, membership information for EUROSIM and Simulation Societies.

Editor-in-Chief: Felix Breitenecker, Inst. f. Analysis and Scientific Computing, Vienna University of Technology, Wiedner Hauptstrasse 8-10, 1040 Vienna, Austria; Felix.Breitenecker@tuwien.ac.at

Layout: Markus Wallerberger, markus.wallerberger@gmx.at

Administration, Web: Anna Mathe, anna.mathe@tuwien.ac.at

Printed by: Grafisches Zentrum, TU Vienna, Wiedner Hauptstrasse 8-10, 1040, Vienna, Austria

Publisher: ARGESIM/ASIM; c/o Inst. for Scientific Computing, TU Vienna, Wiedner Hauptstrasse 8-10, 1040 Vienna, Austria, and ASIM (German Simulation Society), c/o Wohlfartstr. 21b, 80939 Munchen;

© ARGESIM/ASIM 2009

Model-based Development of Self-organizing Earthquake Early Warning Systems

Joachim Fischer, Frank Kühnlenz, Klaus Ahrens, Ingmar Eveslage, Humboldt-Universität zu Berlin

SNE Simulation Notes Europe SNE 19(3-4), 2009, 9-20, doi: 10.11128/sne.19.on.09941

A new approach for *e*arthquake *e*arly *w*arning *s*ystems (EEWS) is presented that uses wireless, self-organizing mesh sensor networks. To develop the prototype of such IT infrastructures, we follow a model-driven system development paradigm. Structure and behaviour models of network topologies in specific geographic regions are coupled with wave signal analysing algorithms, alarming protocols, convenient visualisations and earthquake data bases to form the basis for various simulation experiments ahead of system implementation and installation. The general objective of these studies is to test the functionality of an EEWS and to optimize it under the real-time, reliability and cost-depended requirements of potential end-users. For modelling a technology mix of SDL/ASN.1/UML/C++ is used to generate the code for different kind of simulators, and for the target platform (several node types).
This approach is used for realizing a prototype EEWS developed within the EU project SAFER (*S*eismic E*a*rly Warning *f*or *Eu*rope) in cooperation with the *Geo*forschungszentrum Potsdam (GFZ). The first operational area of that EEWS is preparation for Istanbul in a region threatened by strong earthquakes. The presented paper focuses on our adopted and developed tool-based modelling and data base techniques used in that project, that are general and flexible enough for addressing similar prototyping use cases of self-organizing sensor-based IT infrastructures.

Introduction

The concept of Self-Organizing Seismic Early Warning Information Networks (SOSEWIN) is being developed within the EU-project SAFER (*S*eismic E*a*rly warning *f*or *Eu*rope) [1] in cooperation with the *Geo*forschungszentrum Potsdam (GFZ). The work benefits from the Graduate School METRIK [2] on disaster management, supported by the DFG (German Research Society). It focuses on the adoption of METRIK-technologies concerning self-organizing, ad-hoc communication infrastructures and model-based software development for prototyping Earthquake Early Warning Systems (EEWS).

The SAFER project aims to fully exploit the possibilities offered by the real-time analysis of the signals coming from seismic networks for a wide range of actions, performed over time intervals of a few seconds to some tens of minutes. These actions include the shutting down of critical systems of lifelines and industrial processes, closing highways, railways, etc., the activation of control systems for the protection of crucial structures, as well as supporting the rapid response decisions that must be made by emergency management (continuously updated damage scenarios, aftershocks hazard etc.) [4, 5].

Present EEWS have a number of problems related to insufficient node density due to the high costs per node necessary for the purchasing, installation and maintenance of the usual more sophisticated seismological stations. However, such problems can be solved by using a low-cost, self-organizing, ad-hoc mesh sensor network that avoids more costly planned infrastructure. Such self-organizing communication networks were already successfully used within other application areas. One example is the *Berlin RoofNet* [3], which demonstrates the feasibility to build an autonomous wireless communication network in the city of Berlin at a moderate budget.

This paper demonstrates how the concept of such self-organizing mesh networks can be extended and adopted for the development of low-cost EEWS prototypes. As in Berlin RoofNet inexpensive commercial off-the-shelf (COTS) hardware is used with Linux as operating system and existing communication technologies, such as IEEE 802.11g WLAN, which operates in the unlicensed 2.4 GHz ISM band. Communication is close to realtime (delay ~ 0.5 - 1.0s), robust (mesh-structure with redundant paths) and based on the Internet Protocol, allowing for easy integration with existing applications and with the external public Internet (where available) [6].

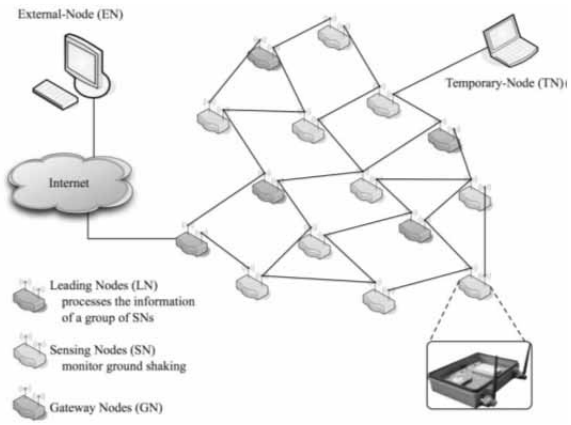

Figure 1. A SOSEWIN example topology with typical nodes.

Low-cost ground acceleration seismometer and GPS receiver are the basic components to recognize wave signals in dependence of time and locality.

A SOSEWIN network consists of nodes of different types with slightly different tasks. The elementary tasks are

- Routing Task: forwarding of received messages by wireless communication,
- Sensing Task: monitoring ground shaking using seismometer and GPS functionality,
- Alerting Task: issuing signals for alarms and reset alarms at different levels,
- Management Task: supporting installation, maintenance and control SOSEWIN for different manager types (seismological or network experts),
- Visualizing Task: supporting visualisation of SOSEWIN state information for different end users (public, decision maker in disaster's management).

In principle, each of the SOSEWIN nodes must undertake all of these tasks. However, there are different restrictions, depending upon the node's equipment and the task requirements. Figure 1 shows a simplified SOSEWIN topology with typical nodes.

Developing the complex IT-infrastructure, we follow a model-driven system development paradigm. Structure and behaviour models of network topologies in specific geographic regions are coupled with wave signal analysing algorithms, alarming protocols, convenient visualisations and earthquake data bases to form the basis for various simulation experiments ahead of system implementation and installation.

The general objective of these studies is to test the functionality of an EEWS and to optimize it under the real-time, reliability and cost-depended requirements of potential end-users. For modelling a technology mix of SDL/ASN.1/ UML/C++ is used to generate the code for different kind of simulators, and for the target on several nodes. This approach is used for realizing a prototype-EEWS developed within the EU project SAFER in cooperation with the GFZ. The first operational area of that EEWS is already installed in Istanbul, a region threatened by strong earthquakes. However, first SOSEWIN model tests were realized by using historical earthquake data, recognized by a centralized seismometer network in Taiwan and synthetic sensor data generated by a tool based on the work of Wang [7].

Our paper is structured into several sections. The next Section 1 gives some background information to the application area and motivates the impact of earthquake wave signal analysing approaches. Section 2 summarizes the current situation in the development of EEWS. Especially the advantages of self-organized systems are discussed here.

Section 3 describes the general concepts of our SOSEWIN prototype, developed in the on-going SAFER project. The principles of our Alarming Protocol (AP) are outlined in section 4. Section 5 discusses this infrastructure, especially modelling concepts, the SDL compiler and simulation components. The current status of the SOSEWIN development is given by Section 6 including a short description of the testbed installation in Istanbul. The last Section 7 summaries the results.

1 Earthquake Waves, Early Warning and Rapid Response

Earthquakes produce different types of seismic waves. These waves travel through the earth and provide an effective way to create an image of both sources and structures deep within the Earth. In addition their analysis is the foundation for different activities in a disaster's management process, so for earthquake classification, early warning and first response.

There are four types of seismic waves: P-waves and S-waves (called body waves), Rayleigh waves and Love waves (called surface waves).

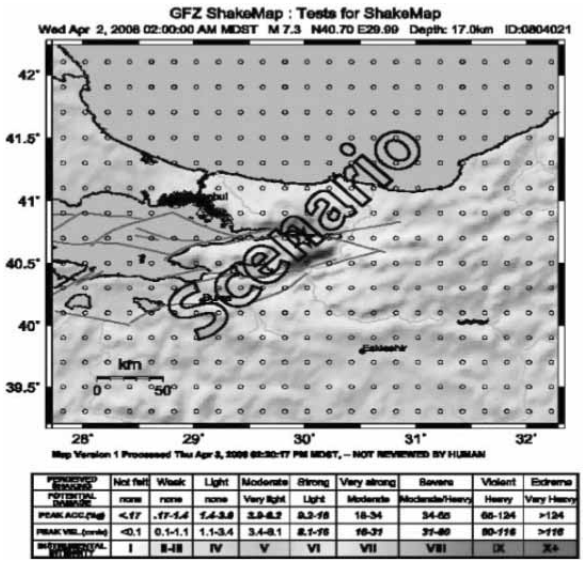

Figure 2. ShakeMap example of a scenario earthquake.

Body waves travel through the interior of the Earth. P-waves (primary waves) are longitudinal or compression waves, which brings the ground into alternately compressed and dilated movement in the direction of propagation. In solids, these waves generally travel almost twice as fast as S-waves (secondary waves) and can travel through any type of material. In air, these pressure waves take the form of sound waves, hence they travel at the speed of sound.

Typical speeds are 330 m/s in air, 1450 m/s in water and about 5000 m/s in granite (dependent upon the geology of the specific region and the hypocenter depth, P-waves travel at 5-8 km/s, and S-waves at 3-7 km/s). When generated by an earthquake they are less destructive than the S-waves and surface waves that follow them. Surface waves remain below the Earth's surface. They can be much larger in amplitude than body waves, and can form the largest signals seen in earthquake seismograms. Seismograms are more strongly excited by surface waves particularly when the seismic source (hypo centre) is in close to the surface of the Earth.

It is not possible to predict an earthquake event. The only chance for preparation on the coming disaster is to use the most of the time delay between the arrival times of the P- and S-wave. In dependence of the distance between the epicentre of the earthquake (transferred hypocentre on the Earth's surface) and the critical area locations only few seconds to some tens of minutes remain for an early warning.

The other important task in analysing earthquake waves, which supports to save human life, is rapid response. This is a fast generation of so-called ShakeMaps, which show the wave peaks in the area (influenced by the earthquake event) in form of isobar lines or different colours. The combination of such ShakeMaps with existing building and inhabitation structures can offer start estimations of the disasters when these information would be available very fast after an event.

A special kind of ShakeMap is an AlertMap. It is based on incomplete earthquake event descriptions (only on entrance signal data series) during the earthquake itself. The generation of such maps is an actual engineering challenge.

2 Earthquake early warning systems

EEWS are based on the detection of P-waves that do not cause damage but precede the slower and destructive S-waves and surface waves. Dependent upon the distance between the hypocentre and the target area, a maximum early warning time before the S-wave arrives can be computed, based on wave travel characteristics and ground parameters. Therefore, the primary goal of an EEWS is simple: maximizing the early warning time under a minimal number of false alarms (which includes false positives and false negatives). An important secondary goal is to generate AlertMaps.

In the next subsection the existing approach for EEWS are described, followed by a statement about the problems these systems are faced. Subsection 2.3 illustrates how the vision of a decentralized sensor network can aim the disadvantages and lead to a better solution.

2.1 Present: Centralized Approach

Present EEWS always use a centralized approach (for example in the Marmara region, Turkey [9], Southern Apennines, Italy [10] and Taiwan [11]). Each station delivers its measured data or the alarm message for the case of P-wave detection over a (more or less) direct connection to a central data centre (which usually has a secondary data centre for backup).

Within the data centre, it can then be decided whether an early warning message should be issued to the end users (e.g. nuclear power plants) who can then decide what actions will be instigated.

In the case of the already existing Istanbul Earthquake Rapid Response and Early Warning System (IERREWS), ten strong-motion stations were placed as close as possible to the Great Marmara Fault zone, forming the online-sensor-part of the early warning system [9]. These stations are connected to the data centre of the Kandilli Observatory and Earthquake Research Institute via a digital spread spectrum radio link and continuously deliver ground-motion data for archiving and early warning purposes.

Depending upon the location of the earthquake's epicentre and the recipient facility, the early warning time can be as high as about 8s [9].

2.2 Dilemma of current EEWS

Current early warning systems, like the above described IERREWS, often consist of only a few, but expensive (several thousand Euros) stations. This fact results in a number of problems:

Malfunction: If one station breaks down, then the area that it would normally observe can now only be monitored from afar, resulting in time delays that could seriously compromise the network's early warning capacity.

Instrumental Density: This problem is related to the generation of precise information about an earthquake's intensity for city square cells, the size necessary being generally of the order of 500 m. Civil protection experts need such detailed information for reliable loss estimation maps (destroyed buildings, injured people and fatalities) that are the basis for effective planning by rescue teams. By comparison, EEWS usually have a station spacing of several kilometres.

Cost: However, increasing the density of seismic stations is limited by their expense.

Communication: The reliable transmission of all station information to central data stations or civil protection headquarters is very important, especially following an earthquake, where usually centralized communication infrastructures may have collapsed.

2.3 Vision: decentralized approach based on low-cost wireless ad-hoc mesh sensor networks

The basic idea presented in this work aims to avoid the problems identified above by deploying a much higher number of much cheaper stations (costing only a few hundreds of Euros per station, which is of the order of 10% compared to a classical station).

Another cost factors are the communication modules necessary for the link to the central data centres (in some cases within IERREWS, involving several hundred kilometres).

Wireless, ad-hoc mesh sensor networks will allow much cheaper radio modules because a single station needs only to reach the nearest neighbour station, which would be only a few hundred meters away.

In addition, the reliability of such a mesh sensor net is a crucial point, since while single sensors may be destroyed, the whole system nonetheless can still detect the earthquake. This can be achieved because the sensor nodes act cooperatively in a self-organizing way.

However, a number of challenging problems must be solved first (e.g. development of strategies for self-organization regarding the special requirements of EEWS; routing in huge multi-hop networks; deployment of software components).

The main advantages of such an approach, besides providing a more robust and cheaper architecture than centralized systems, may be summarized as follows:

- The simple deployment and installation of a temporary sensor net. This would be of particular value to, for example, groups such as the German Earthquake Taskforce, who deploy temporary arrays for the detection of aftershocks. Time consuming planning and (costly) installation of a traditional infrastructure-based system can thus be avoided.
- As mentioned above, in the event of an individual sensor node being destroyed, the self-organizing nature of the network will allow alternate communication routes to be established, while the information regarding the loss of the sensor or sensors may be utilized in damage assessments.
- At a later stage it is planned to provide the capability of using the network as an information system. In the event of a damaging earthquake, individuals will be able to send short messages such as "I am alive." or "I need help!" through a reliable mesh network that is still functional when other systems such as GSM may have collapsed.

3 SOSEWIN Overview

In contrast to existing EEWS, which are planned and centralized, we propose the use of a self-organizing ad-hoc wireless mesh network to overcome the problems of planning such a large network and administrating potentially thousands of Sensing Nodes (SNs). The advantages of such a network include robustness, independence of infrastructure, spontaneous extensibility as required, and a self-healing character in the event of failing SNs.

However, these networks still pose a great research challenge, particularly regarding a routing-strategy to accomplish scalability requirements and time constraints.

To realise a hierarchical alarming system, each node runs the Alarming Protocol (AP) with different roles at runtime. The SOSEWIN nodes are organised into clusters using criteria that determines the optimum communications efficiency. Each cluster is headed by a SN that is designated, again based on communications efficiency, as a Leading Node (LN), with whom the other SNs within its cluster communicate general "housekeeping/status" information and initial alarms. The LN in turn communicated with other LNs, including the issuing of system alarms, based on each LN knowing the status of the nodes that make up their clusters.

For SOSEWIN, the following node types have been defined:

- *Sensing Nodes* (SN) monitor ground shaking. Most nodes in the network are of this type.
- *Leading Nodes* (LN) are basically Sensing Nodes as they consist of the same hardware. The “leading” property is a role that any SN can fulfil. A leading node processes the information of a group of SN in its neighbourhood (usually not more than five SN).
- *Gateway Nodes* (GN) represent information sinks in the SOSEWIN that have connections to the end users (via the internet/satellite/cable) outside of the network, and are used for sending early warning messages. It includes the functionality of a SN.
- *External nodes* (EN) are outside of the SOSEWIN and are connected via Gateway Nodes. They are to be informed first in the event of an alarm (e.g. GFZ, HU, Kandilli Observatory KOERI, police stations)
- *Temporary Nodes* (TN) are present in the network only for a short time to access data. An example of a temporary node is the laptop of an earthquake task force member, who wants to access ground shaking maps or waveform data.
- *Routing Nodes* (RN) ensure that communications between far-away nodes, which could not communicate otherwise. A Routing Node only delivers messages that it receives and undertakes no analysis. It is useful in being a low-cost way of extending the monitoring to a larger area.
- *Visualizing Node* (VN) A Laptop acting as a TN is a typical VN, which is able to come with a GUI to visualize subsequent SOSEWIN states on different abstraction levels by request. It is also easy to imagine that some of the SNs also have restricted visualization capabilities.

The AP uses peer-to-peer communication services realized by the underlying communication layer (TCP/UDP, OLSR [12], WLAN). To reduce the network load and the latency the messages are encoded using ASN.1 standard [14, 15] developed by ITU-T.

4 Alarming protocol

The AP is one part of the SOSEWIN software architecture which specifies the algorithm and the rules how the sensor network detects an earthquake and issues the alarm to the end user. It consists of an ensemble of entities described in this section. Each entity is modelled as an extended finite state machine.

4.1 Overview of the system hierarchy

SOSEWIN supports a hierarchical alarming system. That is why the network is composed of node clusters, each cluster headed by a LN, where the cluster members are ordinary SNs or GNs. The definition of the clusters and the designation of which nodes are the LNs (which are themselves simply normal SNs within the network) are given by the initial installation.

However, this can be changed dynamically if the network topology is changed. In principle, every sensor node can play two roles, a sensing and a leading role.

As Fig. 3 shows, the AP is realized by different asynchronous communicating protocol entities. Each entity is formally described by a state machine using the SDL-RT model description language:

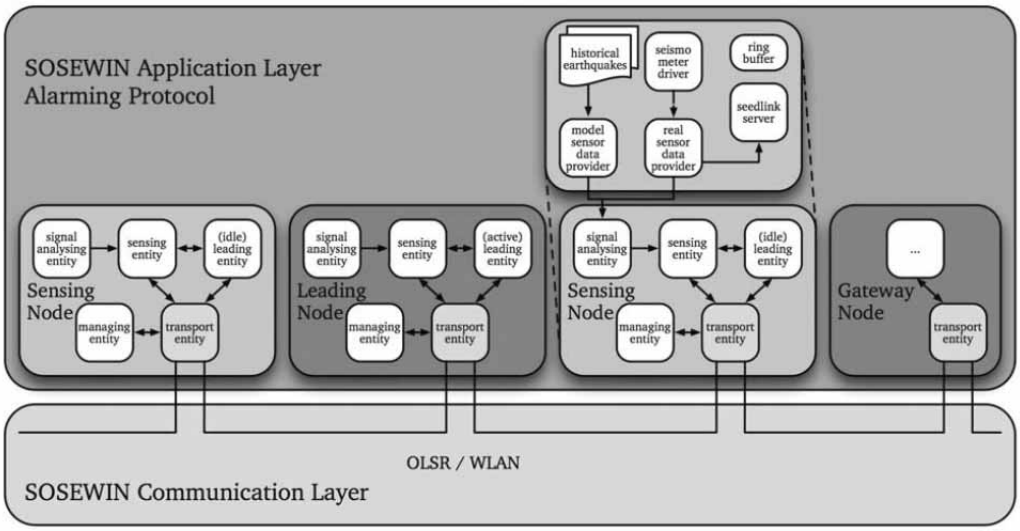

Figure 3. Nodes and the associated protocol entities of the SOSEWIN Application Layer.

- *Signal Analysing Entity* (SAE): This one is responsible for analysing the incoming streams of accelerometric raw data and informing the SE in the event of certain state changes. As presented in Fig. 3 we distinguish two different data sources for SAE. Alternately to a seismometer driver a stored data file (containing synthesized data) can be used here. This is controlled by data provider functions. An additional procedure is to save the raw data in a special data format (SEEDLink [13]) in a ring buffer.
- *Sensing Entity* (SE): It reacts on the results from the SAE trigger by informing its associated LE itself if the hosting node is a leading node (otherwise the LE of another node). To improve the SAE-SE-communication they operate over a semaphore-controlled common data base.
- *Transport Entity* (TE): It implements the message transport from the communications layer to the corresponding AP entities and vice versa. There are different message types (signal description, alarming, management…) with individual signatures. To do so it has the knowledge of the member node IP numbers of that cluster where it belongs to. A special task is the coding and decoding of all AP messages to and from other nodes. The coding/decoding procedure is realized by an ASN.1 compilation [14, 15]. For that, a C++ library modelling ASN.1 data types was used, developed by an earlier SDL/ASN.1-C++ compiler project [14].
- *Leading Entity* (LE): The LE monitors all associated SEs (that is the SE of the same node and the SEs of the Sensing Nodes within its cluster). An LE is able to cause or invoke group alerts and is also able to cause system alerts to be issued after communicating with other LEs; each system alert will sent to the TEs of all GNs. When a node is not a LN, then this entity is idle.

4.2 Informal Protocol Description

Besides event detection, a general goal of the AP is to offer a network service that actualizes the knowledge about the states of all distributed SOSEWIN seismometers by their associated LEs as fast as possible after an individual change. The AP functionality is defined by two sub layers, an internal cluster protocol and a protocol for cluster-interaction. The internal cluster protocol defines the communications between a SAE and SE, and the communication between all SEs of a cluster and their representing LN.

The inter-cluster protocol defines the communications between all LEs. If a critical number of P-wave triggers have reached the LE of a cluster's LN, this node informs its neighbouring LNs. In the case that a LE of a LN has received enough cluster alarms, a socalled system alarm will be sent as fast as possible to the GNs of SOSEWIN that are responsible for forwarding those alarms to defined ENs by peer-to-peer communication.

According to this hierarchical principle, three alarm levels are recognized by the SOSEWIN:

- Pre-alarm (recognized by the LE of a LN, the requirement being a registration of a P-wave trigger by at least one SN of its cluster);
- Group alarm (recognized by the LE of a LN, the requirement being a certain number of node alarms of this cluster have been registered);
- System alarm (recognized by the LE of a LN, requires a certain number of group alarms registered by this LE).

Because of the independent reaction of the distributed nodes and their corresponding protocol entities, these alarm levels are reached by the individual nodes in a time-displaced manner. In addition to the three alarm states of the nodes represented by their protocol entities, two other states can be distinguished:

- Idle (recognized by the SE of each node, in that no event is occurring and preliminary analysis of the data input is going on);
- Final reporting (recognized by the LE of a LN, and the SE of all nodes, that the event is considered to be finished and the final data/result files (e.g. for ShakeMap) are being produced.

The AP is characterized by the principle that all SNs inform their LNs with as short time delays as possible about their current state without any explicit demand. Doing so, the LNs will be informed about the whole life cycle of an earthquake event according to their SNs. An explicit demand is necessary if ENs (via GNs) or TNs want to collect detailed information on the last event observed by the SOSEWIN. Once the first SN of a cluster has been triggered, the LN assigns an ID to the event, which will be based on the GPS time of the trigger at the first SN that detected it. The ID of the event is therefore the minimum event time, and maybe also with a code identifying the SN. Hence, both the real and false events will be recognized by the network by that code.

4.3 Formal Protocol Description

All of the protocol entities were described in detail by us in SDL, where in the first design stage the Real Time Developer Studio (RTDS) in version 3.4 was used, which supports an SDL dialect (SDL-RT [8]) in combination with UML class diagrams and C++ for activity and data type descriptions. This toolkit was extended in the context of the development of our EEWS prototyping infrastructure. Our extension allows not only a simulated execution and testing of the protocol entities, it also simplifies the code generation for an available cross compiler for the target hardware/operating system architecture. In addition to that the coding/decoding of messages for the node-to-node communication is realised by a developed ASN.1 compiler. To ease the management of the complex prototyping task of EEWS an infrastructure was developed in parallel to the model development itself.

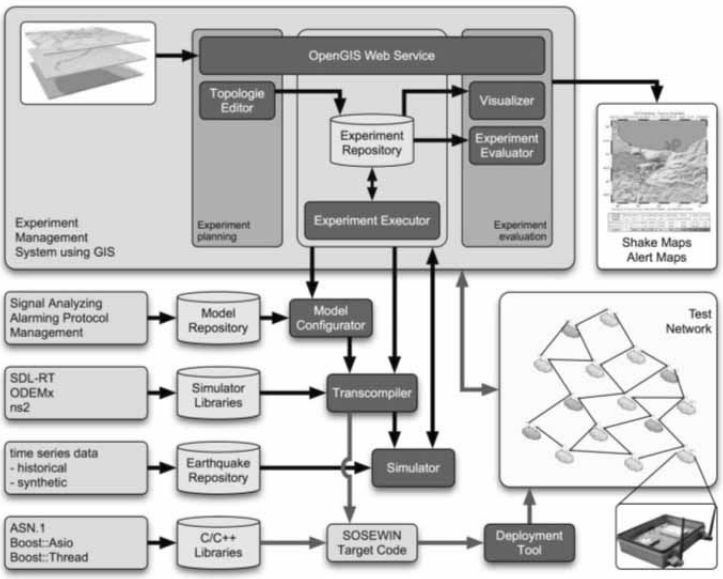

Figure 4. Model-based Prototyping Infrastructure for EEWS.

5 Prototyping Infrastructure

5.1 Infrastructure Components

The foundation of the tool integration in our EEWS prototyping infrastructure is a centralized management of models, software artefacts, and simulation results by several repositories that are implemented by data base technologies. Figure 4 shows an overview on the core components realizing the identified requirements and concepts, which are shortly described in the following (from top to down in Fig. 4).

- *The Experiment Management System* supports planning, configuration, automated execution of simulations and storage of simulation results. It provides additionally GIS-based visualization capabilities for simulation results (e.g. Detection Maps) that can also be used for planning software deployment and monitoring of an installed SOSEWIN network.

- *The Model Repository* stores used SDL(-RT), UML and C++ models defining the entities of the AP. It also holds models of the environment (e.g. for network clustering, message transport properties or node breakdowns).
- *The Model Configurator* knows the target platform and uses platform dependent artefacts to configure the compiler (e.g. cross-compilation). It also specifies certain input parameters (e.g. threshold values or network clustering) and stores the whole configuration into the Experiment Repository.
- *The Transcompiler* is indeed a tool chain of several transcompilers, which accept SDL-RT models and compile C++ code at the end into different executable binaries (simulators, target code).
- *The Simulator* represents in fact a collection of several simulators of different functionality (derived from different simulation frameworks).
- *The Simulator Libraries* is a pool of simulation frameworks used by the simulators. They are used by the transcompiler to generate the executable binaries. Each simulator uses a different library with different features and restrictions.
- *The Earthquake Repository* comprises time series of historical recorded or synthetic generated earthquake data stored in a relational database system. Various input formats, such as (Mini)SEED, SAC and several well-known-text (WKT) formats where mapped to the same database scheme, that is used as an uniform interface for simulations.
- *The C/C++ Libraries* providing the target code binary with threading and networking capabilities and with the necessary functions to decode and encode the network messages using the ASN.1 standard.
- *The Deployment Tool* enables the developer to distribute the AP in the testbed network from a remote site without access the nodes physically. Presently this is done by SFTP access from a central temporary node but a distributed approach is subject of actual research activities.

Using this infrastructure, different testbeds can be offered, namely for the detection of P-waves, for the functional correctness of different protocol concepts, and for the simulation of complete EEWS models. In addition, our infrastructure will be used for prototyping software components of the target EEWS.

Additional a TN equipped by components of this infrastructure can play a temporary manager of the EEWS to visualize different dynamic installation, maintenance and operating activities.

Some of the concepts will described now more in detail.

5.2 Experiment Management System (EMS)

The results of the simulator runs (event traces) will also be stored within the relational database Experiment Repository (by import log files or direct access through an API), which is part of the Experiment Management System (EMS). Experimental results can then be evaluated manually by the Visualizer. This tool allows the presentation of a P-wave travelling through the network, with its detection (or non-detection) being marked by the sensor nodes changing colour (green to red, Detection Map). Other experimental output would include the so-called AlertMaps and ShakeMaps [12].

Both maps describe the spatial variation in the maximum ground shaking resulting from an earthquake for a given ground motion quality. A ShakeMap is generated from the complete time series of an event for each sensing node. In contrast, AlertMaps follow an evolutionary approach. Based only on the first few seconds of an earthquake's time series, a predicted ShakeMap is computed.

Hence, while AlertMaps have a lower quality and accuracy than ShakeMaps, they are generated during an earthquake and are an early warning tool while ShakeMaps are used for post-event response planning.

For the configuration of EEWS models (network topology, software architecture of nodes, geographic area) under load (earthquake events, transmission disturbances) a graphical Topology Editor based on a Geographic Information System (GIS) is necessary. Adding and removing nodes is implemented using the OGC standard Web Feature Service (WFS). With WFS, a layer of spatial objects (e.g. points and lines with additional attributes) defined by the OGC standard Simple Features for SQL can be placed in a topographic map (overlay).

With our EMS, various automatic evaluations of the experiments can be computed. It considers the seismic wave velocities for a certain area and computes the estimated arrival of the P- and S-wave for each sensing node based on the hypocentre information in the repository.

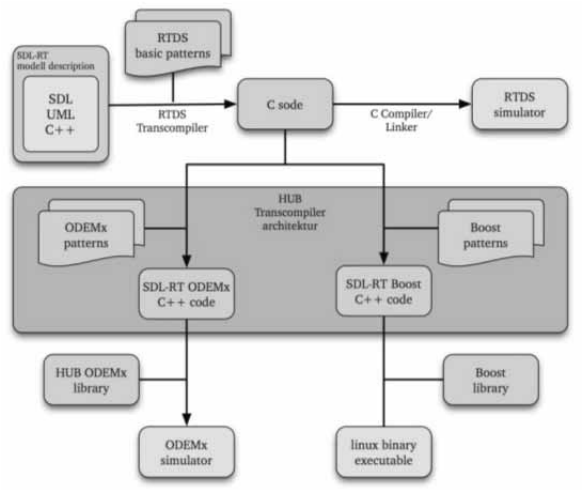

Figure 5. SDL-UML-C++ Transcompiler Architecture.

Then it checks the P-wave arrival time as determined by the sensing node, and determines whether this time is within a certain tolerance. Based on that mechanism, our EMS offers a comparison feature to evaluate different experimental results, for example the efficiency of different detection methodologies. Furthermore, it ensures reproducibility and consistency between the various development cycles of the simulator.

5.3 Transcompiler

By adopting PragmaDev-tools [23] our transcompiler follows the UML MDD approach to produce code for different platforms starting from SDL-RT model descriptions. This allows to process compositions of UML (class, use case and sequence diagrams), SDL [22] (communicating processes) and C++ (data structures and sequential actions). We are able to use the RTDS[1] simulator to debug the model execution by SDL interpretation.

In addition to this technique, other simulation frameworks can be coupled according to specific modelling and investigation requirements. Whereas by an SDL-based simulation, so far "only" functional characteristics have been examined, the ODEMx library ([17], [18], [19]) will allow non-functional performance characteristics of self-organizing systems to be determined by simulation, while varying the topology and environmental influences. The RTDS compiler is currently adopted by following extensions (shown in Figure 5):

- annotations (prefixed SDL identifiers) in the SDL-RT source code allow a post-processing of the generated C-code, produced by RTDS,
- additional pattern-controlled transcompiler which transforms the generated C-code of RTDS to C++ supporting different targets. Using these patterns special parts of the structured RTDS C-Code will be substituted in each case following the related substitution patterns. Currently two alternatives are supported by our transcompiler:
  - transcompilation to ODEMx simulator, described in section 6.4, using the network simulator library ODEMx[2] which also handles time dependencies of state machine actions and message transportations by the network (as a main preposition for a model-based performance evaluation of SOSEWIN networks),
  - transcompilation by using Boost library thread and network functionality [20] to C++ as target code for the SOSEWIN nodes running a POSIX-compliant Linux, as they are currently installed in a testbed (see section 6).

5.4 Simulator

Our prototyping infrastructure integrates various simulators for different evaluation goals under common experiment management strategies. The last section has demonstrated different kinds of C/C++ code generations, where two of them were related with the simulation framework.

For the simulated execution of our formal described protocol entities we have to distinguish different main analysing goals, where each of them is of certain complexity:

- functional evaluation of a single SAE SDL process by varying historical or synthesised earthquake data to check and improve the used signal analysing numerical methods.
- functional evaluation of a single SN as an ensemble of different communicating state machines.

[1] Real Time Developer Studio (V3.4) supports SDL-RT (a combination of UML, SDL, and C/C++) as a suited representation in the embedded / real time world today because it is basically a set of graphical representations of classical concepts such as tasks, messages, states, timers, and semaphores.

[2] Object-oriented Discrete Event Modelling is a C++ library for modelling and simulation of ensembles of discrete event driven processes combined with time-continuous processes.

Figure 6. Actual SOSEWIN testbed installation in Istanbul.

- functional evaluation of a configuration of SNs and LNs by varying historical or synthesized earth quake data,
- performance evaluation of a configuration of SNs and LNs by varying historical or synthesized earthquake data to estimate the capability of early warning.

A lot of parameters have to be tuned by the above scenarios in dependence on the target local area, the network size and topology, on the influence of environmental noise, on the behaviour of used underlying transport protocols.

The successful realisation of this complex task to fulfil a compromise of different requirements is the base of continuation of further development steps, so for code generation, software deployment, network installation, network test, and finally for network operating.

All simulators produce MSCs and other event traces for a further information aggregation or visualisation. To simplify this kind of operations the trace raw data are managed by our experiment repository, realized as a data base system.

Simulator I: Functional evaluation of signal analysing algorithms of a single node. This simulator executes for a given number of SNs and provided time series of sensor's raw data (for each of them) the behaviour of their SAEs without any communication between themselves. With the help of this simulator an isolated test of the signal analysing functionality can be realized.

With the EMS topology editor the nodes can be positioned in a map.

Using their GPS coordinates a synthesiser of an Earthquake can produce event data individually for each node by fixing a hypocentre and the earthquake parameters (e.g. rupture length, depth, energy). The simulator visualizes on one hand side the distribution of the earthquake waves in dependence of time and on the other side the P-wave detection by switching a virtual light controller from green to red by each of the node (Detection Map).

Simulator II: Functional evaluation of alarming protocol. Here we use the RTDS SDL-RT-simulator to test the functional behaviour of smaller ensembles of the SOSEWIN nodes. We abstract from concrete earthquakes, and underlying protocol layers. One further important preposition is perfect transmission behaviour of used communication channels over the air. The results of functional tests allow us to evaluate and improve the logic of our alarming protocol. Typical outputs here are MSCs, which can be represented as XML and also stored in the experiment repository for further filtering by using data base functionalities.

Simulator III/IV: Performance evaluation of alarming protocol in geographic context. Here we use the capability of our general-purpose ODEMx library [19], which supports the modelling and simulation of parallel process, where their state changes are described by discrete events in combinations with differential equations.

This library contains especially concepts for simulation computer networks, where the protocol entities are extensions of the built-in ODEMx process concepts. Using this library two different simulators are produced by our transcompiler technology:

- Simulator III allows an integrated test of all developed software components in a large network of sensor nodes. Every node processes its own set of sensor data provides by a synthetic earthquake generator [7]. This simulator allows the estimation of required transmission times and transmission quality of alternative SOSEWIN configuration which guarantees the early warning functionality in dependence on different earthquake scenarios.
- Simulator IV should support in extension of Simulator III the simulation of node breakdowns and of the behaviour of underlying protocol layers. Especially this simulator could be used for the training of disaster's management experts.

6 Current status – a prototype for Istanbul

Besides an existing small laboratory testbed of 10 SOSEWIN nodes at Humboldt-Universität, the main field test is installed in Istanbul. In order to establish a small network in the city of Istanbul, in 2008 a scientists group installed 20 nodes in the Ataköy area in the Bakirköy district (see Figure 6) [24].

The testbed runs the SOSEWIN software architecture including the network communication layer and und application layer. The actual performance of the wireless network is satisfying and guaranties a reliable communication between the nodes. Two SOSEWIN nodes are connected with the internet, so the testbed is accessible from remote site.

The installation of the alarming protocol is planned in February 2009. In the test phase of the installed alarming protocol, the already mentioned generated synthetic sensor data will be used as input for the signal analysing algorithms.

The experiments will give information about the performance of the early warning and rapid response capabilities.

7 Conclusion

We have presented a prototyping infrastructure for the model-driven development of EEWS based on selforganizing sensor networks. This architecture is based on OGC, OMG and ITU-T standards and combines different technologies for GIS, databases, behaviour modelling, code generation and simulation according to a special application domain by one integrated framework.

So, it allows the evaluation of the real-time behaviour of projected earthquake monitoring and alarming systems and supports automatic code generation from evaluated structure and behavioural models.

Modelling techniques which we used here are based on SDL and UML under special real-time requirements. Our prototyping infrastructure, implemented in C++, is used in the project SAFER for optimizing self-organizing seismic earthquake early-warning and rapid response systems, a real testbed is established in Istanbul.

An evaluation of the real-time behaviour of such complex systems is almost impossible or too expensive without prior modelling experiments, involving computer simulations. For that we identified several investigation goals supported by different simulators. This involves functional and performance evaluation of EEWS models by tuning topologies and parameters. Additionally to the model-based development our prototyping infrastructure supports also the installation, test, and operating of the network.

Currently the concepts of a cooperative signal analyzing are tested and the compiler technology reached a stable level. Now experiments have to evaluate and improve performance characteristics of the alarming protocol.

Although this contribution is naturally focussed on earthquake driven applications, the presented architecture of prototyping system may be adopted to those use cases where meshed sensor-based self-organizing infrastructures in combination with GIS are applied, such as in Heat Health Warning Systems [21].

Acknowledgements

The work was supported by the SAFER project partners at the GFZ J. Zschau, C. Milkereit, K. Fleming and M. Picozzi and by our colleagues from the Humboldt University J.-P. Redlich, B. Lichtblau and S. Heglmeier (Systems Architecture Group).

References

[1] http://saferproject.net, Seismic early warning for Europe

[2] http://www.gk-metrik.de, Model-based Development of Technologies for Self-organizing Systems.

[3] http://www.berlinroofnet.de.

[4] Wieland, M.: *Earthquake Alarm, Rapid Response, and Early Warning Systems: Low Cost Systems for Seismic Risk Reduction.* Electrowatt Engineering Ltd. Zurich, Switzerland 2001.

[5] Allen, R. M., and Kanamori, H.: *The Potential for Earthquake Early Warning in Southern California.* Science, 300, 786-789, 2003.

[6] Kurth, M., Zubow, A. and Redlich, J.P.: *Multichannel link-level measurements in 802.11 mesh networks*. IWCMC '06, Canada 2006.

[7] Wang, R.: *A Simple Orthonormalization Method for Stable and Efficient Computation of Green's Functions*. Bulletin of the Seismological Society of America, 89:733–741, Juni 1999.

[8] http://www.sdl-rt.org, 2008/05/28.

[9] Erdik, M., Fahjan, Y., Ozel, O., Alcik, H., Mert, A. and Gul, M.: *Istanbul Earthquake Rapid Response and the Early Warning System*. Bulletin of Earthquake Engineering, 1(1):157–163, 2003.

[10] Weber, E. et al.: *An Advanced Seismic Network in the Southern Apennines (Italy) for Seismicity Investigations and Experimentation with Earthquake Early Warning.* Seismological Research Letters, 78, 622–634, 2007.

[11] Lee, W. H. K., Shin, T. C. and Teng, T. L.: *Design and implementation of earthquake early warning systems in Taiwan.* Proc. 11th World Conf. on Earthquake Engineering, Acapulco, Mexico, Oxford, England: Pergamon, Disc 4:2133, 1996.

[12] http://ietf.org/rfc/rfc3626.txt, Optimized Link State Routing Protocol (OLSR), RFC.

[13] http://www.iris.washington.edu/data/dmc-seedlink.htm.

[14] Fischer; J. et. al: *A Run Time Library for the Simulation of SDL'92 Specifications.* Proc. 6th SDL Forum.

[15] ITU-T X.690 *ASN.1 Encoding Rules: Specification of Basic Encoding Rules (BER).* International Telecommunication Union, 1992.

[16] Wald, D. J., Worden, B. C., Quitoriano, V. and Pankow, K. L.: *ShakeMap Manual; Technical Manual, Users Guide and Software Guide*. U.S. Geological Survey, version 1.0 6/19/06 edition, 06 2006.

[17] Fischer, J. and Ahrens, K.: *Objektorientierte Prozeßsimulation in C++*. Addison-Wesley, 1996.

[18] Gerstenberger, R.: *ODEMx: Neue Lösungen für die Realisierung von C++-Bibliotheken zur Prozesssimulation*. Diplomarbeit Humboldt-Universität Berlin, 2003.

[19] http://sourceforge.net/projects/odemx, 2008/05/28.

[20] http://www.boost.org, 2008/05/28.

[21] Endlicher, W., Jendritzky, G., Fischer, J. and Redlich, J.-P.: *Heat waves, urban climate and human health.* In: F. Kraas, W. Wuyi, and T. Krafft, editors, Global Change, Urbanization and Health, pages 103 – 114. China Meteorological Press, 2006.

[22] ITU-T Z.100: *Specification and Description Language (SDL).* International Telecommunication Union, 2002.

[23] http://www.pragmadev.com (RTDS V3.4), 2008/05/28.

[24] Milkereit, C., Fleming, K., Picozzi, M., Jackel, K.H. and Honig, M.: *Deliverable D4.4: Development of the seismological analysis software to be implemented in the Low Cost Network.* SAFER project report, 2008/05/09.

Corresponding author: Joachim Fischer
Humboldt-Universität zu Berlin
Department of Computer Science
Unter den Linden 6, 10099 Berlin, Germany;
fischer@informatik.hu-berlin.de

Received & Accepted: MATHMOD 2009
Revised: September 18, 2009
Accepted: October 15, 2009

SNE 13/3-4, December 200709

A Quantistic Modelling of Wine Evaluation in Oenology – Probability Analysis

S. Giani, CERN, Geneva, Switzerland, Simone.Giani@cern.ch

SNE Simulation Notes Europe SNE 19(3-4), 2009, 17-24, doi: 10.11128/sne.19.tn.09943

This paper describes a formalization of the essential organoleptic characteristics assessed in the wine evaluation process. A scalar quality metrics is associated and bound to 3 dimensions and 6 variables representing standard organoleptic wine features detected by mouth-tasting (visual-tasting and nose-tasting are not the subject of this work). The correlation existing between such wine characteristics is mathematically modelled by a matrix of operators' values acting on the corresponding variables. An algebraic notation is developed to express the multi-dimensional nature of the wine quality and to provide a measurement tool for the still subjective evaluation of a wine. Probability distributions are computed, or deduced from frequency distributions, for the values measured on a sample of over 100 wines in order to test the metrics performance in terms of phase-space and bias. The statistical meaning of the empiric distributions obtained by applying such a wine evaluation metrics is analysed by benchmarking them versus known theoretical mathematical conditions: this reverse-engineering of the metrics allows the factorization of the intrinsic metrics features from the effects due to the interaction with the "observer" and his preferences. Finally, the relation between the independent and correlated quantities in the evaluation of the wines is emphasized, and a conditional probability model is proposed.

Introduction

A metric for wine evaluation in the domain of Oenology is introduced and its mathematical aspects are studied in this paper. A main concept is that any metrics in Oenology [1] must be benchmarked from a mathematical and quantitative point of view [2], as it is the case for a numerical fit or for a pseudo-random generator. In particular, the objectives of this work are:

- To define a metrics for quantitative assessments of wine evaluations, including the implementation of the existing correlations between the variables expressing the organoleptic characteristics of the wine.
- To benchmark the performance of the metrics by analysing the statistical distributions of the results it produces on a sample of over 100 wines.
- To understand the nature and the mathematical meaning of the interaction of the "observer" (human evaluating the wine subjectively) with the system represented by the sample of wines being "measured".

A proper wine evaluation represents a multidimensional system [3], involving dependencies between different variables. Consequently the occurrence of the evaluations' results can be expressed by conditional probability relations.

The corresponding equations are derived by modelling and renormalizing the probabilities according to the correlations.

1 Definitions

Let us define Q to be the scalar expressing the overall quality score of a wine and let us define it to assume the following values:

$$Q = [0.1; 0.2; 0.3; 0.4; 0.5; 0.6; 0.7; 0.8; 0.9; 1.0; 1^{*}; 1^{**}; 1^{***}]$$

The range of Q can also be transformed to an integers' space: $Q = [-9; +3]$.

Let us define α, ϕ, π as three independent dimensions in the evaluation of wine characteristics, representing the following:

α … Architecture; ϕ … Finesse; π … Power

Each dimension holds two correlated signed directions and operators, identified as $<$ (left), and as $>$ (right), representing and valuing the specific organoleptic features (variables) of the wine:

	$<$	$>$
α	Structured, Complex	Equilibrated, Harmonious
ϕ	Sec, Dry	Fine, Aged
π	Sensory, Intense	Bodied, Full

SNE 13/3-4, December 2007009

< \ >	1	0	-1	-2	-3
1		ok			
0	ok	ok	ok	ok	ok
-1		ok	ok	ok	
-2		ok	ok		
-3		ok			

Table 1. Operators correlation: matrix of allowed "< left operator" values for each "> right operator value" (and vice versa).

Let us define each operator to apply the values:

$[+1; 0; -1; -2; -3]$, also noted as [*; *id*; -; --; ---]

with the constraints defined by the correlations/vetoes set in Table 1. These also imply that the sum of the left/right operators on each dimension is contained in the range $[-3\,;\,+1]$. (Note: the notations "0" or "*id*" represent the identity operator).

2 Metrics

The wine organoleptic features can thus be treated as eigenstates with discrete eigenvalues to quantitatively measure their quality. For example, the $< \pi$ characteristics of a wine can map the incremental values in their range $[-3; +1]$ to the usual scale of adjectives used in Oenology: "weak", "short", "light", "sensory", "intense". The same approach is valid for the other defined organoleptic variables and related operators' values (the complete "dictionary" is included in the Appendix). The defined wine evaluation procedure can be interpreted via a tasting operator bringing the wine system into the eigenstates corresponding to the wine organoleptic characteristics (the eigenvalues giving a measure for their quality), and with the eigenvalues of a given state putting limits to the possible outcomes of the measurements on the coupled observable.

The constraints on the operator values applied to each dimension allow a discretized sampling of the correlation existing between pairs of organoleptic features of the wine: for example, considering the submatrix $[0, -3] \times [0, -3]$ in Table 1 and in the Appendix for the case of the α dimension, it is evident how a very structured wine has more channels open to be unbalanced (to different extents) than a monotonic wine has; similarly, in the π dimension, a high alcohol content poses a more severe challenge to the wine body than what can be the case for lighter wines. A special case is given by the $+1$ values of the operators, for which a 0 of the coupled operator is required (excellence on one side requires the highest constraint from the other side). The recognition of correlations between variables is essential to avoid biases (e.g. accumulation points with respect to the average due to empty regions in the allowed phase space) in the data distribution estimators. Hence any multi-variable wine evaluation form [4] should be tested statistically by checking in these terms the results it produces.

As a consequence of the definitions seen previously and of the exclusion rules in Table 1, each of the three α, ϕ, π dimensions can assume all (and only all) the following 12 patterns:

[*X; X*; X; -X; X-; -X-; --X; X--; --X-; -X--; ---X; X---]

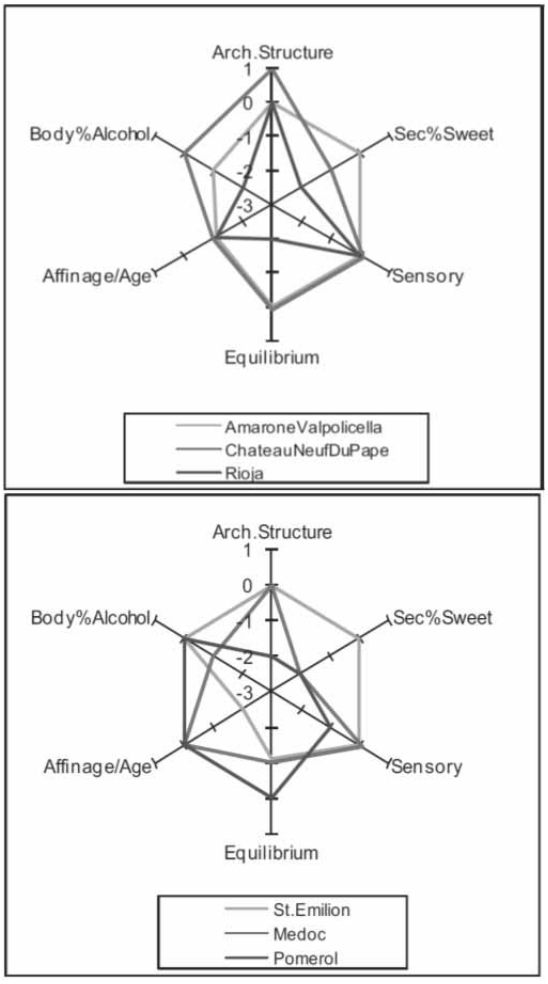

Figure 1. Graphical notation: charts comparing tasted wines belonging to different 'appellations'. The 3 axis represent independent dimensions for wine evaluation. The organoleptic characteristics, which are on the opposite directions of each axis, are anticorrelated.

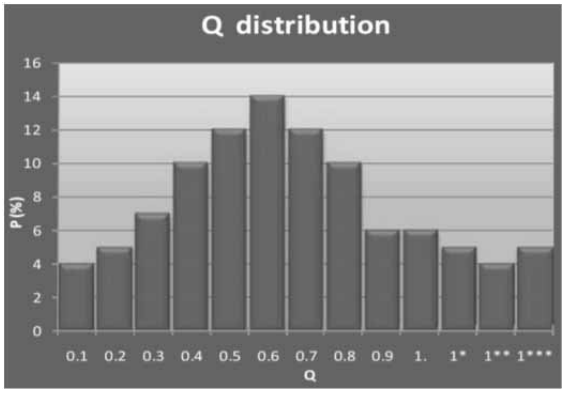

Figure 2. Q probability distribution.

Therefore the total number of allowed combinations supported by the metrics for expressing a wine evaluation is: $12^3 = 1728$.

The sum/combination of the six operators on the three α, ϕ, π dimensions is contained in the range $[-9\,;\,+3]$ and it coincides numerically with the Q value, thus binding a scalar measure to the underlying multidimensional wine system. Examples:

$Q = 0.7$ [*α -ϕ-- π-] $Q = 0.1$ [α--- ---ϕ --π-]

$Q = 1^{***}$ [α* *ϕ π*]

Such algebraic notation of the kind $[_i\alpha_j\ _i\phi_j\ _i\pi_j]$ maps directly to standard graphical representations, of which some examples are shown in Figure 1.

3 Metrics benchmarks

Q is distributed within a range of 13 values. The probability distribution of the Q scalar has been computed on a sample of 109 wines tasting [5] and is shown in Figure 2. It is observed that the peak and the median of the distribution are left-shifted with respect to the centre of the range.

The Q value histogrammed for these 109 degustations is not statistically compatible with a flat random distribution, but it rather seems to follow a combinatorial distribution. The probability P of the empiric Q values could not possibly be constant; in fact~~s~~ if $P(Q) = \text{const}$, then $P(Q) = 7.7\%$ for all Q values (range of 13 values); in such a case, also $P(Q = +3) = 7.7\%$; but $P(Q = +3) = 8 \cdot P(^*X)3$ (because there are 8 possible permutations for all the three dimensions to be in the status *X or X* to give $Q = 1^{***}$).

Q	Integer Q	Configurations (out of 1728)	Relative frequency
0.1	-9	64	3.7%
0.2	-8	144	8.3%
0.3	-7	204	11.8%
0.4	-6	219	12.7%
0.5	-5	270	15.6%
0.6	-4	255	14.8%
0.7	-3	206	11.9%
0.8	-2	144	8.2%
0.9	-1	114	6.6%
1.0	0	61	3.5%
1*	1	30	1.7%
1**	2	12	0.7%
1***	3	8	0.5%

Table 2. Theoretical Q distribution in case $12 \times 12 \times 12 = 1728$ α, ϕ, π configurations would have the same probability to occur.

The solution of that equation gives $P(^*) \approx 21.5\%$ (which would bring *X and X* together to hold about 43% of the total P), i.e. an absurd requirement on the allowed operator patterns.

The mean of the distribution result to be more probable. This may be for combinatorial reasons or it may be intrinsic in the wine subjective taste (it is evident that the extremes of the range represent exceptional cases, good or bad, while the central values represent more normal situations). In any case, one could even consider Q as the independent variable in a wine assessment (evaluated first), and α, ϕ, π could be constrained consequently: however, Q being a scalar, and the wine evaluation being a multidimensional problem involving different wine characteristics [6], it is implied that any value assigned to Q "averages" anyway over the different wine variables during the tasting; i.e. the same value of Q can derive from different wines configurations. Hence the Q distribution is expected to hold always a strong combinatorial component.

In fact~~s~~, it has been seen how a wine evaluation is expressed by the configuration obtained by the valued operators applied on all the α, ϕ, π dimensions (e.g. [*α -ϕ-- π-]); it has also been mentioned that since each dimension can assume 12 patterns independently from the others, it follows that the metrics can support $12 \times 12 \times 12 = 1728$ configurations, i.e. 1728 different combinations.

Consequently, if the 12 patterns of operators allowed on each dimension would have the same probability to occur, then all 1728 configurations would have the same probability to occur (by product of probabilities), and it would be possible to predict and compute theoretically the Q distribution: the probability of each Q value would depend on the number of α, ϕ, π configurations leading to that value in the $[-9, +3]$ range. Such a computation leads to the results shown in Table 2.

The qualitative agreement of these results with the shape, the maxima, and the asymptotic minima of the empirical Q distribution in Figure 1 appears to confirm the underlying combinatorial nature of the system: also the left shift of the peak with respect to the range middle-point is evident. On the other hand, the significant quantitative differences of the distributions (the median of the data in Table 2 is shifted towards lower values with respect to the median of the empirical Q distribution, and their right-end tail is shorter and lower) confirm that the 1728 α, ϕ, π configurations seem to be not-equiprobable, hence the 12 operator patterns on each α, ϕ, π dimension would not be equiprobable.

In summary:

- There is evidence for the signature of the combinatorial nature underlying the Q metrics.
- The 1728 configurations appear to be not-equiprobable, hence the 12 patterns of possible operators per dimension would not have the same probability to occur.

In facts, it has been found that the Q distribution is peaked and has median at values lower than the middle of the Q range, however such shifts are smaller than what required by an equiprobable operators $P({}_iX_j)$ distribution (thus the Q distribution has a trend towards "better wines"). The crucial question is why the 12 operator patterns are not equiprobable (i.e. why there is such a trend on Q):

1. It is conceivable that the metrics is not centred in the phase space, and that de-facto it behaves like a decimal system plus degenerated solutions above $Q = 1$.
2. It is conceivable that the analysed wines sample is not fully random, and that with an infinite random sample $P({}_iX_j)$ will be flat and $P(Q_k)$ will be fully combinatorial.

Q mean	0.1	0.2	0.3	0.4	0.5	0.6	0.7	0.8	0.9	1.	1*	1**	1***
M types	1	3	7	7	4	8	6	4	4	4	1	0	0
N wines	1	5	10	10	8	21	10	9	18	15	2	0	0

Table 3. Distribution of the mean Q values obtained for the different types (appellation, denominazione) of wine. Multiplicity of tasted wines summed for all types falling in each Q-mean bin. The median is at the 2nd entry of the bin 0.6.

In addition, the role of the observer in the wine tasting operation has to be considered.

4 Data analysis and interpretation

In order to answer the questions raised in the previous section, it is convenient to analyse the results of the wine evaluations for each wine type ("appellation", e.g. AOC in France; or "denominazione", e.g. DOCG in Italy): it is legitimate to assume that different wine types do not need to produce identical Q distributions from the sets of wines they include in the various "appellations" and "denominazioni"; hence, the average of the Q values obtained from the wines of each "appellation" and "denominazione" is taken to represent the relative wine type; the obtained averages are histogrammed (one Q mean value for each wine type) as function of Q_k bin.

The list of wine types used in the sample of 109 wines [5] tasted for this analysis is expected to represent a rather standard sample, not too dependent on the observer's preferences, and it is expected to follow a distribution representative of the overall Q distribution; this allows the study of the weight, in terms of wines multiplicity M, found for each "appellation" or "denominazione" and, ultimately, given to each bin or sub-range of Q values. Table 3 shows the distribution of the mean Q values and shows that its median is comprised between 0.55 and 0.60; moreover it shows that 37% of the total 109 wines are belonging to the wine types before the median (Q mean value lower than the median), while 63% are belonging to the wine types after the median (Q mean value greater than the median).

Therefore the sample of 109 wines is not uniform and its distribution represents the observer's trend to interact with wines closer to his taste. It is noted that the insight given by this kind of analysis allows equalization options a posteriori for the wine sampling, otherwise very unlikely to be realized [2].

Q	Equi-P	Ntypes-P	Exp-P
0.1	3.7%	2.0%	4.0%
0.2	8.3%	6.1%	5.0%
0.3	11.8%	14.3%	7.0%
0.4	12.7%	14.3%	10.0%
0.5	15.6%	8.2%	12.0%
0.6	14.8%	16.3%	14.0%
0.7	11.9%	12.2%	12.0%
0.8	8.2%	8.2%	10.0%
0.9	6.6%	8.2%	6.0%
1.0	3.5%	8.2%	6.0%
1*	1.7%	2.0%	5.0%
1**	0.7%	0.0%	4.0%
1***	0.5%	0.0%	5.0%

Table 4. Comparison of the distributions of, respectively: Q for equi-probable 1728 α, ϕ, π configurations, Q mean for the wine types, and the experimental Q on all wines.

In facts, every observer is faced not only with an extremely large spectrum of wines and related characteristics [3], but also with a remarkably large variance of wine performance for his taste as function of how many years after vintage the very same wine is tasted.

However, the most important result of this analysis is derived from the comparison of the distributions of, respectively, the mean Q value per wine type, the overall empirical Q on all wines (from Figure 2), and Q for the full combinatorial case (i.e. equiprobability of the 12 operator patterns). The relevant data are shown in Table 4.

In facts, straightforward fits to the data tabulated above, as shown in Figure 3, show that the Q mean distribution on all considered wine types ("appellations", "denominazioni") tends closely to the full combinatorial case (the differences are explainable as residual observer's neglecting of not favourite or known wine types), consistently with the hypothesis of a more truly random sample.

It is concluded that:

- The shape of the scalar Q probability distribution is quantitatively determined by a pure combinatorial effect (due to the binding to a 6-dimensional system), superimposed by an observer's specific and not constant probability distribution of the 12 allowed operators patterns on each dimension, which represents a trend to taste (and consequently to include in the analysis sample) favourite wines.

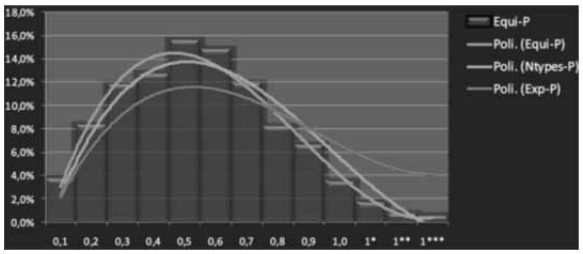

Figure 3. Comparison of the 3rd order polynomial fits to the distributions of, respectively: Q for equi-probable 1728 α, ϕ, π configurations, Q mean for the wine types, and the experimental Q on all wines. The data show that the distribution of Q mean on the sampled types of wine tends towards the fully combinatorial case (though a small trend remains to test types of wine which one knows better or is more likely to appreciate positively).

- Such an observer's interference, with respect to a neutral random sampling of the wines to be evaluated by the metrics, has to be measured and characterised.
- Due to the required modelling of the correlations between pairs of the 6 dimensions of the wine system, the metrics is intrinsically unbiased in the phase space of the wine evaluations measurements (in facts, the case of wines total sampling with large statistics tends to the pure combinatorial condition, i.e. to the equiprobability of the allowed operators patterns on each dimension.

The observer-specific probability distribution derived (using the sample of 109 wine evaluations [5]) for the 12 different patterns of possible operators per dimension (α, ϕ, π) is tabulated in Table 5 and plotted in Figure 4.

P%	*	id	-	-,-	--	--,-	---
$< \alpha$	7,3	16,5	12,8	10,1	8,3	3,7	2,8
$> \alpha$	6,4	16,5	14,7	10,1	7,3	6,4	3,7
$< \phi$	8,3	19,3	11,9	8,3	6,4	6,4	4,6
$> \phi$	4,6	19,3	15,6	8,3	7,3	4,6	2,8
$< \pi$	8,3	19,3	13,8	11,0	6,4	5,5	2,8
$> \pi$	5,5	19,3	13,8	11,0	7,3	3,7	2,8
Mean	6,7	18,3	13,8	9,8	7,2	5,0	3,2
Fluct	2,6	4,3	3,7	3,1	2,7	2,2	1,8

Table 5. Probability distribution of the absolute valued configurations that can result for α, ϕ, π. For X= α, ϕ, π, the notation used for the operators' values in the table header means the following: *X, X, -X, -X-, --X, --X-, ---X for the left operator <X ; and X*, X, X-, -X-, X--, -X--, X--- for the right operator X> .

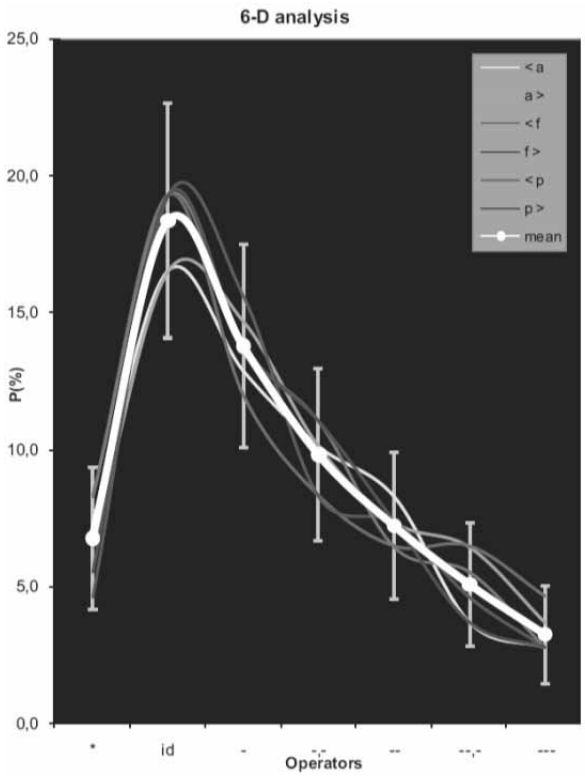

Figure 4. Trend lines relative to the observer-specific probability distributions for the allowed operators' patterns per dimension (α, ϕ, π), as tabulated in Table 5. The mean distribution (white thick line) represents the calibration function for the interaction of the observer with the benchmarking of the wine evaluation metrics.

Such a distribution is sampled 6 times via the organoleptic variables associated to α, ϕ, π (left and right operators) and obtained as their average, showing a consistent functional dependence. It should be noted that the average function shown in Figure 4 refers to operators patterns in abscissa for which a symmetric counterpart exists (except for X and -X-): these should be taken into account for computing correctly the total probability normalization. It is also noted that those probability distributions fluctuate about twice less than what allowed by a Poissonian statistics (computed for reference in the line fluct of Table 5), consistently with the systematic boundary conditions they have to obey to.

The white trend-line in Figure 4, relative to the averaged (mean) data distribution, is the calibration function for the observer's interaction with the wine evaluation metrics benchmarking.

P	*****	**id**	**-**	**--**	**---**
Mean	6.7%	49.2%	28.6%	12.2%	3.2%

Table 6. Mean probability distribution of an operator value to appear at a given side of a variable, regardless (i.e. integrating probabilities) what happens on the opposite side of the variable.

As mentioned previously, the analysis of the non-uniformity of the probability distribution in Table 5 or Figure 4 (equivalent to shifting the Q distribution away from the pure combinatorial shape) provides useful feedback on the sample of the selected wines from a statistical point of view: for example, it might indicate that the wines sample used has an average quality superior/inferior (for the observer) to a world-wide random selection [6].

Finally, questions such as why patterns like -X- vs. --X (and -X-- vs. X---) have different probability to occur, despite they contribute with the same number of minuses to the overall score for a wine, will be addressed in the following section: this is due to the inherent combinatory triggered by the particular correlation matrix defined.

5 Probability modelling

At the level of research interest, it remains to be studied the direct effect determined by the organoleptic variables correlations onto the probabilities of occurrence for the values applied by the left and right operators on the same α, ϕ, π dimension. This means analysing the probability of finding any of the values $+1, 0, -1, -2, -3$ (or *, id, -, --, ---) on a given side of α, ϕ, π, regardless what is present on the opposite side of each variable α, ϕ, π: such a probability can be expressed as $P(i)$, with $i = +1, 0, -1, -2, -3$ (or i = *, id, -, --, ---). Hence by construction the following formula holds:

$$P(i) = \sum_j P({}_iX_j) = \sum_j P(i \,\&\, j)$$

where: $X = \alpha, \phi, \pi$; $i, j = +1, 0, -1, -2, -3$; and & stands for the logical AND.

By scanning the same sample of 109 wine evaluations [5] analysed so far, the $P(i)$ distributions for the various dimensions are obtained empirically; they represent the probability distributions of valued operators applied to "a" side of α, ϕ, π. By averaging the results from all dimensions, the following data are produced and recorded in Table 6.

If there would be no correlations between the values $+1,0,-1,-2,-3$ obtainable on the two sides of a given α, ϕ, π variable, the probability P of finding the patterns *X, X, -X, -X-, --X, --X-, ---X (and of course their symmetric cases) during the wines evaluation would be given by the products of the probabilities seen in Table 6.

The resulting probability distributions for the configurations listed above already show that the probability of patterns such as -X- vs. X-- (and -X-- vs. X---) is not necessarily identical (just for combinatorial reasons); in fact, the following numbers would be found, apart from a constant multiplicative term of renormalization of the total probability:

$$P(\text{*X}) = P(\text{X*}) = 6.7\% \cdot 49.2\% = 3.3\%$$
$$P(\text{X}) = 49.2\% \cdot 49.2\% = 24.2\%$$
$$P(\text{-X}) = P(\text{X-}) = 28.6\% \cdot 49.2\% = 14.1\%$$
$$P(\text{-X-}) = P(\text{-X-}) = 28.6\% \cdot 28.6\% = 8.2\%$$
$$P(\text{--X}) = P(\text{X--}) = 12.2\% \cdot 49.2\% = 6.0\%$$
$$P(\text{--X-}) = P(\text{-X--}) = 12.2\% \cdot 28.6\% = 3.5\%$$
$$P(\text{---X}) = P(\text{X---}) = 3.2\% \cdot 49.2\% = 1.6\%$$

The most interesting challenge introducing the correlations comes from the difficulty that one gets an under-determined system, when trying to derive mathematically the probability of the 12 operator patterns on the three dimensions by using the empirical knowledge of the $P(i)$ recorded in Table 6: in facts the matrix in Table 1 does not contain the sufficient information.

Therefore it is necessary to develop a model to express the results via conditional probabilities:

$$P(\text{*X}) = P(\text{* \& } id) = P(id) \cdot P(\text{* } | \text{ } id);$$
$$P(\text{--X-}) = P(\text{-- \& -}) = P(\text{-}) \cdot P(\text{-- } | \text{ -}); \text{ etc.}$$

In the present work, it is proposed to use a first order expansion of the probabilities renormalizations due to the exclusion constraints by Table 1. This gives the following results (which are compared below vs. the mean data of Table 5, reported in the right-aligned brackets):

$$P(\text{*X}) = P(\text{* \& } id) = P(\text{*}) \cdot P(id) \cdot [1 - P(\text{*}) - P(\text{-}) - P(\text{--}) - P(\text{---})]^{-1} \cdot 1 = 6.70\% \quad (\text{vs. } 6.70\%)$$
$$P(\text{ X }) = P(id \text{ \& } id) = P(id) \cdot P(id) \cdot [1 - P(\text{*}) - P(\text{---})] \cdot [1 - P(\text{*}) - P(\text{---})] = 19.62\% \quad (\text{vs. } 18.35\%)$$
$$P(\text{-X}) = P(\text{- \& } id) = P(\text{-}) \cdot P(id) \cdot [1 - P(\text{*}) - P(\text{---})] \cdot [1 - P(\text{*}) - P(\text{---})]^{-1} = 14.07\% \quad (\text{vs. } 13.76\%)$$
$$P(\text{-X-}) = P(\text{- \& -}) = P(\text{-}) \cdot P(\text{-}) \cdot [1 - P(\text{*}) - P(\text{---})]^{-1} \cdot [1 - P(\text{*}) - P(\text{---})]^{-1} = 10.09\% \quad (\text{vs. } 9.82\%)$$
$$P(\text{--X}) = P(\text{-- \& } id) = P(\text{--}) \cdot P(id) \cdot [1 - P(\text{*}) - P(\text{---})] \cdot [1 - P(\text{*}) - P(\text{--}) - P(\text{---})]^{-1} = 6.94\% \quad (\text{vs. } 7.16\%)$$
$$P(\text{--X-}) = P(\text{-- \& -}) = P(\text{--}) \cdot P(\text{-}) \cdot [1 - P(\text{*}) - P(\text{---})]^{-1} \cdot [1 - P(\text{*}) - P(\text{--}) - P(\text{---})]^{-1} = 4.98\% \quad (\text{vs. } 5.05\%)$$
$$P(\text{---X}) = P(\text{--- \& } id) = P(\text{---}) \cdot P(id) \cdot [1 - P(\text{*}) - P(\text{-}) - P(\text{--}) - P(\text{---})]^{-1} \cdot 1 = 3.21\% \quad (\text{vs. } 3.21\%)$$

Such a modelling gives satisfactory results, by matching the empirical mean values of Table 5 with a precision at the level of few percent (and fits the total normalization with a 1.5% precision, which is of the same order of magnitude as the numerical rounding and error propagation derived from the empiric data, which is for example 0.7% on the total normalization for the mean data in Table 5).

6 Conclusions

The essential organoleptic characteristics assessed in the wine evaluation process have been formalized via a scalar quality metrics associated and bound to 3 dimensions and 6 variables.

The mathematical modelling of the existing correlations between the variables expressing such organoleptic features has been proven to play a key role in the performance of any wine quality metrics.

Consequently, a dedicated algebraic notation has been developed to express the multi-dimensional nature of the wine quality and to provide a suitable measurement tool. The use of an equivalent graphical notation has also been demonstrated.

The statistical distribution of the scalar wine-quality measure is quantitatively determined by a pure combinatorial effect (due to the binding to a 6-dimensional system), superimposed by the effect of an observer's specific sampling of the wines phase space.

The mathematical meaning of the interaction of the "observer" (human evaluating the wine subjectively) with the system represented by the sample of wines being "measured" has been quantified and calibrated.

The relation between the independent and correlated quantities in the evaluation of the wines has been formalized via a conditional probability model, which has been shown to be precise at the few percent level.

Appendix

A complete mapping of the operators' values on α, ϕ, π to a standard scale of adjectives used in Oenology is included in the following "dictionary":

			α---: aciadic	
		-α--: less structured, not equilibrated	α--: saturating	
	--α-: not structured, less equilibrated	-α-: less structured, less equilibrated	α-: unbalanced	
---α: flat	--α: monotonic	-α: simple	α: structured, equilibrated	*α: complex
			α*: harmonious	

			ϕ---: sour	
		-ϕ--: less sec, not fined	ϕ--: tannic	
	--ϕ-: not sec, less fined	-ϕ-: less sec, less fined	ϕ-: bitter	
---π: flabby	--π: mellow	-π: rounded	π: sec, fined	*π: dry
			π*: aged	

			ϕ---: syrupy	
		-ϕ--: less sensory, not bodied	ϕ--: alcoholic	
	--ϕ-: not sensory, less bodied	-ϕ-: less sensory, less bodied	ϕ-: thin	
---ϕ: weak	--ϕ: short	-ϕ: light	ϕ: sensory, bodied	*ϕ: intense
			ϕ*: full	

References

[1] C. G. Raptis, C. I. Siettos. *Classification of aged wines distillates using fuzzy and neural network systems*. Journal of Food Engineering, Elsevier Science, 2000, volume: 46 issue: 4, 267-275.

[2] S. De Marchi. *Some mathematics in the wine*: *Part I*. MathematicaMente, Mathesis, Verona, 2007, numero: 113.

[3] R. S. Jackson. *Wine tasting: a professional handbook*. Food Science and Technology – International Series, Academic Press, 2002.

[4] R. Garr. *Wine tasting 101*. Cliffwood Organic Works, 2008

[5] S. Giani. *The wines' records data file*. Sixth International Vienna Conference on Mathematical Modelling, MathMod '09, Vienna, 2009 – Appendix to oral presentation.

[6] F. Guatteri, C. Morondo. *La degustazione del vino*. Eds. Gribaudo, Cuneo, 2005.

Corresponding author: S. Giani,
CERN, PH Dpt.
Geneva 23, CH-1211, Switzerland; *Simone.Giani@cern.ch*

Received & Accepted: MATHMOD 2009
Revised: September 15, 2009
Accepted: October 10, 2009

Modelling of Heat Transfer Processes with Compartment/Population Balance Model

Z. Süle, B.G. Lakatos, Cs. Mihálykó, University of Pannonia, Veszprém, Hungary

SNE Simulation Notes Europe SNE 19(3-4), 2009, 25-32, doi: 10.11128/sne.19.tn.09945

A compartment/population balance model is presented for describing heat transfer in gas-solid fluidized bed heat exchangers, modelling the particle-particle and particle-surface heat transfers by collisions. The results of numerical experimentation, obtained by means of a second order moment equation model indicate that the model can be used efficiently for analysing fluidised bed heat exchangers recovering heat either by direct particle-fluid heat exchange or indirect tube-in-bed operation mode. The population balance model is validated with physically measured data taken from the literature [6].

SNE 19/3-4, December 2009

Introduction

Fluidised bed heat exchangers, widely used in the metallurgical and process industries are important tools for recovering heat from hot solid particles [1-7]. In these systems heat exchange with the wall usually is modelled by means of suspension-wall heat transfer coefficients which, in principle, are aggregates of two transfer components: gas-wall and particle-wall heat transfers.

However, because of intensive motion of particles, the particle-wall, and also the particle-particle heat transfers are collision induced processes thus it seems to be significant to model these processes by themselves. Using such modelling approach the gas-wall and particle-wall components can be separated that allows understanding the transfer mechanisms involved.

For modelling and simulation of collisional heat transfer processes in gas-solid systems, an Eulerian-Lagrangian approach, with Lagrangian tracking for the particle phase [8-11], and a population balance approach [12-16] have been applied.

The population balance model, involving both the collisional particle-particle and particlewall heat transfers, was extended by Süle *et al*. [17, 18] for describing the spatial distributions of temperatures in deep or long fluidised beds developing a compartment model.

The aim of the paper is to extend the compartment population balance model to describe the heat transfer processes in fluidised bed heat exchangers in which the heat of hot solid particles is used to heat water flowing in tubes immersed in the bed. We apply a two-phase model of gas-solid fluidisation assuming that no bubbles are formed in the bed.

The particle-particle and particle-tube heat transfers are modelled by collisions, while the gasparticle, gas-tube and tube-water heat transfers are described as continuous processes using linear driving forces.

1 Physical model

Consider a shallow fluidised bed in which particles transported horizontally through the bed are fluidised by cross-flow air fed into the system in equally distributed gas streams along the bed. Cold water to be heated is flowing inside a tube immersed in the bed. The fluidising air induces intensive particle-particle and particle-tube collisions, and heat transfer between the gas, particles and water through the wall of the tube.

The assumptions concerning the system are as follows: 1) The particles are of constant size and are not changed during the process; 2) The system is operated under steady state hydrodynamic conditions, and the influence of thermal changes on the hydrodynamics is negligible. 3) There is no heat source inside the particles. 4) The heat transfer by radiation is negligible.

The structure of the compartments, as well as of the mass and heat flows of the system is shown in Figure 1. In this system the following mass transport processes are distinguished.

1. Volumetric cross-flow q_g of the fluidising gas through the ideally mixed cells between which some crossmixing occurs. The temperature of gas in the k-th cell is denoted by $T_{g,k}$, and there occurs continuous heat transfer between the gas and particles, and the gas and wall, characterised by the heat transfer coefficients h_{gp}, h_{gw}. and h_{wl}, respectively.

SNE 19/3-4, December 2009

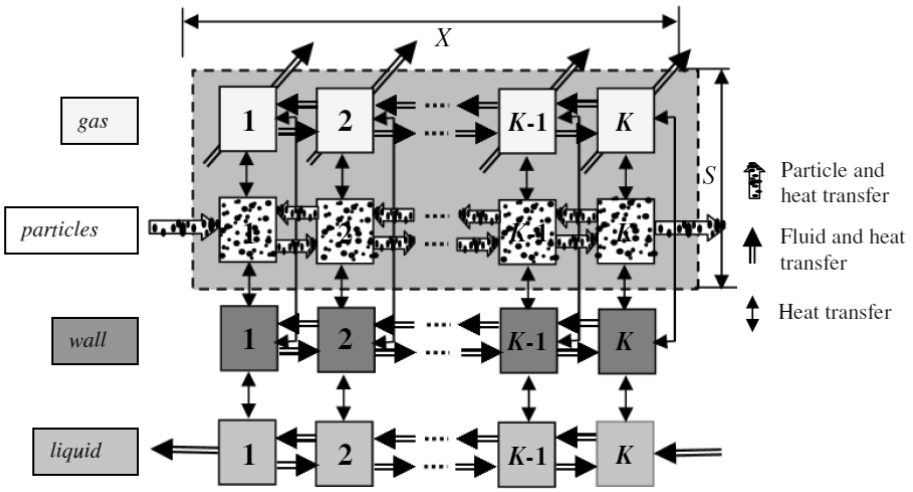

Figure 1 :the scheme of the system.

2. Dispersed plug flow of particles through the bed modelled by the cells-in-series with back-flow model. Here, $n_k(T_p,t)$ denote the population density function for the k^{th} cell by means of which $n_k(T_p,t)\,dT_p$ provides the number of particles from the interval $(T_p,\ T_p+dT_p)$ in a unit volume of the cell at time t. Inter-particle heat transfer occurs by collisions, and is described by the random variable $\Omega_{pp}\in[0,1]$ with probability density function f_{pp}, while the particle-wall heat transfer also occurs by collisions that are characterised by the random variable with probability density function f_{pw}.
3. The heat in the wall of the tube is transported by conduction, and the continuous wall-liquid heat transfer is characterised by the heat transfer coefficient h_{wl}.
4. The volumetric flow q_l of water inside the tube is modelled also by the cells-in-series with back-flow model. It is assumed to be counter-current one with respect to the volumetric flow of particles.

In the present model, as it is illustrated in Figure 1, all compartments (cells) describing the shallow fluidised bed are of the same volume V_k, while, for the sake of computational simplicity, the number of discrete elements of the tube wall and of the cells of model of flowing liquid, although their volumes are quiet different, are the same as that of the bed compartments along the axial direction x.

2 Mathematical model

Under these conditions, the mathematical model of the heat transfer processes of the system is formed by a mixed set of partial integral-differential, partial differential and ordinary differential equations.

The population balance equation, which governs the variation of the population density function of particle population in the individual cells, is a partial integral-differential equation and can be written as

$$\begin{aligned}&\frac{\partial}{\partial t}n_k(T_p,t)+\frac{a_{gp}h_{gp}}{c_pm_p}\frac{\partial}{\partial T_p}\left[(T_{g;k}(t)-T_p)n_k(T_p,t)\right]\\&=\frac{(1+S_kR_p)q_p}{V_k}n_{k-1}(T_p,t)+\frac{S_{k+1}R_pq_p}{V_k}n_{k+1}(T_p,t)\\&\quad-\frac{(1+Z_kR_p)q_p}{V_k}n_k(T_p,t)-S_{pw}n_k(T_p,t)\\&\quad+S_{pw}\int_0^1 n_k\left(T_p-\frac{p_w\omega_{pw}T_{w;k}}{1-p_w\omega_{pw}},t\right)\frac{f_{pw}(\omega_{pw})}{1-p_w\omega_{pw}}d\omega_{pw}\\&\quad-S_{pp}n_k(T_p,t)+\frac{2S_{pp}}{M_{0;k}}\int_{T_{p;min}}^{T_{p;max}}\int_0^1\frac{f_{pp}(\omega_{pp})}{\omega_{pp}}\times\\&\qquad\times n_k\left(\frac{2(T_p-\tau)}{\omega_{pp}}+\tau,t\right)n_k(\tau,t)\,d\omega_{pp}\,d\tau\\&k=1,2,\dots,K,\ \tau>0\end{aligned}\qquad(1)$$

where the variables

$$\omega_{pp}:=1-\exp\left[-\frac{2h_{pp}a_{pp}\theta_{pp}}{m_pc_p}\right],\text{ and}$$

$$\omega_{pw}:=1-\exp\left[-\frac{h_{pw}a_{pw}\theta_{pw}(m_pc_pm_wc_w)}{m_pc_pm_wc_w}\right]\qquad(2)$$

represent the realizations of the random variables Ω_{pp} and Ω_{pw} which express, in principle, the efficiencies of the collisional particle-particle and particle-tube wall heat transfers [16].

Here, a_{gp}, a_{pp} and a_{pw} denote, respectively, the gas-particle, particle-particle and particle-wall contact area, while θ_{pp} and θ_{pw} denote the corresponding contact times. Parameter p_w expresses the ratio of thermal properties of particles and the wall, while parameters S_l and Z_l were introduced for characterising the compartmental structure of the system in a compact way where: $S_1 = 0,\ S_K = 1,\ Z_1 = Z_K = 1,$ $S_l = 1, Z_l = 2, l = 2 \dots, K-1.$

The first term on the left hand side of Eq.(1) denotes the rate of accumulation of particles having temperature $(T_p, T_p + dT_p)$, while the second term describes the change of the number of particles with temperature $(T_p, T_p + dT_p)$ due to the gas-particle heat transfer. The first three terms on the right hand side represent the input and output rates of particles from and to the neighbouring cells, as well as to and from the system, the next two terms describe the variation of the population density function due to the collisional particle-tube wall heat transfer, while the last two terms describe the change of $n_k(T_p, t)$ because of the collisional heat exchange between the particles.

The heat balance equations for the temperature of fluidising gas in the individual cells become

$$\begin{aligned}\frac{d}{dt}T_{g,1}(t) = {} & \frac{q_{g,1}}{\varepsilon_1 V_1}T_{g,1,in}(t) - \frac{q_{g,1}}{\varepsilon_1 V_1}T_{g,1}(t) + \\ & + \frac{\varepsilon_2 R_g q}{\varepsilon_1 V_1}T_{g,2}(t) - \frac{\varepsilon_1(1+R_g)q}{\varepsilon_1 V_1}T_{g,1}(t) - \\ & - \frac{a_{gw}h_{gw}}{c_g\rho_g}\int_0^{x_1}\Big(T_{g,1}(t) - T_w(x,t)\Big)\,dx - \\ & - \frac{a_{gw}h_{gw}}{c_g\rho_g}\int_{T_{p,min}}^{T_{p,max}}\big(T_{g,1}(t) - T_p\big)n_1\big(T_p,t\big)dT_p\end{aligned} \tag{3}$$

$$\begin{aligned}\frac{d}{dt}T_{g,k}(t) = {} & \frac{q_{g,k}}{\varepsilon_k V_k}T_{g,k,in}(t) - \frac{q_{g,k}}{\varepsilon_k V_k}T_{g,k}(t) - \\ & - \frac{\varepsilon_{k-1}(1+R_g)q}{\varepsilon_k V_k}T_{g,k-1}(t) + \frac{\varepsilon_{k+1}R_g q}{\varepsilon_k V_k}T_{g,k+1}(t) - \\ & - \frac{\varepsilon_k(1+2R_g)q}{\varepsilon_k V_k}T_{g,k}(t) - \\ & - \frac{a_{gw}h_{gw}}{c_g\rho_g}\int_{x_{k-1}}^{x_k}\Big(T_{g,k}(t) - T_w(x,t)\Big)\,dx - \\ & - \frac{a_{gw}h_{gw}}{c_g\rho_g}\int_{T_{p,min}}^{T_{p,max}}\big(T_{g,k}(t) - T_p\big)n_k\big(T_p,t\big)dT_p\end{aligned} \tag{4}$$

$$\begin{aligned}\frac{d}{dt}T_{g,K}(t) = {} & \frac{q_{g,K}}{\varepsilon_K V_K}T_{g,K,in}(t) - \frac{q_{g,K}}{\varepsilon_K V_K}T_{g,K}(t) - \\ & - \frac{\varepsilon_{K-1}(1+R_g)q}{\varepsilon_K V_K}T_{g,K-1}(t) - \frac{\varepsilon_K(1+R_g)q}{\varepsilon_K V_K}T_{g,K}(t) - \\ & - \frac{a_{gw}h_{gw}}{c_g\rho_g}\int_{x_{K-1}}^{x_K}\Big(T_{g,K}(t) - T_w(x,t)\Big)\,dx - \\ & - \frac{a_{gw}h_{gw}}{c_g\rho_g}\int_{T_{p,min}}^{T_{p,max}}\big(T_{g,K}(t) - T_p\big)n_K\big(T_p,t\big)dT_p\end{aligned} \tag{5}$$

where ε_k denotes the bed voidage in the k-th cell, q stands for the volumetric gas flow between the cells causing some cross-mixing between the neighbour cells, and coefficient h_{gw} represents the gas-wall heat transfer rate.

Since the gas is assumed to be fed into the system equally distributed along the axial coordinate x we can write $\varepsilon_k = const.$ for all $k = 1, \dots, K$.

Heat in the wall of tube is transported with conduction hence the differential equation describing the temperature of the wall can be written in the form

$$\begin{aligned}\frac{\partial}{\partial t}T_w(x,t) = {} & \frac{k_w}{\rho_w c_w}\frac{\partial^2}{\partial x^2}T_w + \\ & + \frac{a_{gw}h_{gw}}{c_w\rho_w}\Big(T_{g,k}(t) - T_w(x,t)\Big) + \\ & + \frac{a_{wl}h_{wl}}{c_w\rho_w}\Big(T_w(x,t) - T_{l,k}(t)\Big) + \\ & + S_{pw}\int_{T_{p,min}}^{T_{p,max}}\int_0^1 p_p\omega_{pw}\Big(T_p - T_w(x,t)\Big)\times \\ & \times\ n_k(T_p,t)f_{pw}\big(\omega_{pw}\big)\,d\omega_{pw}\,dT_p \\ & t > 0,\ x \in [(k-1)\Delta x, k\Delta x],\ k = 1, \dots, K\end{aligned} \tag{6}$$

subject to the boundary conditions

$$\frac{k_w}{\rho_w c_w}\frac{\partial}{\partial x}T_w(x,t)\Big|_{x\in\{0,X\}} = 0 \tag{7}$$

Here, k_w denotes the thermal conductivity of the wall, while the coefficient h_{wl} denotes the wall-liquid heat transfer rate. Parameters a_{gw} and a_{wl} denote the surface area of gas-wall and wall-liquid heat transfers in a unit length of tube.

Finally, the set of differential equations for the temperature of liquid phase compartments is written as

$$\begin{aligned}\frac{d}{dt}T_{l,k}(t) = {} & \frac{S_{k-1}R_l q_l}{V_{l,k}}T_{l,k-1}(t) + \frac{(1+S_k R_l)q_l}{V_{l,k}}T_{l,k+1}(t) \\ & - \frac{(1+Z_k R_l)q_l}{V_{l,k}}T_{l,k}(t) + \\ & + \frac{a_{wl}h_{wl}}{c_l\rho_l}\int_{x_{k-1}}^{x_k}\big(T_w(x,t) - T_{l,k}(t)\big)\,dx\end{aligned} \tag{8}$$

where the values of the S and Z parameters, characterising the structure of the system are: $S_0 = S_K = 0,$ $S_{K+1} = 0, \quad Z_0 = Z_K = 1, \quad S_l = 1, \quad Z_l = 2, \quad l = 1, \dots, K-1.$

The additional boundary conditions to (1) – (8) can be written as

$$n_0(T_p,t) = n_{in}(T_p,t) \text{ and } T_{l,K+1} = T_{l,in} \qquad (9)$$

which, naturally, should be completed with the appropriate initial conditions.

3 Solutions of the model equation

The mixed set of differential equations (1)-(9) was solved by reducing the population balance equation (1) and the heat conduction equation (6) into two sets of ordinary differential equations applying, respectively, a moment equation reduction and a finite difference discretion, obtaining in this way together with the gas phase equations (3)-(5) and liquid phase equation (8) a closed set of ordinary differential equations.

The moments and normalized moments of the temperature of particle population are defined as

$$M_{I;k}(t) = \int_{T_{p,min}}^{T_{p,max}} T_p^I \, n_k(T_p,t)\, dT_p$$
$$m_{I;k}(t) = \frac{M_{I;k}(t)}{M_{0;k}(t)};\ I = 0,\dots,k;\ k = 1,\dots,K \qquad (10)$$

which are useful for the basic characterisation of the temperature distribution of particles. The zero order moments $M_{0;k}$ provide the total numbers of particles in a unit volume of cells by means of which the solids concentrations can also be computed, while the mean temperature of particles in the k-th cell is expressed by $m_{1;k}(t)$.

Completing the zero and first order moments $M_{0;k}$ and $M_{1;k}$ with the second order one $M_{2;k}$, the variance of temperature, defined as

$$\sigma_k^2 = \frac{M_{2;k}}{M_{0;k}} - \left(\frac{M_{1;k}}{M_{0;k}}\right)^2 \qquad (11)$$

can also be computed.

The infinite hierarchy of the moment equations generated by the population balance equation (1) has the form

$$\frac{d}{dt}M_{i;k} = IK_{gp}\left(M_{I-1;k}(t)T_{f;k}(t) - M_{i;k}(t)\right) +$$
$$S_{pp}\left[\frac{1}{M_{0;k}(t)}\sum_{i=0}^{I} M_{i;k}(t)\, M_{i-I;k}(t) b_{i,I}^{(1)} - M_{I;k}(t)\right]$$
$$+ S_{pw}p_1\Big[-M_{I;k}(t) + \sum_{i=0}^{I}\binom{I}{i} b_i^{(2)} \times$$
$$\times \sum_{j=0}^{i}\binom{i}{j}(-1)^{i-j} T_{w;k}^{j} M_{I-j;k}(t)\Big] +$$
$$+ \frac{(1+S_kR_p)q_p}{V} M_{I;k-1}(t) + \frac{R_pq_p}{V} M_{I;k+1}(t) -$$
$$- \frac{(1+Z_kR_p)q_p}{V} M_{I;k} \quad I = 0,1,\dots \qquad (12)$$

where

$$b_{i,I}^{(pp)} = \int_0^1 \binom{I}{i}\left(\frac{\omega_{pp}}{2}\right)^2 \left(1-\frac{\omega_{pp}}{2}\right)^{I-i} f_{pp}(\omega_{pp})\, d\omega_{pp}$$
$$\text{and } b_i^{(pw)} = \int_0^1 \omega_{pw}^i\, f_{pw}(\omega_{pw})\, d\omega_{pw} \qquad (13)$$

Since the infinite set of moment equations can be closed at any order, the second order moment equation reduction can be computed exactly by solving the equations for the first three leading moments. This reduction is obtained by using the following equations.

The total number of particles in the k-th cell:

$$\frac{d}{dt}M_{0;k}(t) = \frac{(1+S_kR_p)q_p}{V} M_{0;in}(t) + \frac{R_pq_p}{V} M_{0;k+1}(t)$$
$$- \frac{(1+Z_kR_p)q_p}{V} M_{0;k}(t) \quad k = 1,\dots,K \qquad (14)$$

The first order moment of the particulate phase in the k-th cell:

$$\frac{d}{dt}M_{1;k}(t) = \frac{a_{gp}h_{gp}}{c_g\rho_g}\left(M_{0;k}(t)T_{g;k}(t) - M_{1;k}(t)\right)$$
$$+ S_{pw}p_w b_1^{(2)}\left(M_{0;k}(t)T_{w;k}(t) - M_{1;k}(t)\right) +$$
$$+ \frac{(1+S_kR_p)q_p}{V} M_{1;in}(t) + \frac{R_pq_p}{V} M_{1;k+1}(t) -$$
$$- \frac{(1+Z_kR_p)q_p}{V} M_{1;k}(t), \quad k = 1,\dots,K \qquad (15)$$

The variance of temperature of the particulate phase in the k-th cell:

$$\frac{d}{dt}\sigma_k^2(t) = -\Big[2\frac{a_{gp}h_{gp}}{c_g\rho_g} + S_{pp}b_{1,2}^{(pp)} + S_{pw}p_w\left(2b_1^{(pw)} -\right.$$
$$\left. - p_w b_2^{(pw)}\right) + \frac{q_p}{VM_{0;k}(t)}\left(R_pM_{0;k+1}(t)\right)\Big]\sigma_k^2(t) +$$
$$+ \frac{q_p}{V}\frac{(1+S_kR_p)M_{0;in}(t)}{M_{0;k}(t)}\left(\sigma_{in}^2(t) - \sigma_k^2(t)\right) +$$
$$+ S_{pw}b_2^{(pw)}p_w^2\left(\frac{M_{1;k}(t)}{M_{0;k}(t)} - T_{(w;k)}(t)\right)^2 +$$
$$+ \frac{q_p(1+S_kR_p)M_{0;in}(t)}{VM_{0;k}(t)}\left(\frac{M_{1;in}(t)}{M_{0;in}(t)} - \frac{M_{1;k}(t)}{M_{0;k}(t)}\right)^2 +$$
$$+ \frac{R_pq_pM_{0;k+1}(t)}{VM_{0;k}(t)}\sigma_{k+1}^2(t) +$$
$$+ \frac{R_pq_pM_{0;k+1}(t)}{VM_{0;k}(t)}\left(\frac{M_{1;k+1}(t)}{M_{0;k+1}(t)} - \frac{M_{1;k}(t)}{M_{0;k}(t)}\right)^2 \qquad (15)$$

The set of equations provided with finite difference discretion of the heat conduction equation (6) for the wall has the form:

$$\frac{d}{dt}T_{w,1}(t) = \frac{D_T}{\Delta x^2}\left(T_{w,2}(t) - T_{w,1}(t)\right) - \frac{a_{gw}h_{gw}}{c_w\rho_w}\left(T_{g,1} - T_{w,1}\right) - \frac{a_{wl}h_{wl}}{c_w\rho_w}\left(T_{w,1}(t) - T_{l,1}(t)\right) - S_{pw}\int_{T_{p,min}}^{T_{p,\max}}\int_0^1 p_p\left(T_{w,1}(t) - T_p\right) n_1\left(T_p, t\right) \times \omega_{pw} f_{pw}\left(\omega_{pw}\right) d\omega_{pw}\, dT_p \quad (17)$$

$$\frac{d}{dt}T_{w,k}(t) = \frac{D_T}{\Delta x^2}\left(T_{w,k+1}(t) - 2T_{w,k} + T_{w,k-1}\right) + \frac{a_{gw}h_{gw}}{c_w\rho_w}\left(T_{g,k}(t) - T_{w,k}(t)\right) - \frac{a_{wl}h_{wl}}{c_w\rho_w}\left(T_{w,k}(t) - T_{l,k}(t)\right) - S_{pw}\int_{T_{p,min}}^{T_{p,\max}}\int_0^1 p_p\left(T_{w,k}(t) - T_p\right) n_k\left(T_p, t\right) \times \omega_{pw} f_{pw}\left(\omega_{pw}\right) d\omega_{pw}\, dT_p \quad (18)$$

$$\frac{d}{dt}T_{w,k}(t) = \frac{D_T}{\Delta x^2}\left(T_{w,K}(t) - T_{w,K-1}(t)\right) + \frac{a_{gw}h_{gw}}{c_w\rho_w}\left(T_{g,K}(t) - T_{w,K}(t)\right) - \frac{a_{wl}h_{wl}}{c_w\rho_w}\left(T_{w,K}(t) - T_{l,K}(t)\right) - S_{pw}\int_{T_{p,min}}^{T_{p,\max}}\int_0^1 p_p\left(T_{w,K}(t) - T_p\right) n_K\left(T_p, t\right) \times \omega_{pw} f_{pw}\left(\omega_{pw}\right) d\omega_{pw}\, dT_p \quad (19)$$

so that the integrals of variable x in (3 – 5) for the fluidising gas and (8) for the liquid flowing in the tube are also rewritten for the discrete values $T_{w,k}$, k = 1, 2, …, K.

Finally, because of the second order moment equations reduction (14 – 16), in (3 – 5) for the fluidising gas and (17 – 19) for the wall in finite difference form the integrals of variable T_p have to be changed rewriting these integrals applying the moments of the temperature of particle population:

$$\int_{T_{p,min}}^{T_{p,\max}} \frac{a_{gp}h_{gp}}{c_g\rho_g}\left(T_{g,k}(t) - T_p\right) n_k\left(T_p, t\right) dT_p = \frac{a_{gp}h_{gp}}{c_g\rho g}\left(M_0(t)T_{g;k}(t) - M_{1;k}(t)\right) \quad (20)$$

and

$$\int_{T_{p,min}}^{T_{p,\max}}\int_0^1 p_p\left(T_{w,K} - T_p\right) n_K\, \omega_{pw}\, f_{pw}\, d\omega_{pw}\, dT_p = p_p b_1^{(2)}(M_0(t)T_{w;k}(t) - M_{1;k}(t) \quad (21)$$

4 Simulation results and discussion of the model

A computer program was developed in MATLAB environment for solving the set of ordinary differential equations (3 – 5), (8) and (14 – 19) taking into account all modifications of the integral terms. The program can generate and handle a compartment/moment equations model consisted of cells of arbitrary number, and the resulted set of ordinary differential equations is solved by means of an ode-solver of MATLAB.

The transient and steady state simulation results presented here were obtained for 9 cells using the basic constitutive expressions presented in detail in [16].

The predictions of the second order moment equation reduction model were validated using the experimental data measured in a laboratory shallow fluidized bed heat exchanger published by Pécora and Parise [6].

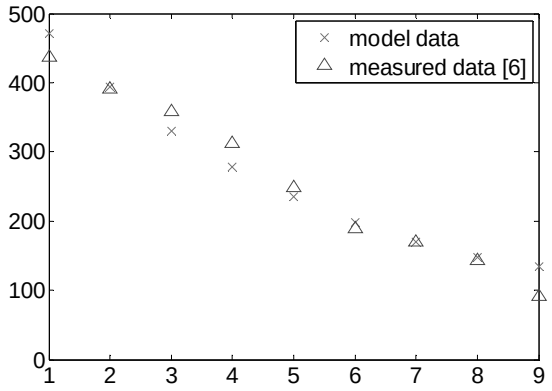

Figure 2. The results of the compartment/population balance model compared with the experimental data by Pécora and Parise [6]

Figures 2 and 3 present the bed temperature profiles for 9 cells comparing the model data with the measured ones [6] when the input temperatures of particles were 650 °C and 708 °C, respectively. The parameters were fitted to the measured values using a least squares method. The results in both cases show rather good correspondence but it has to be taken only as preliminary ones since the heat transfer coefficients have been compared yet.

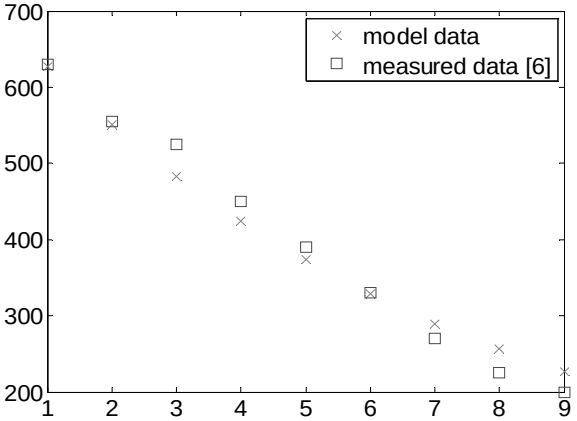

Figure 3. The results of the compartment/population balance model compared with the experimental data by Pécora and Parise [6]

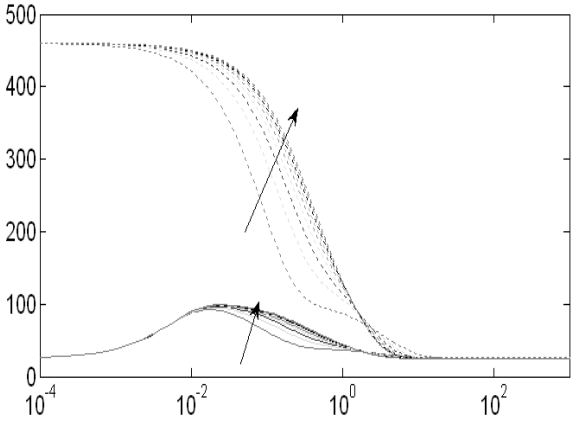

Figure 4. Transients of the mean temperature of particles and the temperature of air in the cells

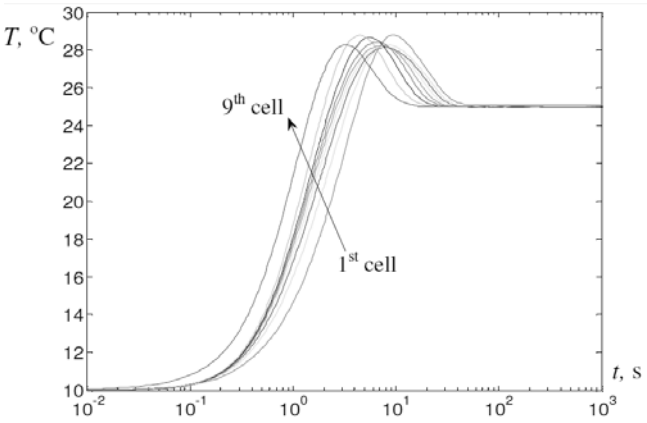

Figure 5. Transients of the temperature of water flowing in the tube

Figure 4 presents the transients of the mean temperature of particles and the temperature of the fluidizing air in the cells along the heat exchanger. It is seen that in steady state these temperatures become almost equal and the heat of hot particles becomes transferred to the cold water.

Under such conditions, the temperature of gas passes a maximum in each cell but delayed to each other in time. Similar maxima can be observed also in the transient processes of the wall and in the temperature of liquid, as it is presented in Figure 5, heated by the hot particles through the tube wall.

Figure 6 shows the variation of the variance of temperature of particle population as a function of time. The temperature of particles at the input was homogeneous but it became strongly distributed during the transient process showing rather large variances.

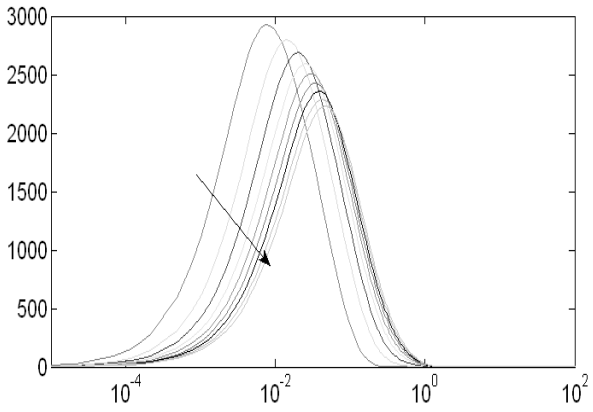

Figure 6. Transients of the variance of temperature of particle population.

The simulation results have shown that the gas-particle and particle-wall heat transfers induce inhomogeneities of the temperature of particles but the particle-particle collision heat transfer shows a strong indirect effect.

5 Conclusions

The compartment/population balance model, developed for describing heat transfer processes in gas-solid fluidized bed heat exchangers, and modelling the particle-particle and particle-surface heat transfer processes by collisions can be used efficiently for analysing the fluidized bed heat exchangers recovering heat from hot particles and heating some liquid flowing in a tube immersed in the bed.

The model describes the temperature distribution of the particle population, and allows separating the effects of the fluidizing gas-immersed surface and particle-immersed surface heat transfers.

The second order moment equation reduction, generated from the population balance equation has proved to be an efficient tool for studying the behaviour of heat exchangers.

Acknowledgements

This work was supported by the Hungarian Scientific Research Fund under Grant K 77955 what is gratefully acknowledged.

	Parameter	Basic value
Solid particles: sand	Diameter, d_p	2.54×10^{-4} m
	Density, ρ	2650 kg m^{-3}
	Specific heat, c_p	835 J kg^{-1} K^{-1}
	Thermal conductivity, k_p	0.35 W m^{-1} K^{-1}
	Volumetric flow rate, q_p	1.5×10^{-5} m^3 s^{-1}
	Mean inlet temperature, m	460
Gas: air	Density, ρ	0.946 kg m^{-3}
	Specific heat, c_g	1010 J kg^{-1} K^{-1}
	Viscosity, μ	2.17×10^{-5} Pa s
	Thermal conductivity, k_g	2.39×10^{-2} W m^{-1} K-1
	Volumetric flow rate, q_g	1.4×10^{-2} m^3 s^{-1}
	Inlet temperature, °C	25
Tube wall: stainless steel	Diameter, D_l	0.0065 m
	Mass, m_w	1.2 kg
	Specific heat, c_w	465 J kg^{-1} K^{-1}
	Thermal conductivity, k_w	44 W m^{-1} K^{-1}
Heated medium: water	Density, ρ_l	998 kg m^{-3}
	Specific heat, c_l	4182 J kg^{-1} K^{-1}
	Thermal conductivity, k_l	0.606 W m^{-1} K^{-1}
	Viscosity, μ_l	10-3 Pa s
	Volumetric flow rate, q_l	1.5 × 10-5 m^3 s^{-1}
	Inlet temperature, °C	25
Fluidized bed	Width, W	0.15 m
	Length, L	0.9 m
	Collision freq., S_{pp}, S_{pw}	103 s^{-1}, 10 s^{-1}
	Heat transfer eff. μ_{pp}, μ_{pw}	0.5, 0.8
Back flow ratio	R_p, R_g, R_l	1, 0.1, 0.01

Table 1. The basic constitutive and process parameters used in simulation

Table of Symbols

a	surface area, m^2
c	specific heat, J kg^{-1} K^{-1}
W	width of the bed, m
D	diameter of the tube, m
D_T	thermal diffusivity, $D_T = k_w/(\rho_w c_w)$, m^2 s^{-1}
f	probability density function
h	heat transfer coefficient, W m^{-2} K^{-1}
k	thermal conductivity, W m^{-1} K^{-1}
m	mass, kg
M_k	k-th order moment of particle temperature
m_k	normalised k-th order moment of particle temperature
n	population density function, no m^{-3} K^{-1}
p_p	parameter in Eq.(1), $p_p = \frac{m_w c_w}{m_p c_p + m_w c_w}$
p_w	parameter in Eq.(1), $p_w = \frac{m_p c_p}{m_p c_p + m_w c_w}$
q	volumetric flow rate, m^3 s^{-1}
R	back-flow ratio
T	temperature, K
t	time, s
V	volume, m^3
x	axial variable, m
θ	contact time, s
ω	random variable of collision heat transfer
μ	viscosity, Pa s
ε	void fraction of the bed
σ^2	variance of the temperature of particle population
ρ	density, kg m^3

Table of subscripts and superscripts

g	gas
in	input
l	liquid
max	maximal value
mf	incipient velocity of fluidisation
min	minimal value
p	particle
gp	gas-particle
pp	particle-particle
pw	particle-wall
w	wall
gw	gas-wall
wl	wall-liquid

References

[1] Elliot D.E. and Holme B.G.: *Fluidized bed heat exchangers*, IChemE, London, UK, 1976.

[2] Rautenbach R. and Katz T.: *Survey of long time behaviour and costs of industrial fluidized bed heat exchangers, Desalination*. 108 (1996) 335.

[3] Rodriguez, O.M.H , Pecora, A.A.B., and. Bizzo, W.A.: *Heat recovery from hot solid particles in a shallow fluidized bed*. Applied Thermal Engineering, 22 (2002) 145-160.

[4] Aghajani, M., Müller-Steinhagen, H., Jamialahmadi, M.: *New design equations for liquid/solid fluidized bed heat exchangers*, Int. J. Heat Mass Transfer, 48 (2005) 317.

[5] Ahn, S.W., Bae S.T., Lee B.C., Kim W.C., Bae M.W., *Fluid flow and heat transfer in fluidized bed vertical shell and tube heat exchanger*. Int. Comm. Heat Mass Transfer, 32 (2005) 224.

[6] Pécora A.A.B. and Parise M.R., *Heat transfer coefficient in a shallow fluidized bed heat exchanger with a continuous flow of solid particles.* Journal of the Brazilian Society of Mechanical Sciences and Engineering, 28 (2006).

[7] Rajan K.S., Srivastava S.N., Pitchumani B., Mahonty B., *Simulation of countercurrent gas-solid heat exchanger: Effect of solid loading ratio and particle size*, Appl. Therm. Eng. 27 (2007) 1345.

[8] Boulet P., Moissette S., Andreaux R., Osterlé B., *Test of an Eulerian–Lagrangian simulation of wall heat transfer in a gas–solid pipe flow*, Int. J. Heat Fluid Flow. 21 (2000) 381.

[9] Mansoori Z., Saffar-Avval M., Basirat-Tabrizi H, Ahmadi G., Lain S., *Thermo-mechanical modeling of turbulent heat transfer in gas-solid flows including particle collisions*, Int. J. Heat Fluid Flow Transfer. 23 (2002) 792.

[10] Chagras V., Osterlé B., Boulet P., *On heat transfer in gas-solid pipe flows: Effects of collision induced alterations on the flow dynamics*, Int. J. Heat Mass Transfer. 48 (2005) 1649.

[11] Mansoori Z., Saffar-Avval M., Basirat-Tabrizi H., Dabir B., Ahmadi G., *Interparticle heat transfer in a riser of gas-solid turbulent flows*, Powder Tech. 159 (2005) 35.

[12] Mihálykó Cs., Lakatos B.G., Blickle T., *Modelling heat transfer between solid particles*, Math. Comp. Simul. 53 (2000) 403.

[13] Mihálykó Cs., Lakatos B.G., Matejdesz A. and Blickle T., *Population balance model for particle-to-particle heat transfer in gas-solid systems*. Int. J. Heat Mass Transfer, 47 (2004) 1325-1334.

Corresponding author: Z. Süle,
University of Pannonia
Dept. Computer Science and Systems Technology
Egyetem u. 10, H-8200 Veszprém, Hungary
sule@dcs.uni-pannon.hu

Received & Accepted: MATHMOD 2009
Revised: September 5, 2009
Accepted: October 10, 2009

TN

Modelling Biochemical Reaction Networks with BIOCHAM Extracting Qualitative and Quantitative Information from the Structure

Sylvain Soliman, INRIA Rocquencourt – Projet CONTRAINTES, France

SNE Simulation Notes Europe SNE 19(3-4), 2009, 33-40, doi: 10.11128/sne.19.tn.09947

Recent advances in Biology have shown that the amount and heterogeneity of the (post-genomic) data now available call for new techniques able to cope with such input and to build high-level models of the complex systems involved [18].

Arguably two key open issues in this emerging area of Computational Systems Biology concern the integration of qualitative and quantitative models and the revision of such integrated models.

The purpose of the Biochemical Abstract Machine (BIOCHAM) modelling environment is to provide formalisms to describe biological mechanisms, including both the studied system and its properties, at different abstraction levels. Based on these formalisms it gives access to a set of tools, mostly focused around model-checking, that help the user in developing, curating, exchanging and refining his models.

In this article we will take as an example invariant computation of the Petri net representing a biological reaction system, and show both a new efficient method for this step, as resolution of a constraint problem, and also how this analysis brings both qualitative and quantitative information on the models, in the form of conservation laws, consistency checking, etc. ranging over all the above defined abstraction levels.

SNE 19/3-4, December 2009

Introduction

Starting from the inspiring use of the π-calculus in [25] to model signaling pathways in a cell, there has been a large amount of work around process calculi and of their stochastic extensions [23, 7] to formalize biochemical interactions. These stochastic versions allowed to link with the usual mathematical biology view of a system of ordinary differential equations (ODEs). However most of these formalisms only bring simulation tools to the modeller. On the other hand, the modelling of gene-regulatory networks through influence graphs along the work of Thomas [30] provided interesting analyses but often impossible to use for post-transcriptional regulation.

The Biochemical Abstract Machine [5] (`http://contraintes.inria.fr/BIOCHAM`) was built as a simplification of the process algebras, using instead a simple rule-based language focused on reactions to describe biological systems. This point of view is shared with all the Systems Biology Markup Language (SBML) [17] community (see for instance databases like `reactome.org`, KEGG [19] or `biomodels.net`) and enables exchanging of models but also, as we shall see, reasoning at different levels on a same model.

BIOCHAM also adds the use of Temporal Logics as a second formalism to encode the expected or observed properties of the system, from a purely qualitative view to a completely quantitative one. This allows to automatically check that the model behaves as specified through model-checking tools adapted to the considered level.

The use of Petri-nets to represent those reaction models, taking into account the difference between compounds and reactions in the graph, and make available various kinds of analyses is quite old [24], however it remains somehow focused towards mostly qualitative and structural properties. Some have been used for module decomposition, like (I/O) T-invariants [13, 14], related to dynamical notions of elementary flux modes [29]. However, there is, to our knowledge, very little use of P-invariant computation, which provides both qualitative information about some notion of module related to the “life cycle” of compounds, and quantitative information related to conservation laws and Jacobian matrix singularity. Conservation law extraction is actually already provided by a few tools, but then using numerical methods, based on the quantitative view of the model, and not integer arithmetic (as in direct P-invariant analysis).

After an illustration of the different views provided for a given reaction model, we present a very simple way to incorporate invariant computation in an existing biological modelling tool, using constraint programming with symmetry detection and breaking. We compare it to other approaches and evaluate it, for the case of P-invariants, on some examples of various sizes, like the MAPK cascade models of [6] and [28]. This experimentation is done through an implementation of the described method in the BIOCHAM modelling environment [3, 11][1] allowing to see the use of invariants for different abstraction levels of the same model, and illustrated on some examples and a few benchmarks.

1 Boolean and bounded views

The simplest view one can have of a system of reactions is purely qualitative and relies on a boolean (presence/absence) semantics. For systems like Kohn's map of the mammalian cell cycle regulation [20], with about 500 compounds and 800 reactions but very little quantitative information, this is the natural level. It is also the choice made in the Pathway Logic of [8].

The parallel with electronic circuits becoming obvious when looking at the drawing of the map, the same tools can be applied with certain success: the reactions define a concurrent transition system on which model-checking allows to verify very efficiently some quite complex properties. For instance, that the original map, as published, does not provide synthesis reactions for all cyclins.

This method can also be turned into a machine learning system where a model not verifying a specification can be automatically revised into one that does [2].

Moreover under simple hypotheses on the possible kinetics of each reaction (and verified by Mass Action Law, Michaelis Menten or Hill kinetics for instance) [10] it is possible to automatically derive the influence graph between compounds from the reaction model. This result linking formally reaction graph and influence graph permits to benefit from the known necessary conditions for multi-stability or oscillations proven in that context, from a reaction network with very little knowledge on the kinetics, and especially no hypothesis of linearity.

This approach is quite complementary with Feinberg's Chemical Reaction Network Theory, which also relies on the reaction graph.

The same kind of view, but with an integer number of compounds, can be applied to smaller models, leading to a Petri-net representation of the system, places corresponding to compounds and transitions to reactions in an immediate way [24]. Once again model-checking can be used to ensure the reachability of some states. This level will be detailed further in Section 3 with invariant computation as a means to extract quantitative as well as qualitative information from the structure of the model.

2 Continuous and Stochastic views

Associating rates or kinetics to each reaction, one can view the system at a stochastic level, with simulation of the corresponding continuous time Markov chain thanks to Gillespie's algorithm(s) and stochastic model-checking.

For efficiency reasons, when the number of compounds considered is big enough, the continuous view of that same system, with ODEs derived automatically from the reactions, is preferred. If the dimension is small enough, mathematical tools like bifurcation theory will bring results about ranges of parameters for which a specific dynamical behavior can be obtained.

In any case, we can use simulations as a basis for continuous model-checking [1, 2] to once again provide automatic verification that the model behaves as specified for either high dimensional systems or for properties outside of the usual scope (e.g. properties about the maximal concentration reached by a transitory peak of the system and its time frame).

Recent works generalizing this model-checking step to constraint-solving allowed us to define a continuous degree of satisfaction of a specification by a model. Using it as a fitness function one can apply state of the art optimization techniques to obtain parameter learning with respect to both qualitative and quantitative information coded as a specification [26]. The same technique also allows to define some new notion of robustness, with respect to a given temporal logic specification.

[1] The most advanced optimizations described in Section 6.3 are currently only available in the Nicotine tool described in that section.

3 Petri-net view of a reaction model

A Petri-net is a bipartite oriented (weighted) graph of transitions, usually represented as square boxes, and places, usually represented as circles, that defines a (actually not only one) transition relation on *markings* of the net, i.e. multisets of tokens associated to places. The relation is defined by *firings* of transitions, i.e. when there are tokens (as many as the weight of the incoming arc) in all pre-places of a transition, they can be consumed and as many tokens as the weight on the outgoing arc are added to each post-place.

The classical Petri-net view of a reaction model is simply to associate biochemical *species to places* and biochemical *reactions to transitions.*

Example 1. *For instance the enzymatic reaction written (in BIOCHAM-like syntax),* $A + E <=> A - E => B + E$ *corresponds to the Petri-net depicted in Figure 1.*

In this Petri-net, starting from a marking with at least one token in A and in E, one can remove one of each to produce one token in A-E (firing of t_1*) and then either remove it to add again one token to A and one to E (firing of* t_{-1}*), or to add one B and one E (firing of* t_2*).*

P (resp. T) invariants are defined, as usual, as vectors V representing a multiset of places (resp. of transitions) such that $V \cdot I = 0$ (resp. $I \cdot V = 0$) where I is the incidence matrix of the Petri net, i.e. I_{ij} is the number of arcs from transition i to place j, minus the number of arcs from place j to transition i. Intuitively, a P-invariant is a multiset representing a weighting of the places and such that any such weighted marking remains invariant by any firing; a T-invariant represents a multiset of firings that will leave invariant any marking (see also Section 5).

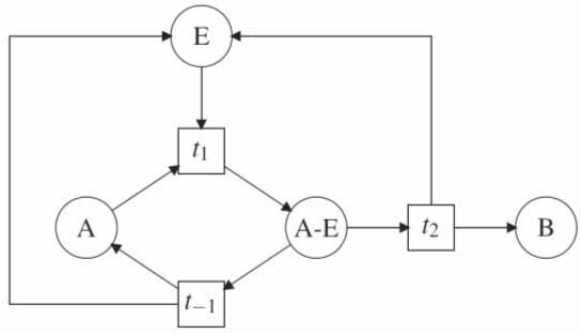

Figure 1. Petri-net corresponding to the biochemical model of example 1.

As explained in introduction, for reaction models these invariants are used for flux analysis, variable simplification through conservation law extraction, module decomposition, etc. More precisely, invariants, being based on the structure, provide of course qualitative information that can be used for instance for model-checking (e.g. reachability analysis). It is however interesting to note that some non-trivial quantitative information is also captured. For instance a semi-positive P-invariant defines a (quantitative) conservation law, whatever the dynamics of the system.

Note that there are other ones, like the following when $k1 = k2$:

$MA(k1)\ for\ A => A + B.$
$MA(k2)\ for\ A => \_.$

Where `MA(k)` denotes that the kinetics of the reaction follow the Mass Action law with rate `k`. The resulting ODEs would have the following property:

$$\frac{d[A]+[B]}{dt} = -k_2 * [A] + k_1 * [A] = (k_1 - k_2) * [A]$$

In the same manner, as pointed out in Section 1 links have been found between the structure of the graph and the dynamical behavior (through positive and negative cycles in the influence graph or CRNT) from the structure of the reaction model.

There is also information lying between quantitative and qualitative, like the definition of modules from T-invariants as explored recently in [13, 14], and to sum this up, the structure of the reaction model contains information that can be used at any abstraction level.

4 Related work

To compute the invariants of a Petri net, especially if this computation is combined with other Petri-net analyses, like sinks and sources, traps, deadlocks, etc. the most natural solution is to use a Petri-net dedicated tool like INA, PiNA, or Charlie for instance through the interface of Snoopy [15], which will soon allow the import of SBML models as Petri-nets. Standard integer methods like Fourier-Motzkin elimination will then provide an efficient means to compute P or T-invariants. These methods however generate lots of candidates which are afterwards eliminated and also need to incorporate some means (like equality class definition) to avoid combinatorial explosion at least in some simple cases, as explained in Section 6.

Another way to extract the minimal semi-positive invariants of a model is to use one of the software tools that provide this computation for biological systems, generally as "conservation law" computation, and based on linear algebra methods like QR factorization [31]. This is the case for instance of the METATOOL [32] and COPASI [16] tools. The idea is to use a linear relaxation of the problem, which suits well very big graphs, but needs again a posteriori filtering of the candidate solutions. Moreover, these methods do not incorporate any means of symmetry elimination (see section 6).

5 Finding invariants as a Constraint Solving Problem

We will illustrate our new method for computing the invariants with the case of P-invariants (but T-invariants, being dual, work in the same fashion). For a Petri net with p places and t transitions ($L_i \rightarrow R_i$), a P-invariant is a vector $V \in \mathbb{N}^p$ s.t. $V \cdot I = 0$, i.e. $\forall 1 \leq i \leq t\ V \cdot L_i = V \cdot R_i$. Since those vectors all live in N_p, it is quite natural to see this as a Constraint Solving Problem (CSP) with t (linear) equality constraints on p Finite Domains variables.

Example 2. *Using the Petri-net of example 1 we have:*

$$A + E => A - E$$
$$A - E => A + E$$
$$A - E => B + E$$

This results in the following equations:

$$A + E = AE \quad (1)$$
$$AE = A + E \quad (2)$$
$$AE = B + E \quad (3)$$

where obviously equations (2) is redundant.

The task is actually to find invariants with minimal support (a linear combination of invariants belonging to $\mathbb{N}^p$ also being an invariant), i.e. having as few non-zero components as possible, these components being as small as possible, but of course non trivial, we thus add the constraint that $V \cdot \mathbf{1} > 0$.

Example 3. *In our running example we thus add* $A + E + AE + B > 0$.

Now, to ensure minimality the labelling is invoked from small to big values and a branch and bound procedure is wrapped around it, maintaining a partial base $\mathcal{B}$ of P-invariant vectors and adding the constraint that a new vector V is solution if $\forall B \in \mathcal{B}$ $\prod_{B_i \neq 0} V_i = 0$, which means that its support is not bigger than that of any vector of the base.

Unfortunately, even with the last constraint, no search heuristic was found that makes removing subsumed Pinvariants unnecessary. Thus, if a new vector is added to $\mathcal{B}$, previously found vectors with a bigger support must be removed.

This algorithm was implemented directly into BIOCHAM [3], which is programmed in GNU-Prolog, and allowed for immediate testing.

Example 4. *In our running example we find two minimal semi-positive P-invariants*:

- $E = AE = 1$ and $A = B = 0$
- $A = B = AE = 1$ and $E = 0$

6 Equality classes

6.1 A hard problem

The problem of finding minimal semi-positive invariants clearly suffers from a computational blowup since there can be an exponential number of such invariants. For instance the model given in example 5 has 2n minimal semi-positive P-invariants (each one with either Ai or Bi equal to 1 and the other equal to 0).

Example 5. *The model:*

$$A1 + B1 => A2 + B2$$
$$A2 + B2 => A3 + B3$$
$$\ldots$$
$$A3 + B3 => A4 + B4$$

is depicted in figure 2

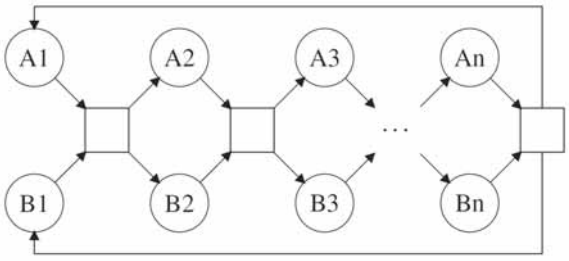

Figure 2. Example net with 2n minimal semi-positive P-invariants.

6.2 CSP-like Symmetry breaking

A first remark is that in this example, there is a variable symmetry [12] between all the pairs (A_i,B_i) of variables corresponding to places. This symmetry is easy to detect (purely syntactical) and can be eliminated through the usual ordering of variables, by adding the constraints $A_i \leq B_i$.

This classical CSP optimization is enough to avoid most of the trivial exponential blow-ups and corresponds to the initial phase of *parallel places* detection and merging of the equality classes optimization for the standard Fourier-Motzkin algorithm [21]. Note however that in that method, classes of equivalent variables are detected and eliminated before and *during* the invariant computation, which would correspond to local symmetry detection and was not implemented in our prototype.

Moreover, in [21], *equality class* elimination is done through replacement of the symmetric places by a represen-tative place. The full method reportedly improves by a factor two the computation speed. Even if in the context of the original article this is done only for ordinary Petri-nets (only one edge from one place to a transition and from one transition to one place), we can see that it can be even more efficient to use this replacement technique in our case:

Example 6

…

$A + B => 4 * C$

…

Instead of simply adding $A \leq B$ *to our constraints, which will lead to 3 solutions when C = 1 before symmetry expansion:* $(A, B) \in \{(0,4), (1,3), (2,2)\}$, *replacing* A *and* B *by* D *will reduce to a single solution* $D = 4$ *before expansion of the subproblem* $A + B = D$.

This partial detection of independent subproblems, which can be seen as a complex form of symmetry identifica-tion, can once again be done syntactically at the initial phase, and can be stated as follows: replace $\sum_i k_i * A_i$ by a single variable A if all the A_i occur only in the context of this sum i.e. in our Petri net all pre-transitions of A_i are connected to A_i with k_i edges and to all other A_j with k_j edges and same for post-transitions. For a better constraint propagation, another intermediate variable can be introduced such that $A = gcd(k_i) \cdot A'$. In our experiments the simple case of *parallel places* (i.e. all k_i equal to 1 in the sum) was however the one encountered most often.

6.3 Going farther

In our Nicotine tool (available at `http://contraintes.inria.fr/~soliman/nicotine/`), we extended SBML support to also include APNN and PNML import/export. We then proceeded to add one more step of optimization.

The point is to note that if a place (in the case of P-invariants) P has only one single input transition I and one single output transition O, and if there exists a path between I and O such that it goes only through such places (with single input and output) P_i, whatever the intermediate transitions, then there is a bijection between minimal semi-positive P-invariants such that $P > 0$ and those where $P = 0$ and $min(Pi) > 0$.

It is thus possible to look only for solutions where $P = 0$ and to obtain the other ones by "symmetry". Actually this bijection consists in mapping all P_i to $P_i - min(P_i)$ and P from 0 to $min(P_i)$. Intuitively the "flow" going through the P_i is redirected through P. More precisely, for the intermediate transitions we get equations of the form $P_j + \cdots = P_j + 1 + \cdots$, which are unchanged by our bijection, and for I (resp. O), P replaces the first (resp. last) P_i. The bijection only maps minimal invariants to minimal invariants (since at least one of the P_i gets removed from the support when P gets added and reciprocally).

7 Example, the MAPK Cascade

The MAPK signal transduction cascade is a well studied system that appears in lots of organisms and is very important for regulating cell division [27]. It is composed of layers, each one activating the next, and in detailed models shows two intertwined pathways conveying EGF and NGF signals to the nucleus.

A simple MAPK cascade model, that of [22] without scaffold, is used here as an example to show the results of P-invariant computation.

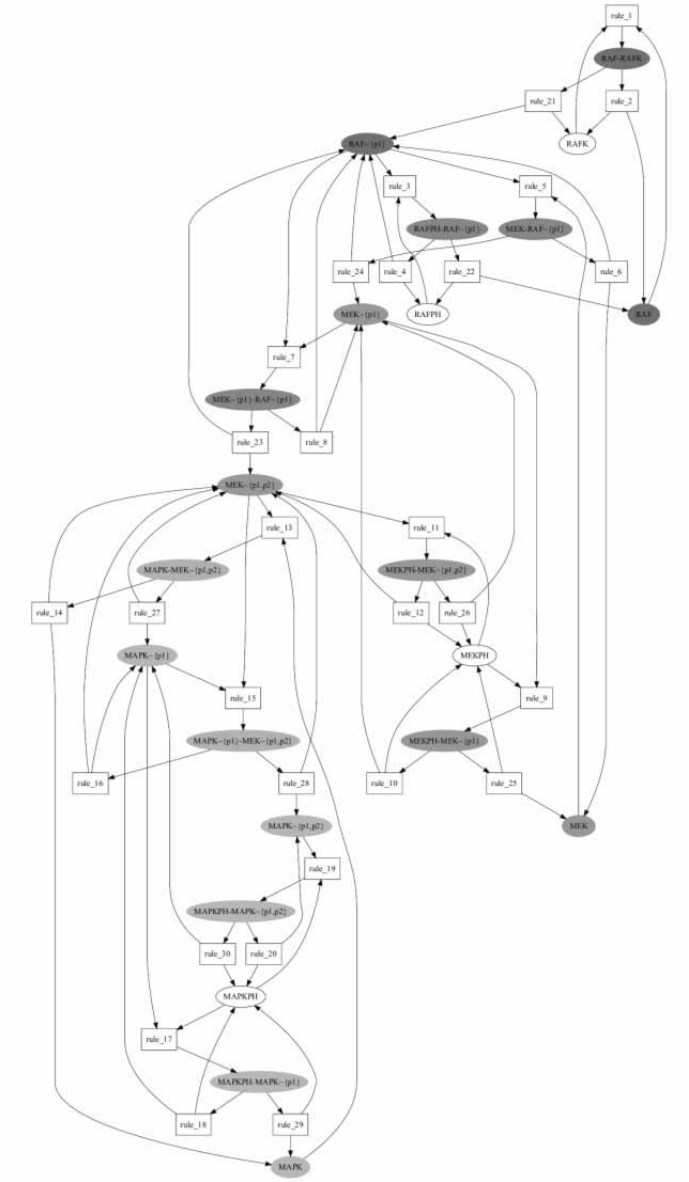

Figure 3: 3 of the 7 P-invariants found in the MAPK cascade model of [22]. The blue one (RAF), the pink one (MEK) and the green one (MAPK) with intersections in purple (blue+pink) and khaki (pink+green).

Seven minimal semi-positive P-invariants are found almost instantly: RAFK, RAFPH, RAF, MEKPH, MEK, MAPKPH, MAPK. Three of them are depicted in figure 3, the full list is given in table 1.

Note that these 7 P-invariants define 7 algebraic conservation rules and thus decrease the size of the corresponding ODE model from 22 variables and equations to only 15.

8 Evaluation on other examples

Schoeberl's model is a more detailed version of the MAPK cascade, which is quite comprehensive [28], but too big to be studied by hand. It can however be easily broken down into fourteen more easily understandable units formed by P-invariants, as shown in table

2, along other examples representing amongst the biggest reaction networks publicly available in Systems Biology.

All the curated models in the December 2008 release of `biomodels.net` were also tested and none of them required more than 1s to compute all its minimal P-invariants. All the Petri-nets of `www.petriweb.org` were also tested, though they do not correspond to reaction models, only one took more than 1s: model 1516, which took about 3s to compute 1133 minimal P-invariants. We think that the structure of this kind of net is however very different from that of usual biochemical reaction models and intend to explore this distinction further in the future.

We could not compare our results with those provided in [31] since the models they use, coming from metabolic pathways flux analyses, do not have an integer stoichiometry matrix, however the examples of table 2 show the feasibility of P-invariant computation by constraint programming for quite big networks.

Note that for networks of this size, the upper bound of the domain of variables had to be set manually (to a reason-able value like 8 since actually only 2 or 3 was needed in all the biological models we have encountered up to now). Otherwise, the only over-approximation of the upper bound found was the product of the l.c.m. of stoichiometric coefficients of each reaction, which explodes really fast and leads to unnecessarily long computation. We thereby lose completeness, but it is not enforced either by QR-factorization methods, and does not seem to miss anything on real life examples.

RAFK, RAF-RAFK
RAFPH, RAFPH-RAF~{p1}
RAF, MEK-RAF~{p1}, RAF-RAFK, RAFPH-RAF~{p1}, MEK~{p1}-RAF~{p1}, RAF~{p1}
MEKPH, MEKPH-MEK~{p1}, MEKPH-MEK~{p1, p2}
MEK, MAPK-MEK~{p1, p2}, MEK-RAF~{p1}, MEKPH-MEK~{p1}, MEKPH-MEK~{p1, p2}, MAPK~{p1}-MEK~{p1, p2}, MEK~{p1}-RAF~{p1}, MEK~{p1}, MEK~{p1, p2}
MAPKPH, MAPKPH-MAPK~{p1}, MAPKPH-MAPK~{p1, p2}
MAPK, MAPK-MEK~{p1, p2}, MAPKPH-MAPK~{p1}, MAPK~{p1, p2} MAPK~{p1}-MEK~{p1, p2}, MAPK~{p1}, MAPKPH-MAPK~{p1, p2},

Table 1: P-invariants of the MAPK cascade model of [22]

9 Conclusion

After the genome sequencing, building and correcting System Biology models is a new and rich domain where lots of mathematics and computer science tools can be used. We argue that to encompass the heterogeneity of the available data it is necessary to provide formal languages for different levels of abstractions and to relate them precisely [9] but also to formalize the properties of the studied system in order to leverage all the automatic tools from machine learning and optimization.

This amounts to more initial work for the modeller who should now both represent his system as a set of reactions but also the experimental data available (either directly in temporal logic or through tools that will extract such specification from other kinds of data like, for instance time series). However after this initial step, lots of different tools, which will complement simulation, become available to automatically curate, refine, modularize, ...his model.

Model	transit	places	P-invar.	Invariant size
Schoeberl's MAPK [28]	125	105	14	from 2 to44
Curie's E2F/Rb [4]	~500	~400	79	from size 1 (EP300) to about 230 (E2F1 box)
Kohn's map [20]	~800	~500	65	from size 1 (Myt1) to about 200 (pRb or cdk2)

Table 2: Minimal semi-positive P-invariant computation on bigger models of biochemical reaction networks, all < 1s

In the BIOCHAM environment we have implemented some of the tools we thought most useful from the modelling point of view, but through SBML import/export it is also possible to rely on the vast body (see `http://www.sbml.org` for a list) of software handling reaction-based biochemical models. The crucial point here is the multiple abstraction levels that can be used to reason about a single reaction model.

We have illustrated this point through invariant computation. We have shown that P-invariants of a biological reaction model are not difficult to compute in most cases.

They do however carry information about conservation laws that are useful for efficient and precise dynamical simulation of the system, and provide some notion of module, which is related to the life cycle of molecules. T-invariants are already used more commonly, and get more and more focus recently.

We introduced a new method to efficiently compute P and T-invariants of a reaction network, based on Finite Domain constraint programming. It includes symmetry detection and breaking and scales up well to the biggest reaction networks found.

The idea of applying constraint based methods to classical problems of the Petri-net community is not new, but seems currently mostly applied to the model-checking. We argue that structural problems (invariants, sinks, attrac-tors, etc.) can also benefit from the know-how developed for finite domain CP solving, like symmetry breaking, search heuristics, etc. and thus intend to generalize our approach to other problems of this category, hoping to bring more and more qualitative and quantitative information from the pure structure of the reaction models.

10 References

[1] Antoniotti, M., Policriti, A., Ugel, N., and Mishra, B. Cell Biochemistry and Biophysics 38, 271–286 (2003).

[2] Calzone, L., Chabrier-Rivier, N., Fages, F., and Soliman, S. In Transactions on Computational Systems Biology VI, Plotkin, G., editor, volume 4220 of Lecture Notes in BioInformatics, 68–94. Springer-Verlag November (2006). CMSB'05 Special Issue.

[3] Calzone, L., Fages, F., and Soliman, S. BioInformatics 22(14), 1805–1807 (2006).

[4] Calzone, L., Gelay, A., Zinovyev, A., Radvanyi, F., and Barillot, E. Molecular Systems Biology 4(173) (2008).

[5] Chabrier-Rivier, N., Chiaverini, M., Danos, V., Fages, F., and Schächter, V. Theoretical Computer Science 325(1), 25–44 September (2004).

[6] Chickarmane, V., Kholodenkob, B. N., and Sauro, H. M. Journal of Theoretical Biology 244, 68–76 (2007).

[7] Danos, V. and Laneve, C. Theoretical Computer Science 325(1), 69–110 (2004).

[8] Eker, S., Knapp, M., Laderoute, K., Lincoln, P., Meseguer, J., and Sönmez, M. K. In Proceedings of the seventh Pacific Symposium on Biocomputing, 400–412, January (2002).

[9] Fages, F. and Soliman, S. Theoretical Computer Science 403(1), 52–70 (2008).

[10] Fages, F. and Soliman, S. In Proceedings of Formal Methods in Systems Biology FMSB'08, number 5054 in Lecture Notes in Computer Science. Springer-Verlag, February (2008).

[11] Fages, F., Soliman, S., and Chabrier-Rivier, N. Journal of Biological Physics and Chemistry 4(2), 64–73 October (2004).

[12] Freuder, E. C. In Proceedings of AAAI'91, 227–233. MIT Press, (1991).

[13] Gilbert, D., Heiner, M., and Lehrack, S. In CMSB'07: Proceedings of the fifth international conference on Computational Methods in Systems Biology, volume 4695 of Lecture Notes in Computer Science. Springer-Verlag, (2007).

[14] Grafahrend-Belau, E., Schreiber, F., Heiner, M., Sackmann, A., Junker, B. H., Grunwald, S., Speer, A., Winder, K., and Koch, I. BMC Bioinformatics 9(90) February (2008).

[15] Heiner, M., Richter, R., and Schwarick, M. In Proceedings of the International Workshop on Petri Nets Tools and APplications (PNTAP 2008) (ACM Digital Library, Marseille, 2008). to appear.

[16] Hoops, S., Sahle, S., Gauges, R., Lee, C., Pahle, J., Simus, N., Singhal, M., Xu, L., Mendes, P., and Kummer, U. BioInformatics 22(24), 3067–3074 (2006).

[17] Hucka, M. et al. Bioinformatics 19(4), 524–531 (2003).

[18] Ideker, T., Galitski, T., and Hood, L. Annual Review of Genomics and Human Genetics 2, 343–372 (2001).

[19] Kanehisa, M. and Goto, S. Nucleic Acids Research 28(1), 27–30 (2000).

[20] Kohn, K. W. Molecular Biology of the Cell 10(8), 2703–2734 August (1999).

[21] Law, C. F., Gwee, B. H., and Chang, J. IEE Proceedings: Computers and Digital Techniques 1(5), 612–624 (2007).

[22] Levchenko, A., Bruck, J., and Sternberg, P. W. PNAS 97(11), 5818–5823 May (2000).

[23] Phillips, A. and Cardelli, L. Transactions on Computational Systems Biology (to appear). Special issue of BioConcur 2004.

[24] Reddy, V. N., Mavrovouniotis, M. L., and Liebman, M. N. In Proceedings of the 1st International Conference on Intelligent Systems for Molecular Biology (ISMB), Hunter, L., Searls, D. B., and Shavlik, J. W., editors, 328–336. AAAI Press, (1993).

[25] Regev, A., Silverman, W., and Shapiro, E. Y. In Proceedings of the sixth Pacific Symposium of Biocomputing, 459–470, (2001).

[26] Rizk, A., Batt, G., Fages, F., and Soliman, S. In CMSB'08: Proceedings of the fourth international confer-ence on Computational Methods in Systems Biology, Heiner, M. and Uhrmacher, A., editors, volume 5307 of Lecture Notes in Computer Science, 251–268. Springer-Verlag, October (2008).

[27] Roovers, K. and Assoian, R. K. BioEssays 22(9), 818–826 August (2000).

[28] Schoeberl, B., Eichler-Jonsson, C., Gilles, E., and Muller, G. Nature Biotechnology 20(4), 370–375 (2002).[29] Schuster, S., Fell, D. A., and Dandekar, T. Nature Biotechnology 18, 326–332 (2002).

[29] Thomas, R., Gathoye, A.-M., and Lambert, L. European Journal of Biochemistry 71(1), 211–227 December (1976).

[30] Vallabhajosyulaa, R. R., Chickarmane, V., and Sauro, H. M. BioInformatics November (2005). Advance Access.

[31] von Kamp, A. and Schuster, S. Bioinformatics 22(15), 1930–1931 (2006).

[32] Sveca J., Söder L.*: Wind power integration in power systems with bottleneck problems.* VIND-2002 conference in Malmö, November 6-7, 2002.

Corresponding author: S. Soliman,
INRIA Rocquencourt - Projet CONTRAINTES
Domaine de Voluceau, Rocquencourt,
BP 105, F-78153 Le Chesnay CEDEX
sylvain.soliman@inria.fr

Received & Accepted: MATHMOD 2009
Revised: September 20, 2009
Accepted: October 10, 2009

Dynamic Optimization of Chemical and Bio-chemical Processes using an Efficient Global Optimization Metaheuristic

J.A. Egea, E. Balsa-Canto, J.R. Banga, Instituto de Investigaciones Marinas (C.S.I.C.), Vigo, Spain

SNE Simulation Notes Europe SNE 19(3-4), 2009, 41-46, doi: 10.11128/sne.19.tn.09949

A metaheuristic based on scatter search for global dynamic optimization of chemical and bio-chemical processes is presented. It is designed to overcome typical difficulties of nonlinear dynamic systems optimization such as noise, flat areas, non-smoothness and/or discontinuities. It balances between intensification and diversification by coupling a local search procedure with a global search and makes use of memory to avoid simulations in previously explored areas. Its application to three dynamic optimization case studies proves its efficiency and robustness, showing also a very good scalability.

Introduction

Dynamic optimization (or open loop optimal control) appears in many industrial applications to optimize a pre-defined performance index (e.g., profitability) subject to some specifications over a time interval. Objective functions and/or constraints formulated from mathematical models describing industrial processes are usually highly nonlinear, which often causes non-convexity. Besides, non-smoothness and discontinuities can be present, thus the use of global optimization methods is needed for many dynamic optimization problems from this field [7]. In recent years, a special class of stochastic global optimization methods called metaheuristics, which provide excellent solutions (often the global optimum) in relatively short computation times, has appeared.

Scatter search is a population-based metaheuristic introduced by Glover [12] which combines a global phase with an intensification method, usually a local search [16]. Compared to other evolutionary or genetic algorithms, scatter search has a small population (called reference set or *RefSet*) consisting of high quality and diverse solutions which are systematically combined. Our scatter search-based algorithm has been written in Matlab under the name *SSm*. This study goes beyond a simple exercise of applying scatter search to dynamic optimization problems, but presents innovative mechanisms to obtain a good balance between intensification and diversification in a short-term search horizon. In many instances, dynamic optimization problems are non-convex and multimodal, thus the use of global optimization techniques becomes crucial for solving them [7]. The application of our algorithm for solving nonlinear optimization problems arising from chemical and biological systems has provided excellent results [10, 18].

This paper is organized as follows: Section 1 states the problem of dynamic optimization. Our algorithm is depicted in Section 2. Section 3 presents the three case studies used in this paper for our experiments as well as the results obtained. The paper finishes with some conclusions.

1 Dynamic optimization: problem statement

The general dynamic optimization problem has the following mathematical form:

$$\min_{\boldsymbol{u}(t),\boldsymbol{v},t_f} C(\boldsymbol{x}(t_f),\boldsymbol{z}(t_f),\boldsymbol{u}(t_f),\boldsymbol{v},t_f) \quad (1)$$

subject to the system's dynamics:

$$\boldsymbol{F}(\dot{\boldsymbol{x}},\boldsymbol{x}_t,\boldsymbol{x}_\xi,\boldsymbol{x}_{\xi\xi},\boldsymbol{x}(t),\boldsymbol{z}(t_f),\boldsymbol{u}(t_f),\boldsymbol{v},t_f)=\boldsymbol{0} \quad (2)$$

$$\boldsymbol{x}(0)=\boldsymbol{x}_0 \quad (3)$$

$$\boldsymbol{u}(0)=\boldsymbol{u}_0 \quad (4)$$

$$\boldsymbol{z}(0)=\boldsymbol{z}_0 \quad (5)$$

$$\boldsymbol{x}(\boldsymbol{\Omega})=\boldsymbol{x}_{\boldsymbol{\Omega}} \quad (6)$$

where $\boldsymbol{x}_t=\partial\boldsymbol{x}/\partial t$, $\boldsymbol{x}_\xi=\partial\boldsymbol{x}/\partial\xi$, $\boldsymbol{x}_{\xi\xi}=\partial^2\boldsymbol{x}/\partial\xi^2$; $\boldsymbol{x}(t)\in\boldsymbol{X}\subset\boldsymbol{R}^{nl+nd}$ (with nl = number of lumped state variables and nd = number of distributed state variables) and $\boldsymbol{z}(t)\in\boldsymbol{Z}\subset\boldsymbol{R}^m$ are the vectors of differential and algebraic states respectively; $\boldsymbol{u}(t)\in\boldsymbol{U}\subset\boldsymbol{R}^p$ is the vector of control (input) variables; $\boldsymbol{v}(t)\in\boldsymbol{V}\subset\boldsymbol{R}^q$ are time invariant parameters; t is the time (and tf is the final time); C is a functional to be minimized; $\boldsymbol{F}$ is the set of partial differential-algebraic equations describing the systems dynamics; finally, $\boldsymbol{x}_0$, $\boldsymbol{z}_0$, and $\boldsymbol{u}_0$ are the values of the respective vectors at the initial time t_0, and $\boldsymbol{x}_{\boldsymbol{\Omega}}$ is the value of $\boldsymbol{x}$ at spatial boundary.

Equality and inequality constraints may be imposed. Some of them must be satisfied over the whole process time (path constraints),

$$\boldsymbol{H}_{\text{path}}(\boldsymbol{x}(t_f), \boldsymbol{z}(t_f), \boldsymbol{u}(t_f), \boldsymbol{v}, t_f) = 0 \quad \forall t \tag{7}$$

$$\boldsymbol{G}_{\text{path}}(\boldsymbol{x}(t_f), \boldsymbol{z}(t_f), \boldsymbol{u}(t_f), \boldsymbol{v}, t_f) = 0 \quad \forall t \tag{8}$$

while others must be only satisfied at the end of the process (endpoint constraints),

$$\boldsymbol{H}_{\text{end}}(\boldsymbol{x}(t_f), \boldsymbol{z}(t_f), \boldsymbol{u}(t_f), \boldsymbol{v}, t_f) = 0 \quad \forall t \tag{9}$$

$$\boldsymbol{G}_{\text{end}}(\boldsymbol{x}(t_f), \boldsymbol{z}(t_f), \boldsymbol{u}(t_f), \boldsymbol{v}, t_f) = 0 \quad \forall t \tag{10}$$

The control variables and/or the time-invariant parameters may be subject to lower and upper bounds:

$$\boldsymbol{u}^{\text{lb}} \leq \boldsymbol{u}(t) \leq \boldsymbol{u}^{\text{ub}} \tag{11}$$

$$\boldsymbol{v}^{\text{lb}} \leq \boldsymbol{v}(t) \leq \boldsymbol{v}^{\text{ub}} \tag{12}$$

In practice, the dynamic optimization of distributed systems typically involves transforming the original system into an equivalent lumped system and applying lumped-system dynamic optimization methods. Therefore, a spatial discretization approach is usually used to transform the original infinite dimension partial differential equations (PDE) into a large-scale, and possibly stiff, set of ordinary differential equations (ODEs) [4]. The accurate solution of the resulting ODE system then often requires the use of an implicit ODE solver.

In this work we will consider the CVP approach [22] using the Piecewise Constant approximation, PC (i.e., zero order polynomial) with fixed-length time intervals. Different number of intervals will be used for each problem in order to check the scalability of the different optimization methods.

2 A scatter search algorithm for dynamic optimization of chemical and bioprocesses

2.1 Diversification Generation Method

SSm begins by generating an initial set of diverse vectors in the search space. The method makes use of memory taking into account the number of times that every decision variable appears in different parts of the search space [13].

2.2 Initial *RefSet* formation

For building the initial *RefSet*, after generating the set of diverse solutions, a subset of high quality and diverse points is selected. The first step consists in evaluating all diverse vectors and selecting some of them in terms of quality. The *RefSet* is completed with the remaining diverse vectors by maximizing the minimum Euclidean distance to the included vectors in the *RefSet*.

2.3 *Subset Generation* and *Solution Combination* methods

After the initial *RefSet* is built, its solutions are sorted according to their quality and we apply the *Subset Generation Method*. In our implementation, it consists in selecting all pairs of solutions in the *RefSet* to combine them. To avoid repeating combinations with the same pair of solutions, we use a memory term which keeps track of the pairs previously combined. Regarding the *Solution Combination Method*, we use a type of combination based on hyper-rectangles [21], which enhances the diversification. Depending on their position in the *RefSet* every pair of combined solutions may generate from two up to four new solutions.

2.4 Updating the *RefSet*

As recommended by Laguna and Marti [17], we update the *RefSet* considering the quality of the elements. This strategy may cause convergence to sub-optimal solutions or stagnation of the search in flat areas. To avoid these effects, we have implemented two filters [10] which restrict the incorporation of solutions that contribute only slight diversity to the *RefSet*.

2.5 Improvement method

The *Improvement Method* consists in a local search, selecting the initial points by means of different filters. In this work, we have considered a gradient-based method [11] and the Nelder and Mead method implemented in Matlab [1]. In applications related to chemical and bioprocess engineering, we often face time-consuming evaluation problems or complex topologies which can make the local search inefficient. This implies that the application of the *Improvement Method* should be restricted to a low number of promising solutions. Here we use merit and distance heuristic filters introduced by Ugray et al. [21] to avoid performing local searches from poor quality solutions or from solutions which are likely to provide already found local minima.

2.6 *RefSet* rebuilding

Due to the memory term which avoids combinations between *RefSet* members previously combined, the optimization procedure may stop if no new solutions enter the *RefSet* in a given iteration. Advanced scatter search designs overcome this problem by resorting a mechanism to partially rebuild the *RefSet*. The method is usually the same as that used to create the initial *RefSet*, in the sense that it uses the max-min distance criterion for selecting diverse solutions.

ρ		CMAES	DE	glcDirect	OQNLP	SRES	SSm
	Best	**20316.11**	**20316.08**	20203.74	**20316.11**	20305.96	**20316.11**
10	Mean	19889.67	20100.72	–	–	20093.14	20291.38
	Worst	18996.02	19672.46	–	–	19554.01	20192.48
	Best	**20412.14**	20404.36	19738.01	**20412.19**	20327.11	**20412.19**
20	Mean	20273.76	20383.95	–	–	20237.58	20412.19
	Worst	19953.39	20341.29	–	–	20095.71	20412.19
	Best	20430.84	20375.32	19544.88	**20444.47**	20214.40	**20444.86**
40	Mean	20360.73	20239.27	–	–	19726.07	20444.86
	Worst	20110.08	19902.08	–	–	19466.64	20444.86

Table 1. Results for the ethanol production problem.

ρ		CMAES	DE	glcDirect	OQNLP	SRES	SSm
	Best	**87.934**	**87.934**	87.258	87.775	**87.927**	**87.931**
10	Mean	87.837	87.914	–	–	87.688	87.906
	Worst	87.340	87.835	–	–	87.348	87.889
	Best	87.948	**88.013**	84.490	87.400	87.671	87.998
20	Mean	87.841	87.955	–	–	86.900	87.885
	Worst	87.599	87.767	–	–	85.064	87.796
	Best	87.914	87.926	80.657	87.547	82.709	**87.999**
40	Mean	87.861	87.802	–	–	82.709	87.863
	Worst	87.745	87.565	–	–	82.709	87.595

Table 2. Results for the penicillin production problem.

We propose an alternative strategy to maximize the number of search directions.

In this strategy, the vectors refilling the *RefSet* are chosen to maximize the number of relative directions defined by them and the existing vectors in the *RefSet* [10].

2.7 Intensification strategies

One of the filters mentioned above may prevent the search from focusing on intensification, especially during the first iterations.

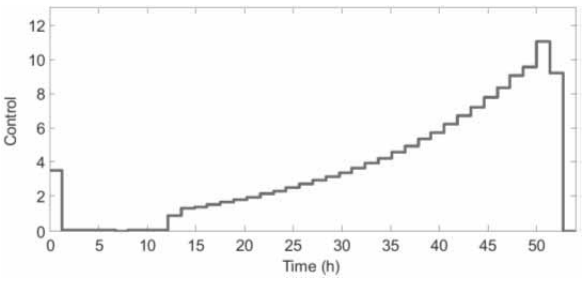

Figure 1. Optimal control profile for the ethanol production problem ($\rho = 40$).

To allow combinations between high quality solutions (which do not apply to enter the *RefSet* because of the distance filter) and *RefSet* members, we store the solutions which can not enter the *RefSet* but have a better function value than the second *RefSet* member.

These stored solutions are then combined with the best *RefSet* solution, increasing the probability of obtaining high quality solutions by combination in early stages of the search [10]. Another advanced strategy (the *go beyond* strategy) to enhance the intensification of the search has been implemented in our algorithm. It consists in exploiting promising directions [9].

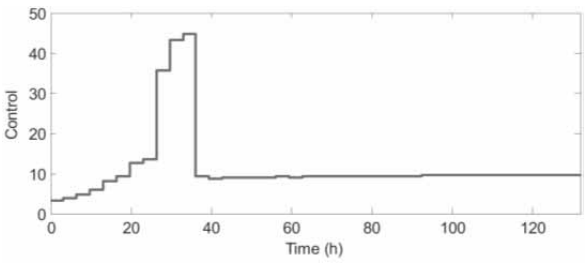

Figure 2. Optimal control profile for the penicillin production problem ($\rho = 40$)

ρ		CMAES	DE	glcDirect	OQNLP	SRES	SSm
	Best	**0.20002**	**0.20003**	0.19979	0.19875	0.20001	**0.20003**
10	Mean	0.19710	0.19683	–	–	0.19894	0.19694
	Worst	0.19108	0.18939	–	–	0.19579	0.18742
	Best	0.19997	0.19913	0.19329	0.15483	0.19989	**0.20010**
20	Mean	0.19696	0.19608	–	–	0.19878	0.19687
	Worst	0.19298	0.19185	–	–	0.19728	0.19326
	Best	**0.19952**	0.19859	0.18848	0.15102	0.19001	0.19788
40	Mean	0.19751	0.19442	–	–	0.18796	0.19618
	Worst	0.19522	0.19103	–	–	0.18623	0.19311

Table 3. Results for the drying process problem.

3 Computational experiments

In this section, a set of bioprocess dynamic optimization problems will be used as case studies to test the performance of the algorithm proposed in this work. A set of different state-of-the-art global optimization methods has been selected to compare their results with those obtained with the algorithm proposed in this study: *CMAES* [2], *DE* [20], *SRES* [19], *DIRECT* [14] and *OQNLP* [15]. Regarding stochastic solvers, ten runs were performed for each problem.

3.1 Ethanol production in a fed-batch reactor

This system is a fed-batch bioreactor for the production of ethanol [6]. The objective is to find the feed rate which maximizes the yield of ethanol. Table 1 presents results for every solver with the different levels of discretization considered. Figure 1 presents the optimal control profile for the highest level of discretization.

3.2 Penicillin production in a fed-batch fermenter

This problem deals with the dynamic optimization of a fed-batch fermenter for the production of penicillin [6]. The optimal control problem is to maximize the total amount of penicillin produced using the feed rate of substrate as the control variable.

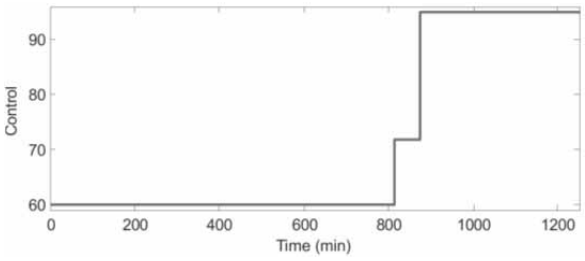

Figure 3. Optimal control profile for the drying process problem ($\rho = 40$)

In our experiments, *SSm* provided the best solution for the levels of discretization $\rho = 10{,}40$. Table 2 presents results for every solver with the different levels of discretization and Figure 2 presents the optimal control profile for the highest level of discretization.

3.3 Drying operation

In this section we consider a food convective drying problem, similar to the one formulated by Banga and Singh [5]. The aim is to dry a cellulose slab maximizing the retention of a nutrient.

The dynamic optimization problem associated with the process consists of finding the dry bulb temperature along the time to maximize the nutrient retention at the final time. Table 3 presents results for every solver with the different levels of discretization and Figure 3 presents the optimal control profile for the highest level of discretization.

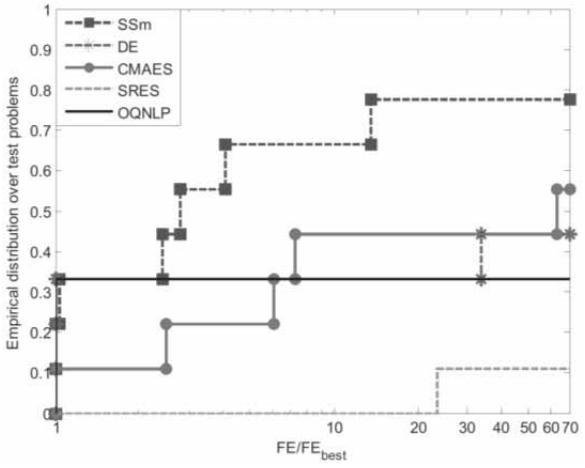

Figure 4. Performance profiles

4 Executive summary of results

In this section we provide a summary of the results obtained in this work by making use of the performance profiles methodology [8]. Following [3], we define the success performance $\boldsymbol{FE}$ for a solver on a specific problem by:

$$\boldsymbol{FE} = eval_{\text{mean}} \frac{\text{\# all runs (10)}}{\text{\# successful runs}} \quad (13)$$

where a run is considered successful if it obtained the optimal solution with a relative error $\leq 0.01\%$ (in our problems, we consider it as the best solution found by any of the solvers). With this definition, the best success performance $\boldsymbol{FE}_{\text{best}}$ is given by the lowest value of $\boldsymbol{FE}$ for every problem. Figure 4 shows the empirical distribution function of the success performance $\boldsymbol{FE}/\boldsymbol{FE}_{\text{best}}$ over all the problems. As shown in the performance profiles, *SSm* solves the highest percentage of problems compared with rest of solvers tested.

5 Conclusions

We have developed a scatter search-based methodology which intends to be effective for solving global dynamic optimization problems from the biotechnological and food industries. The procedure treats the objective function as a black box, making the search algorithm context-independent. We have expanded and advanced knowledge associated with the implementation of scatter search procedures.

We have tested the proposed methodology over a set of dynamic optimization problems from the biotechnological and food industries. In order to have an idea about their efficiency, they have been compared with other state-of-the-art global optimization methods. The results obtained showed that the proposed methodology is adequate for the kind of problems intended to solve. In all cases our algorithm was competitive, providing the best solution among the tested solvers in many of the examples.

It is to note that the algorithm's behaviour is not affected by the problem size since it provides excellent results for every level of discretization considered in this study.

Acknowledgements

The authors acknowledge financial support from EU project BaSysBio LSHG-CT-2006-037469 and Spanish MICINN project MultiSysBio DPI2008-06880-C03-02.

References

[1] The MathWorks Inc: *Optimization Toolbox for Use with Matlab*. User's guide. Version 2.

[2] Auger, A. and Hansen, N.: *A restart CMA evolution strategy with increasing population size*. In: Proc. IEEE Congress on Evolutionary Computation, IEEE CEC 2005, 1769-1776.

[3] Auger, A. and Hansen, N.: *Performance evaluation of an advanced local search evolutionary algorithm*. In: Proc. IEEE Congress on Evolutionary Computation, IEEE CEC 2005, 1777-1784.

[4] Balsa-Canto, E., Banga, J.R., Alonso, A.A. and Vassiliadis, V.S.: *Dynamic optimization of distributed parameter systems using second-order directional derivatives*, Industrial & Engineering Chemistry Research, 43 (2004), 6756-6765.

[5] Banga, J.R. and Paul Singh, R.: *Optimization of air drying of foods*, Journal of Food Engineering, 23 (1994), 189-211.

[6] Banga, J.R., Alonso, A.A. and Singh, R.P.: *Stochastic dynamic optimization of batch and semicontinuous bioprocesses*, Biotechnology Progress, 13 (1997), 326-335.

[7] Banga, J.R., Balsa-Canto, E., Moles, C.G. and Alonso, A.A.: *Dynamic optimization of bioprocesses: Efficient and robust numerical strategies*, Journal of Biotechnology, 117 (2005), 407-419.

[8] Dolan, E.D. and More, J.J.: *Benchmarking optimization software with performance profiles*, Mathematical Programming, Series B, 91 (2002), 201-213.

[9] Egea, J.A.: *New Heuristics for Global Optimization of Complex Bio-Processes*, PhD Thesis, University of Vigo, 2008.

[10] Egea, J.A., Rodriguez-Fernandez, M., Banga, J. R., Marti, R.: *Scatter search for chemical and bioprocess optimization*, Journal of Global Optimization, 37 (2007), 481-503.

[11] Exler, O. and Schittkowski, K.: *A trust region SQP algorithm for mixed-integer nonlinear programming*, Optimization Letters, 1 (2007), 269-280.

[12] Glover, F.: *Heuristics for Integer Programming Using Surrogate Constraints*, Decision Sciences, 8 (1977), 156-166.

[13] Glover, F., Laguna, M., Marti, R.: *Scatter search*. In: Advances in Evolutionary Computation: Theory and Applications, (Eds.A. Ghosh, Tsutsui, S.), Springer-Verlag, New York, 2003, 519–537.

[14] Jones, D.R.: *DIRECT global optimization algorithm*. In: Encyclopedia of Optimization, (Eds.C. A. Floudas and P. M. Pardalos), Kluwer Academic Publishers, Dordrecht, 2001, 431-440.

[15] Laguna, M. and Marti, R.: *The OptQuest Callable Library*. In: Optimization software class libraries, (Eds. S. Voss and D. L. Woodruff), Kluwer Academic Publishers, Boston, 2002, 193-218.

[16] Laguna, M. and Marti, R.: *Scatter search : methodology and implementations in C*. Kluwer Academic Publishers, Boston, 2003

[17] Laguna, M. and Marti, R.: *Experimental testing of advanced scatter search designs for global optimization of multimodal functions*, Journal of Global Optimization, 33 (2005), 235-255.

[18] Rodriguez-Fernandez, M., Egea, J. A., Banga, J. R.: *Novel Metaheuristic for Parameter Estimation in Nonlinear Dynamic Biological Systems*, BMC Bioinformatics, 7 (2006), 483.

[19] Runarsson, T.P. and Yao, X.: *Stochastic ranking for constrained evolutionary optimization*, IEEE Transactions on Evolutionary Computation, 4 (2000), 284-294.

[20] Storn, R. and Price, K.: *Differential evolution - A simple and efficient heuristic for global optimization over continuous spaces*, Journal of Global Optimization, 11 (1997), 341-359.

[21] Ugray, Z., Lasdon, L., Plummer, J., Glover, F., J., K. and Marti, R.: *A Multistart Scatter Search Heuristic for Smooth NLP and MINLP Problems*. In: Metaheuristic optimization via memory and evolution: tabu search and scatter search, (Eds.C. Rego and B. Alidaee), Kluwer Academic Publishers, Norwell, Mass., 2005, 25-58.

[22] Vassiliadis, V.S., Sargent, R.W.H. and Pantelides, C.C.: *Solution of a class of multistage dynamic optimization problems. Problems without path constraints*, Industrial and Engineering Chemistry Research, 33 (1994), 2111-2122. 1593

Corresponding author: J.R. Banga
Process Engineering Group
Instituto de Investigaciones Marinas (C.S.I.C.)
Eduardo Cabello, 6, 36208, Vigo, Spain
julio@iim.csic.es

Received & Accepted: MATHMOD 2009
Revised: September 25, 2009
Accepted: October 20, 2009

Development of a Multi-Rate Simulation Model of an Unmanned Underwater Vehicle for Real-Time Applications

J.J. Zenor[1], D.J. Murray-Smith[2], E.W. McGookin[2] , R.E. Crosbie[1]

[1]California State University, Chico, CA, U.S.A.; [2]University of Glasgow, Glasgow, Scotland, U.K.

SNE Simulation Notes Europe SNE 19(3-4), 2009, 47-54, doi: 10.11128/sne.19.tn.09951

This paper describes work involving the further development and refinement of a mathematical model of an unmanned underwater vehicle (UUV), together with the development of an associated real-time multi-rate simulation that includes both high-speed power electronic sub-systems and slower components. The chosen vehicle uses a battery as its energy source and this feeds an a.c. motor drive through a d.c. to a.c. converter. The drive powers the vessel which is modelled as a six-degree of freedom vehicle with control surfaces. Tests carried out indicate that a careful choice of frame rates can increase the speed of solution by factors of several hundred over solution times when the shortest frame rate is used throughout. These multi-rate solutions were executed faster than real time on a typical laptop even when using 3-D graphical output for visualisation of vehicle motion. The conclusions of the paper are that the modelling and simulation of the UUV has provided a useful test-bed for ideas on multi-rate simulation and has demonstrated that multi-rate real-time simulation is feasible and useful for an application of this kind that includes very fast power electronic sub-systems and relatively slow systems such as the vehicle and battery.

SNE 19/3-4, December 2009

Introduction

A propulsion system for an unmanned underwater vehicle (UUV) involving an electrical drive system presents many interesting design challenges and involves electronic, electrical, mechanical, thermal and fluid dynamic sub-systems. As with any other complex system, analysis of the behaviour of a system of this kind can be greatly facilitated by the use of computer simulation techniques. However, in applications of this kind, simulation-based investigations of the complete system can be computationally very demanding and investigations involving multi-run optimisation studies or real-time simulation can present difficulties.

The conventional approach to simulation of a system of this kind involves the use of a single integration algorithm for all the sub-systems, using an integration step length small enough to produce results with acceptable accuracy for the subsystems with the greatest bandwidth and highest switching frequency. However, the step size chosen to provide adequate accuracy in the high bandwidth components may well be very much smaller than the minimum step length required for the slower sub-systems and the simulation may perform in a very inefficient and slow fashion. In most cases the approach chosen to overcome these problems involves the use of an error-controlled variable-step integration algorithm.

Such algorithms make an estimate of the truncation error arising in each integration step and then automatically adjust the set length so that it is appropriate for the dynamics at all times. This is achieved as follows:

1. if the estimated error is larger than a pre-set tolerance the step is rejected and replaced by a shorter step, or
2. if the estimate is within the tolerance bounds the results of the step are accepted and the simulation continues using that step length, or
3. if the estimated error is much smaller than the pre-set error tolerance the results of the step are accepted and increase the step length in the next integration interval.

In addition, when a model includes switches that require the simulation of very fast changes, an additional feature often is included within the integration algorithm to detect switching events and establish the time (to within a user-defined tolerance) at which each event occurs. The integration step is then adjusted so that one step ends when the discontinuity occurs and the next step starts immediately after the event.

The main benefit of this approach is increased simulation accuracy at the cost, inevitably, of additional computer time.

However, in the case of real-time simulation applications the use of variable step-length integration algorithms and discontinuity detection methods is not appropriate. One possible approach is to sub-divide the complete system model into sub-models having different dynamic ranges. Different time steps can then be used in different parts of the simulation model, giving a simulation which is capable of faster execution because the total number of calculations is significantly smaller. This approach is known as *multiple frame rate* or *multi-rate simulation* and can be applied with many different types of integration algorithm. Although this approach is recognised as offering benefits in terms of reduced computational demands it also raises important issues in terms of the overall accuracy and stability of the simulation.

The task of modelling the power electronic and electrical drive system for an unmanned underwater vehicle (UUV) in real time, or in a time-scale faster than real-time, provides a useful basis for the investigation of general issues arising with multi-rate simulation techniques. Evaluation of the effects of the propeller, control surface and actuator sub-systems on the overall performance capabilities of the vehicle may well require detailed modelling of electrical motors and associated converters coupled to an accurate representation of the relevant actuators and a nonlinear model of the vessel itself. This combination of relatively fast events in the power electronic components and much slower dynamics in the vessel itself raises immediately many of the issues discussed above.

Although multi-rate simulation has been a familiar technique for many years and is featured in a number of commercial simulation software packages, this application is notable because of the combination of a real-time application and the need for very short frame times to handle part of the system. The non-real-time version of this simulation, which has been developed in preparation for the full real-time version, also features use of the Virtual Test Bed (VTB) [1] and its associated 3-D animated graphics output in a faster-than-real-time implementation on a conventional laptop.

1 The underwater vehicle model

The nonlinear dynamic model of an underwater vehicle is commonly represented either in the body-fixed or earth-fixed frames of reference, as described in standard texts on modelling of ocean vehicles (e.g., [2]).

Using the notation adopted by Fossen [2] the general body-fixed vector representation involves the equations:

$$\boldsymbol{M}\dot{\boldsymbol{v}} + \boldsymbol{C}(\boldsymbol{v})\boldsymbol{v} + \boldsymbol{D}(\boldsymbol{v})\boldsymbol{v} + \boldsymbol{g}(\boldsymbol{\eta}) = \boldsymbol{\tau} \quad (1)$$

$$\dot{\boldsymbol{\eta}} = \boldsymbol{J}(\boldsymbol{\eta})\boldsymbol{v} \quad (2)$$

In this representation the matrix $\boldsymbol{M}$ is the inertia matrix and includes added mass effects while the matrix $\boldsymbol{C}(\boldsymbol{v})$ is the matrix of Coriolis and centripetal terms and also includes added mass effects. The matrix $\boldsymbol{D}(\boldsymbol{v})$ is the damping matrix, the vector $\boldsymbol{g}(\boldsymbol{\eta})$ is the vector of gravitational forces and moments and $\boldsymbol{\tau}$ is the vector of external forces and moments. The matrix $\boldsymbol{J}(\boldsymbol{\eta})$ is the transformation matrix relating body-fixed and earth-fixed coordinate systems.

In these equations the body-fixed frame has components of motion defined by the vector $\boldsymbol{v}(t) = [u(t), v(t), w(t), p(t), q(t), r(t)]^T$ relative to a constant velocity coordinate frame moving with the ocean current velocity vector $\boldsymbol{u}_c$. Following the normal convention used in the modelling of marine vehicles (see e.g., [2, 3]) the components of the vector $\boldsymbol{v}(t)$ are the three translational velocities $u(t)$, $v(t)$ and $w(t)$ together with the three angular rates $p(t)$, $q(t)$ and $r(t)$. The six components in the global reference frame involve three variables $x(t)$, $y(t)$ and $z(t)$ that relate to translational motion and three variables $\phi(t)$, $\theta(t)$ and $\psi(t)$ that relate to angular motion of the vehicle. These six components are given by the vector $\boldsymbol{\eta}(t) = [x(t), y(t), z(t), \phi(t), \theta(t), \psi(t)]^T$. The angles $\phi(t)$, $\theta(t)$ and $\psi(t)$ are related through the Euler transformations to the body roll, pitch and yaw motions, while the external forces and moments $[X\ Y\ Z\ K\ M\ N]$ involved in the vector $\boldsymbol{\tau}$ are made up of gravitational, buoyancy, hydrodynamic and propulsive terms. The inputs that generate the external forces and moments required to control the vessel arise from control surface deflections at the rudder ($\delta_r(t)$), port bow plane ($\delta_{bp}(t)$) and starboard bow plane ($\delta_{bs}(t)$), the stern plane ($\delta_s(t)$), together with inputs arising from propeller rotational rate ($n(t)$) and buoyancy adjustment ($B(t)$).

From the above equations it is possible to derive a set of six nonlinear equations for surge, sway, heave, roll pitch and yaw motion [2]. For the purposes of the investigation described in this paper the six degrees of freedom equations of motion of an existing underwater vehicle (the U.S. Naval Postgraduate School (NPS) AUV II) were used.

The specific equations and parameters relating to the NPS AUV II vehicle upon which the work described in this paper is based are those given by Fossen [2], which are, in turn, based on information provided by Healey and Lienard in their paper [3].

The model of the UUV is converted into standard state space form by rearranging Equations (1) and (2) in the following manner:

$$\begin{bmatrix}\dot{\boldsymbol{\eta}}\\ \dot{\boldsymbol{v}}\end{bmatrix} = \begin{bmatrix}\boldsymbol{J}(\boldsymbol{\eta})\boldsymbol{v}\\ \boldsymbol{M}^{-1}\{-(\boldsymbol{C}(\boldsymbol{v})-\boldsymbol{D}(\boldsymbol{v}))\boldsymbol{v}-\boldsymbol{g}(\boldsymbol{\eta})+\boldsymbol{\tau}\}\end{bmatrix} \quad (3)$$

This is the standard state space form for a nonlinear system:

$$\dot{\boldsymbol{x}} = \boldsymbol{F}(\boldsymbol{x},\boldsymbol{u}) \quad (4)$$

where $\boldsymbol{x}$ is the state vector and $\boldsymbol{u}$ is the input vector.

Some important changes had to be introduced to the model, as described by Healey and Lienard [3], in order to get the simulation model to behave in a credible fashion for the range of open-loop conditions and manoeuvres needed in the proposed real-time simulation application. Modifications were made to the equations representing the propeller in order to allow the model to function correctly as the propeller speed dropped to zero.

This involved adopting an approach, first suggested by Fossen [2], in which the original representation of the thrust generated by the propellers was replaced by a quadratic quasi-steady thrust equation relating the propeller speed and the surge velocity of the vehicle. The modifications made to the model also ensured that an undesirable situation involving a divide-by-zero condition that could occur with the original representation with zero initial propeller speed was eliminated.

The main modification involved replacing the thrust equation within the existing model. First it was assumed that the UUV produces a single propulsive force, although it has two propellers.

The resulting thrust produced by the propeller is calculated from the *Bilinear Thruster Model* [2] as:

$$T = T_{nn}|n|n + T_{nu}|n|u \quad (5)$$

The values for the T_{nn} and T_{nu} coefficients can be obtainnn ed from the following equations [2]:

$$T_{nn} = \rho D^4 \alpha_1 \quad (6)$$

$$T_{nu} = \rho D^3 \alpha_2 \quad (7)$$

$$\alpha_1 = 0.12 - 0.5\alpha_2 \quad (8)$$

Here D is the diameter of the propellers, which is given as 30cm. For this application the value for α_2 is chosen to be -0.16, which gives a value for α_1 of 0.019. These values provide the required surge velocity profile for the NPS AUV II. Combining Equations (5) to (8) gives the ideal total thrust produced by the propeller.

However, the efficiency of the propeller is less than 100% and in this case the efficiency has been chosen to be 70%. Therefore, the surge force produced by the propulsion system is found to be:

$$X_{\text{prop}} = 0.7T \quad (9)$$

The other dynamic equations do not have propulsion components since the propeller only produces thrust along the longitudinal axis. Also, the rotational effects of the propellers in roll and yaw are assumed to be negligible since the propellers operate together in a counter-balancing manner.

As well as modelling the propeller in terms of thrust production, this model has an element that approximates the load on the motor shaft caused by the propeller rotating in the water. This approximation is based upon the propeller being considered as a rotating disc.

By applying Newton's Second Law, the moments of the propeller can be considered thus:

$$\sum T_o = I_o \dot{n} \quad (10)$$

Here T_O represents the torques acting on the propeller, I_O is its moment of inertia and n is the rotation speed of the propeller. By considering the total number of moments acting on the propeller, we can derive the equation of motion for the load exerted on the shaft. Firstly there is the lateral drag moment caused by the rotation of the propeller. The drag force generated by the rotating propeller can be calculated using the following standard drag equation [4]:

$$F_{\text{DRAG}} = -\tfrac{1}{2}\rho C_D (n \times R_{\text{DISK}})^2 \quad (11)$$

Here R_{DISC} is the radius of the disc, C_D is the drag coefficient and ρ is the density of water. To calculate the drag moment, the drag force is multiplied by the moment arm of the propeller (i.e., its radius):

$$T_{\text{DRAG}} = F_{\text{DRAG}} R_{\text{DISK}} = -\tfrac{1}{2}\rho C_D n^2 R_{\text{DISK}}^3 \quad (12)$$

Note that the negative sign indicates that the moment is acting in opposition to the rotation of the propeller.

The second moment is the input torque applied by the shaft, T_{SHAFT}. This is the necessary torque needed to be applied to the propeller to make it overcome its drag and inertia components. Both this moment and the drag moment can be combined to give the equation of motion for the propeller:

$$T_{\mathrm{SHAFT}} = I_o\dot{n} + \tfrac{1}{2}\rho C_D n^2 R_{\mathrm{DISK}}^3 \qquad (13)$$

It follows that since the input moment needs to overcome the drag and inertia of the propeller, that it is equal in amplitude to the load on the propeller but acting in the opposite direction. Therefore, the load moment on the propeller, T_{LOAD}, is calculated as:

$$T_{\mathrm{LOAD}} = -T_{\mathrm{SHAFT}} = -I_o\dot{n} - \tfrac{1}{2}\rho C_D n^2 R_{\mathrm{DISK}}^3 \qquad (14)$$

This gives the approximate load on the shaft. The only parameter that is not readily available in this expression is the drag coefficient, C_D, However it is known that a disc rotating about its longitudinal axis has a drag coefficient equal to 1.369×10^{-3} [4] and this value is used in the model. It should be noted that this representation does not take into account added mass and the dynamics of the shaft.

2 The power-electronic and motor drive system model

The vehicle model described in Section 2 was combined with a model of an electrical drive system involving a battery connected to a d.c. to a.c. inverter, consisting of a three-phase six switch network producing a variable-frequency a.c. waveform and an induction motor. The controlled switches in the inverter are operated by on-off commands from a pulse-width modulated controller switching at a frequency of 5kHz. The controller uses a form of proportional plus integral (PI) control for the timing of the on-off pulses supplied to the converter switches to maintain a desired current level in the motor. Switch timings are determined using a well-established approach involving comparison of sinusoidal and triangular waves.

The relative amplitudes of these waveforms are adjusted by the feedback control system and switching occurs when the sine and triangular waves intersect. The a.c. output from the converter is filtered to remove high-frequency harmonics and is then supplied as input to the induction motor. The motor is connected directly to the propeller.

This electrical sub-system has also been described in a number of previous publications (e.g., , [6], [8])

For full mission simulation capability the model must thus be capable of representing accurately the high speed power electronic subsystem, with phenomena involving time intervals of less than 10 μs, over periods of time of the order of seconds, minutes or longer. In some applications it may be important that the simulation model be capable of running in real time or faster than real time.

From the brief description given above, the system is seen to divide naturally into sub-systems that may involve different ranges of frame time for simulation. The convertor is a fast sub-system compared with the dynamics of the vessel and the battery, which can undoubtedly both be classified as slow sub-systems. Between these extremes the controller and motor may be regarded as slow-medium and fast-medium sub-systems respectively. Figure 1 is a schematic diagram of the complete underwater vehicle system showing the interactions between these different sub-systems.

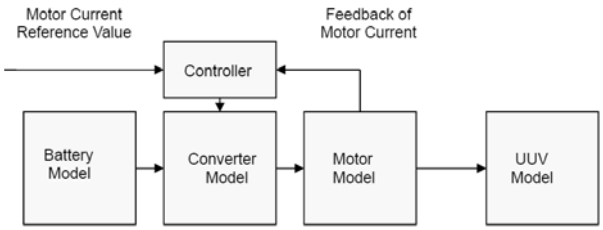

Figure 1. Conventional block diagram representation of UUV model with electrical drive system.

3 Component connections in VTB

The VTB system allows component interconnection without the need for major changes in the coding of those components. This achieved using what are termed “natural” couplings in place of the conventional “signal” connections that are used in traditional continuous system simulation packages. A natural coupling is neither an input nor an output but is a form of connection in which values at each end of the connection must simply be consistent. In the case of an electrical circuit application, for example, the voltage at any connection point is the same for all connected components and the sum of all the currents at that point must be zero.

This is achieved by providing as output the equation that relates the current to the voltage at the connection point, rather than simply outputting a specific value of current given the voltage at that point, as would be the case for a conventional signal connection. An external VTB solver then determines what the voltage would have to be to ensure that the sum of currents from all the connected component models is zero. The equation defining this has the form:

$$\boldsymbol{I} = \boldsymbol{GV} - \boldsymbol{b} \tag{15}$$

Each model is called at time t to output the values of $\boldsymbol{G}$ and $\boldsymbol{b}$ for time $t + \Delta t$. The computation of the elements of $\boldsymbol{G}$ and $\boldsymbol{b}$ involves algebraic manipulation of the difference equations that result from the application of an implicit integration method to the differential equation of the model. Illustrative examples of this procedure may be found in the VTB model development manual [7] and in publications describing the development of the VTB software (e.g., [1]).

A further important feature of the VTB is the provision for "layered models" which allows several versions of a simulation component to be packaged within a single VTB component. Separate icons may be used for each version, with each having different connections.

4 Multi-rate simulation

4.1 Fundamentals of multi-rate simulation techniques

The reason for using multi-rate simulation methods is the fact that this approach can reduce significantly the time for execution of a simulation. This approach was used extensively in the early days of simulation using digital computers but has become less widely used as computers have become more powerful. However the complexity of some present day engineering applications of simulation, such as those arising in the design and development of electric ship systems, makes these techniques potentially attractive, especially in the context of real-time applications or multiple-run simulation studies for design optimisation.

An integration step length of h seconds gives a frame rate of $f = 1/h$ frames per second. In multi-rate simulation it is assumed that integration step lengths $h_1, h_2, h_3, \ldots$ (where h_1 is the smallest) can be chosen so that the ratio of successive step length values

$$r_{ij} = h_i/h_j \tag{16}$$

is an integer.

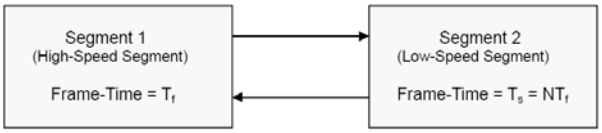

Figure 2: Block diagram illustrating a two-rate simulation with the simulation partitioned into two parts which use different frame times. The slow frame time is an integer multiple of the fast frame time. Communication takes place at the slower frame rate.

Figure 2 illustrates the simplest case of multi-rate simulation with two frame rates corresponding to integration step lengths h_1 and h_2 where $h_2$is related to h_1 through an integer N according to the equation:

$$h_2 = Nh_1 \tag{17}$$

Thus Segment 1 of the model, as illustrated in Figure 2, produces results at a rate of

$$R_1 = \frac{1}{h_1} \tag{18}$$

while Segment 2 produces results at the slower rate of

$$R_2 = \frac{1}{h_2} = \frac{1}{N}R_1 \tag{19}$$

There are several methods that can be used for communicating results between segments. In the case of the two-segment case considered here, the simplest of these involves use of a zero-order hold for transferring data from Segment 2 to Segment 1. Thus Segment 1 uses the same last value received from Segment 2 for N steps until the value from Segment 2 is updated. Values of the output from Segment 1 for communication to Segment 2 have to be averaged in some way over the last N steps of Segment 1 before transfer.

Simple filtering can often provide a natural and convenient form of averaging. An alternative, but more complex, approach to inter-segment communication involves use of a first-order hold involving linear extrapolation to estimate input values for each of the fast steps. An approach which is very similar, but which avoids the use of the first-order hold, can be applied for cases where the value of the derivative of a variable is available as well as the variable itself.

The basis of the method is to calculate both quantities within the slow segment and pass them to the fast segment to allow estimation of the intermediate values using the derivative information.

A further possibility is to stagger the timing of the segments by delaying the slow segment by a time $h_2/2$ so that the slow segment passes values to the faster segment at the mid-point of its cycle of N steps. If there is a significant difference in the step sizes anti-aliasing filters may be required.

4.2 The UUV application

The model of the UUV has been partitioned into sub-systems, as discussed in Section 3 and shown in Figure 1. There is a fast component consisting of the model of the d.c. to a.c. converter which requires step sizes as small as 3 μs, a slow-medium speed component involving the feedback controller, a fast-medium speed component which is electric motor model and a slow component representing the battery, the vehicle and its control surfaces and also involving the interface graphics.

The simulation frame rates used in these four areas correspond to integration periods of 2μs for the converter, 100μs for the motor, 800μs for the feedback controller and 100ms for the battery, vessel and graphical output.

The simulation has been implemented using the Virtual Test Bed (VTB) together with the VXE graphics software which can be used to display graphical and 3-D animations of model behaviour. Both of these software tools were developed at the University of South Carolina [1], [7]. The main benefit of this approach is that the VTB provides a flexible simulation environment which allows sub-system models which have been developed using different simulation tools to be combined. The VTB also incorporates a library which contains a large range of mechanical and electrical components.

Three different programming approaches have been used in the development of the sub-system models because models had been developed by different groups in different locations. The converter, controller and motor sub-models have been programmed using C++ code whereas the model of the vessel is written in Matlab and the d.c. power source is represented using native VTB battery models.

Modules exist in the VTB environment to allow interfacing to many other simulation environments but VTB natural couplings, as described in Section 4, are not directly compatible with traditional signal connections.

Although the converter model is coded using C++, it is implemented as a native VTB simulation model. In this sub-model the d.c. input connection and the a.c. output connections are natural couplings while the connections to the controller are signal couplings. The converter simulation involves Euler integration for the input d.c. filter capacitor and trapezoidal integration for the filter components at the output.

The sine and triangular waveforms of the controller are generated by table lookup with the table entries being scanned at a rate determined by the desired frequency. Linear interpolation is employed with sufficient table entries to ensure a maximum error of one bit. The “layered model” feature of the VTB means that a stand-alone model of the converter can exist alongside a combination system of converter, controller and motor with the icon and executed code being changed by an input parameter. This type of facility has been found to be very useful, especially for fault-finding during the development of the model.

The six degree of freedom simulation model of the vessel was implemented originally in Matlab and involves the use of a fourth-order Runge-Kutta integration algorithm. Fin deflections are applied through the user interface and the propeller shaft RPM is a signal input. The Matlab simulation was translated to C++ and implemented as a native VTB model although the original Matlab model may still be used through the VTB/Matlab interface.

The motor simulation was also implemented in C++ as a native VTB simulation using trapezoidal integration. The a.c. input involves a natural connection but the output connections for the motor model, in terms of the torque and shaft RPM variables, had to be compatible with the model of the vessel. Thus the original VTB model equations for the motor model were re-implemented to have signal connections for the mechanical variables.

Two implementations of the multi-rate simulation have been under development. One of these approaches is based upon a distributed multi-rate solver that forms an integral part of the VTB environment. In this approach the system is partitioned in such a way that each partition contains models that have to be run at the same time step. Connections between the partitions terminate in special VTB “ports”. Each partition has to be distributed to a separately running copy of the VTB, connected using an Ethernet network.

Since the VTB distributed solver was not available when the work started, a less-flexible but simpler, special-purpose, multi-rate solver was developed for initial development and testing of the multi-rate approach. This second "Chico" solver approach involves bundling together the models to be run at different rates within a single VTB "super-model". The VTB then runs at the rate of the slowest model and other models run with a step size that is an integral divisor of the VTB step size.

At each VTB time step the complete bundle of models is called by the VTB and an internal scheduler calls the internal models at the appropriate rate, returning values to the VTB when the elapsed time corresponds to the start of the next VTB step. Natural couplings are handled by a special-purpose internal solver.

Apart from its immediate availability an advantage of the "Chico" solver is a slightly lower computational overhead than that of the general-purpose VTB distributed solver. The main disadvantage is the fact that results could only be displayed at the user interface at the VTB time step.

Other work carried out to support the development of the multi-rate simulation has involved the use of an algebraic manipulation program based on Mathematica. The program takes the differential equations for the model, a list of program names and the corresponding mathematical symbols and a definition of the implicit integration algorithm to be used (e.g., the trapezoidal rule) and computes the difference equations, the equations for $\boldsymbol{G}$ and $\boldsymbol{b}$ and outputs the C++ code for insertion into a VTB program for communicating the values of $\boldsymbol{G}$ and $\boldsymbol{b}$ at each time step. Mathematica could be copied directly into the VTB simulation to implement the changes in a very simple and reliable way.

4.3 Results and verification of the multi-rate simulation

The models were not constrained to real-time execution and faster than real-time execution has been achieved on a typical laptop computer even when using the 3-D graphical output capability provided with the VXE. Work was also carried out to develop non-real-time simulations of the system to allow detailed investigation of the effectiveness of the multi-rate approach, consider detailed issues of frame rates for different sub-systems and prepare the ground for real-time implementation.

The European Simulation Language (ESL) [9] was used to make comparisons of results obtained using multi-rate simulations with conventional simulation results. ESL, which was developed at the University of Salford for the European Space Agency, incorporates a parallel segment feature that supports multi-rate simulations.

One of the important features of ESL is that it can automatically locate switching points, accurately integrate up to the discontinuity and then continue form that exact point. This discontinuity detector allows investigation of the effects of taking fixed time steps in a fast multi-rate simulation and the switching errors introduced for different step lengths. ESL has recently been integrated into the VTB system [10].

5 Discussions and conclusions

The UUV model of Healey and Lienard [3] proved to be a useful starting point in the development of the multi-rate simulation involving the combined model of the vehicle and the electrical drive system. Modifications required in the model of the vehicle were due to problems observed in the behaviour of the model at low values of forward speed and when starting from rest.

These changes in the model, which were successfully implemented in the multi-rate simulation studies, are almost certainly due to the fact that the published model equations were used originally for research involving the development of nonlinear control systems for this underwater vehicle for manoeuvres involving some specific ranges of forward speed.

The observation of some anomalous behaviour in applying the same model for open-loop and manual control investigations over a wider range of speed is perhaps not entirely surprising and emphasises the difficulties likely to be encountered when a model developed for one type application is used for an entirely different type of investigation.

The conclusions of the paper are that the modelling and simulation of the UUV has provided a useful test-bed for ideas on multi-rate simulation and has demonstrated that multi-rate real-time simulation is feasible for an application of this kind that includes very fast power electronic subsystems and relatively slow systems such as the vehicle and the battery.

The VTB software has been a unifying tool in this development work and recent work on the development of an interface between ESL and the VTB makes ESL very attractive as a development tool in work of this kind.

Acknowledgements

The authors acknowledge the financial support from the U.S. Office of Naval Research through Awards N00014-01-1-0394, N00014-04-1-0373, N00014-05-1-0534 and N00014-08-1-0687. They also recognise valuable contributions by Professor Roger Dougal and Antonello Monti and others in the VTB team at the University of South Carolina, and by Dr. John Pearce of ISIM International Simulation Ltd. Contributions made to the development of the simulation by a number of Chico students, including Sourabh Bhalerao and Robert Powelson, are also acknowledged.

References

[1] R.A. Dougal. *Design Tools for Electric Ship Systems*, In Proc. 2005 IEEE Electric Ship Technologies Symp, Philadelphia, PA, July 2005, IEEE, pp 8-11, 2005.

[2] T.I. Fossen. *Guidance and Control of Ocean Vehicles*, John Wiley & Sons Ltd, Chichester, 1994.

[3] A.J. Healey, D. Lienard. *Multivariable Sliding Mode Control for Autonomous Diving and Steering of Unmanned Underwater Vehicles*, IEEE Journal of Oceanic Engineering, Vol. 18, No. 3, pp 327-339, 1993.

[4] S.F. Hoerner, *Fluid Dynamic Drag*, Hoerner Publications, New York, 1968.

[5] D. Word, J.J. Zenor, R. Bednar, R.E. Crosbie, N.G. Hingorani. *Multi-Rate Real-Time Simulation Techniques*. In Proc. 2007 Summer Simulation Multiconf., San Diego, CA, July 2007, SCS San Diego, USA.

[6] J.J. Zenor, R. Bednar, Sourabh Bhalerao, *Multi-Party, Multi-Rate Simulation of an Unmanned Underwater Vehicle*. In Proc. 2007 Summer Simulation Multiconf, Edinburgh, UK, June 2008, SCS San Diego, USA.

[7] The University of South Carolina, The Virtual Test Bed. Online: http://vtb.engr.sc.edu/ [Acc. 23/12/2008]

[8] D. Word, R. Bednar, J.J. Zenor, N.G. Hingorani, *High-Speed Real-Time Simulation for Power Electronic Systems*, Simulation, Vol. 84, pp 441-456, 2008

[9] J.J. Zenor, J.G., Pearce, R. Bednar. *Testing of Multi-Rate Simulations Using the ESL Simulation language*. In Proc. 2007 Summer Simulation Multiconf., San Diego, CA, July 2007, SCS San Diego, USA, 2007.

[10] J.G. Pearce, *Interfacing the ESL Simulation Language to the Virtual Test Bed*. In Proc: 2007 Western Simulation Multiconf., San Diego, CA, January 2007, SCS San Diego, USA, 2007.

Corresponding author: D.J. Murray-Smith
Department of Electronics & Electrical Engineering, University of Glasgow
Glasgow G12 8QQ, Scotland, U.K.
*djms@elec.gla.ac.uk*s

Received:July 2009
Revised: September 5, 2009
Accepted: October 10, 2009

Interpersonal Trust Model

A Netrvalova, J. Safarik, University of West Bohemia, Plzen, Czech Republic

SNE Simulation Notes Europe SNE 19(3-4), 2009, 55-60, doi: 10.11128/sne.19.tn.09953

The paper deals with interpersonal trust modelling. Terms as trust, trust values, trust affecting factors, and representation of interpersonal trust and its implementation are presented. The proposed trust model tries to integrate more factors, which affect trust for trust determination, than usual. The model covers basic factors as reciprocal trust, initial trust, subject reputation, number of subject recommendations, number of mutual contacts, and trusting disposition. The significance of these factors participating in trust forming is discussed. Modifications of parameter values describing mentioned factors and their effects on interpersonal trust evolution are investigated. The interpersonal trust model behaviour is examined by a number of parameter studies. Only some of these studies are presented in this paper and the significant results acquired from them are shown in the graphs.

Introduction

Trust is a unique phenomenon and plays an important role in the relationships among subjects in the communities. These subjects need not be only humans.

In the internet age, the trust among machines, servers, and network nodes gains more and more importance. Widening of e-service [1], e-commerce [2], e-banking, etc., arises the question of human machine trust. Further, trust plays an important role in peer-to-peer networks [3], ad hoc networks, grid computing, semantic web [4], and multi-agent systems, where humans and/or machines have to co0llaborate. Trust models and interpersonal trust models particularly, e.g., [1, 2, 3], are used in those uncertain environments [5, 6, 7].

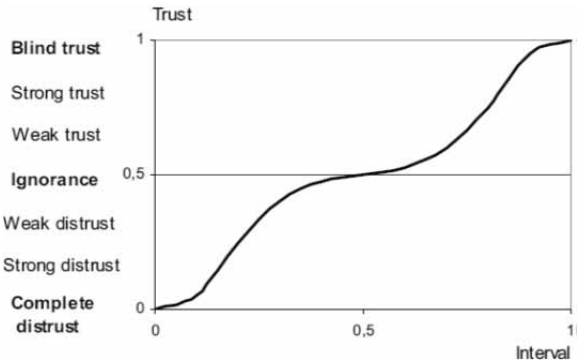

Figure 1. Trust value representation – verbal trust levels are on the vertical axis, real interval ⟨0,1⟩ is on the horizontal axis (example for a trust mapping function).

What is trust and how can it be described? The acceptance of trust is wide and various explanations are offered [8]; from honesty, truthfulness, confident expectation or hope, something managed for the benefit of another, confidence in ability or intention to pay for goods or services in the future, till business credit. A universal trust definition does not exist. Bulk of definitions comes out from Gambetta's definition [9]. We will understand trust as a given credit, hope, confidence in ability or intention of some subject to perform to benefit of another subject at some future time.

Trust models, and interpersonal trust models particularly, e.g., [3, 10, 11], are usually focused on merely one of the factors which trust determine. Each of these factors (reputation, recommendations, and initial trust) can be modelled as an individual component. Our model tries to integrate more of trust affecting factors, i.e. initial trust, reputation, recommendations, mutual contacts, and trusting disposition for trust determination.

1 Interpersonal trust representation

Generally, trust can be quantified by a values from the interval $\langle a, b\rangle$, where a, b $(a < b)$ are integer or real numbers. Value a represents complete distrust and value b is blind trust. Other verbal trust levels are possible to represent by values from this interval. Without loss of generality, we will use real values from the interval $\langle 0,1\rangle$.

A single trust value can be visualized as a point on the line between point 0 and 1 on the horizontal axis, which is acquired by mapping of the respective circumlocution on the vertical axis in Figure 1.

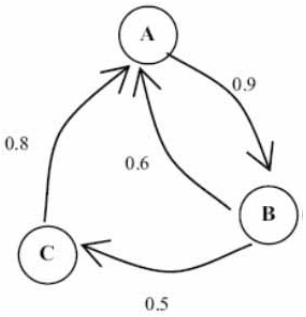

Figure 2. Graph of interpersonal trust in the group – the group consists of three individuals A, B and C, reciprocal trust is between A and B, individual B trusts C and individual C trusts A (example for trust representation).

Generally, the mapping function is neither linear nor symmetrical. Further we will work with trust values from the interval $\langle 0,1\rangle$.

Next, we specify an interpersonal trust representation, i.e. trust between two subjects. Consider a group of n subjects represented as the set $X = \{x_1, x_2, \dots, x_n\}$. The measure of interpersonal trust between the subject x_i and x_j is introduced as follows:

$$t_{ij} = t(x_i, x_j),\ t_{ij} \in \langle 0,1\rangle;\ \ i,j = 1,\dots,n; i \neq j \qquad (1)$$

Further we suppose that both values t_{ij} and t_{ji} exist, thus providing reciprocal trust. The directed weighted graph is applied for interpersonal trust representation in the whole group. Vertices represent the subjects, oriented edges represent trust relations between connected subjects and the weights are trust values. The direction of the edge reflects trust asymmetry, i.e. $t_{ij} \neq t_{ji}$ (trust of the i-th subject in the j-th on may differ, and usually will differ, from trust of the j-th subject in the i-th one).

An example of the representation of interpersonal trust in the group is shown by the graph in Figure 2. The group consists of three individuals A, B and C. The value individual A trusts to B is 0.9, the trust value of individual B to A is 0.6, individual B to C is 0.5, and individual C to A is 0.8. Individual A has no contact to C and C has no contact to B. Note that the graph does not contain self-looped edges.

We use the adjacency matrix, called trust matrix, for graph representations of interpersonal trust in the group. Note that complete distrust is represented by an edge with zero weight, while non-existence of an edge represents the situation when the trust value is not known, e.g., value -1 is used for the matrix element in this case.

The trust matrix for the graph in Figure 1 is following

$$T = \begin{pmatrix} -1 & 0.9 & -1 \\ 0.6 & -1 & 0.5 \\ 0.8 & -1 & -1 \end{pmatrix} \qquad (2)$$

The first line (column) of the matrix represents the trust value of individual A to A, B and C, the second one represents trust of individual B to A, B and C, and the third one describes the same for individual C.

2 Trust affecting factors

Trust forming can be determined by many factors. Based on former related works [3, 10, 11] we consider in our model the following ones: reciprocal trust, initial trust, subject reputation, number of subject's recommendations, number of reciprocal contacts and trusting disposition.

The tendency of reciprocal trust is reflected by the geometric mean. Initial trust to the subject is got on the start. The reputation of the subject comes after individual experience and by some information dissemination about the subject in its neighbourhood and influences trust formation considerably. Trust depends also on the frequency of mutual contacts of subjects.

Next, trust is formed by information about another subject that other subjects have passed on. This information is called recommendation. Trusting disposition representing a degree of non-rational behaviour of a subject is modelled by random factor.

Thus, for trust forming of the i-th subject (trustor) to the j-th subject (trustee) the formula (3) is proposed:

$$T_{ij} = t_{ij} + \sqrt{t_{ij}t_{ji}}\left(\frac{\Delta c_{ij}}{w_{c_i}} + \frac{\Delta d_{ij}}{w_{d_i}}\right)\frac{r_{ij}}{w_{r_i}}\frac{G_{\alpha,\beta}}{w_{g_i}} \qquad (3)$$

where $T_{ij} \in \langle 0,1\rangle$ is the new trust value of the i-th subject on the j-th one, t_{ij} is the previous trust (trust starting value is $t_{0,ij}$) of the i-th subject on the j-th one, t_{ji} is the previous trust of the j-th subject on the i-th one, Δc_{ij} is the relative gain (loss) of the number of contacts between i-th and j-th subject, Δd_{ij} is the relative gain (loss) of the number of recommendations of the j-th subject to the i-th subject, r_{ij} is the reputation of the i-th subject about the j-th one, $G_{(\alpha,\beta)}, 0 < \alpha < \beta \leq 1$ is the trusting disposition expressed by the probability distribution function, w_{c_i} is the weight coefficient of the number of contacts of the i-th subjects, w_{d_i} is the weight coefficient of the number of recommendations of the j-th subject i-th subject, w_{r_i} is the weight coefficient of the effect of

reputation of the i-th subject about the j-th one, and w_{g_i} is the weight coefficient of trusting disposition. Interpersonal trust design is shown in Figure 3.

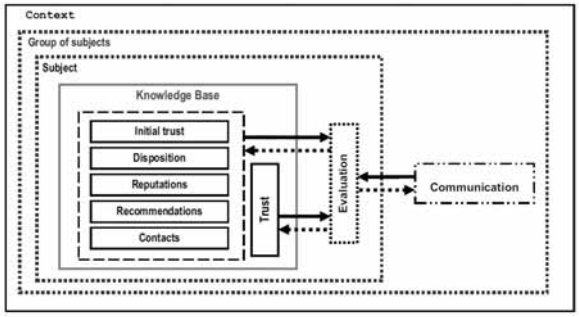

Figure 3. Interpersonal trust design in a group – components of initial trust, reputations, recommendations, contacts, and trusting disposition and trust in knowledge base; evaluation of trust using information from communication between subjects (example for group trust forming).

3 Experiments and results

To pursue trust model behaviour we carried out a series of experiments. The groups of individuals of various sizes have been generated. Reflecting possible non-linearity and/or non-symmetry of the trust distribution, the initial trust matrix and reputation matrix has been chosen with uniform distribution from the interval $\langle 0,1 \rangle$ randomly. The number of contacts among the selected subjects and the number of recommendations of these subjects where stepwise set up and trust forming was pursued. An example is presented below.

Values of initial trust ($t_{0_{ij}}$) and reputation (r_{ij}) of six selected couples are in Table 1 and Table 2. The scenarios of the number of mutual contacts (c_{ij}) and the number of recommendations (d_{ij}) are in Table 3 and Table 4.

First, we have looked how trust is formed in various cases of selected individual relationships. Reputation of individuals is given on the start and as it is rather persistent, it is invariable for all calculated steps. Trusting disposition was generated for each individual of couple. Weight of reputation of individuals was constant, and weight of trusting disposition was not applied ($w_{g_i} = 1$).

$t_{0_{12}}$	$t_{0_{14}}$	$t_{0_{25}}$	$t_{0_{32}}$	$t_{0_{34}}$	$t_{0_{54}}$
0.97	0.35	0.41	0.55	0.03	0.31

Table 1. Initial trust of selected couples – numbers of selected couples are in the 1st line, values of initial trust are in the 2nd line (example for initial trust setting).

r_{21}	r_{41}	r_{52}	r_{23}	r_{43}	r_{45}
0.27	0.14	0.34	0.84	0.74	0.79

Table 2. Reputation of selected couples – numbers of selected couples are in the 1st line, values of reputations are in the 2nd line (example for reputation setting).

Step	c_{12}	c_{14}	c_{25}	c_{32}	c_{34}	c_{54}
0	0	0	0	0	0	0
1	2	1	1	2	0	0
2	4	1	0	0	0	0
3	0	2	0	0	0	0
4	0	2	0	0	0	0
5	0	0	0	0	0	3

Table 3. Numbers of mutual contacts of selected couples – number of selected couples are in the 1st line, step number is in the 1st column (example for number of contacts).

Step	d_{12}	d_{14}	d_{25}	d_{32}	d_{34}	d_{54}
0	0	0	0	0	0	0
1	1	1	1	1	1	1
2	3	0	1	0	0	0
3	0	0	1	0	0	0
4	0	2	1	0	0	0
5	0	0	0	0	0	2

Table 4. Numbers of recommendations of selected couples – number of selected couples are in the 1st line, step number is in the 1st column (example for number of recommendations).

The behaviour of six selected relationships $s_1 \rightarrow s_2, s_1 \rightarrow s_4, s_2 \rightarrow s_5, s_3 \rightarrow s_2, s_3 \rightarrow s_4$ and $s_5 \rightarrow s_4$, where $s_i \rightarrow s_j$ represents relationship involving i-th and j-th subject, is described in short. Trust evolution of selected couples is depicted in Figure 4.

- $s_1 \rightarrow s_2$: Subject s_1 trusts s_2 strongly (0.97), but s_2's reputation is low (0.27). The number of mutual contacts and the number of recommendations influences trust increasing particularly in the first and second step.
- $s_1 \rightarrow s_4$: Subject s_1 distrusts s_4 weakly (0.35), s_4's reputation is even lower (0.14). Influence on trust evolution is low, with exception of the fourth step. This is an example of changing dynamics.

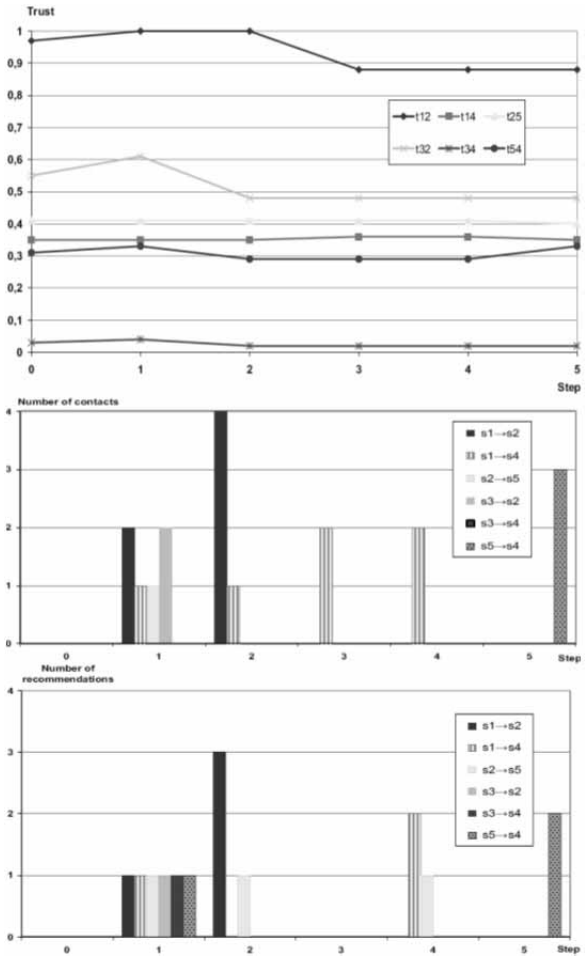

Figure 4. Study of trust forming for six relationships of individuals – upstairs is trust forming for six selected relationships between subjects, in the middle is stepwise number of contacts, at the bottom is stepwise number of recommendations (example for trust forming).

- $s_2 \rightarrow s_5$: Subject s_2 distrusts s_5 weakly (0.41), reputation of s_5 is moderate (0.34). Numbers of contacts and recommendations are low, trust does not change.
- $s_3 \rightarrow s_2$: Subjects s_3 trusts s_2 close to ignorance (0.55), s_2's reputation is high (0.84). Contacts and recommendations noticed in the first step caused trust increase followed by its decrease.
- $s_3 \rightarrow s_4$: Subject distrusts s_4 strongly (0.04), s_4's reputation is high (0.74). High reputation and recommendation produce trust increase in the first step.
- $s_5 \rightarrow s_4$: Subjects s_5 distrusts s_4 weakly (0.31), s_4's reputation is high (0.79). Recommendation in the first step, contacts and recommendations in the fifth step influence trust increase in these steps and decrease in the second step.

Experiments studying the influence of reputation were performed next. The number of contacts and the number of recommendations were stepwise increased to illustrate trust forming.

Trusting disposition was generated randomly for every subject and every step. Five values of reputation were chosen (0.2, 0.35, 0.5, 0.65, and 0.8). This study was performed with the same parameters, trust matrix and number of contacts, recommendations and steps.

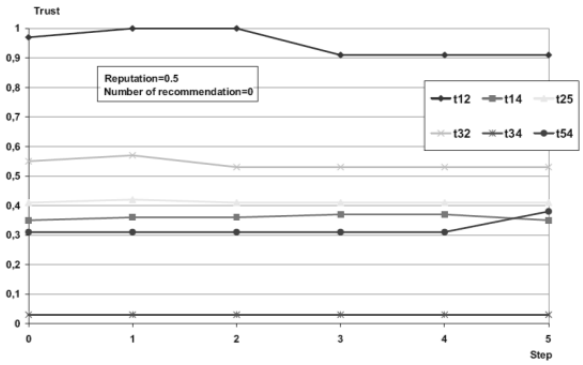

Figure 6. Study of number of contacts influence – reputation size is 0.5; number of recommendations is zero, the results for six couples of individuals (example for study of contacts influence).

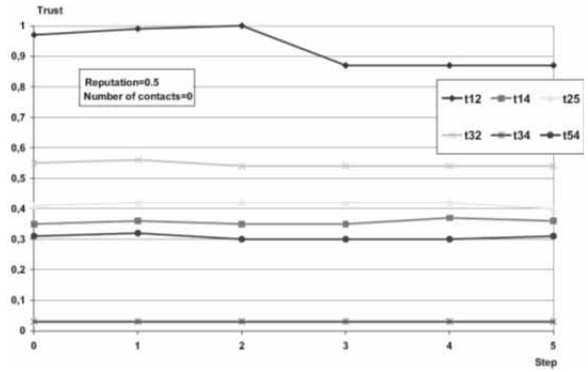

Figure 7. Study of number of recommendations influence – reputation size is 0.5; number of contacts is zero, the results for six couples of individuals (example for study of contacts influence)

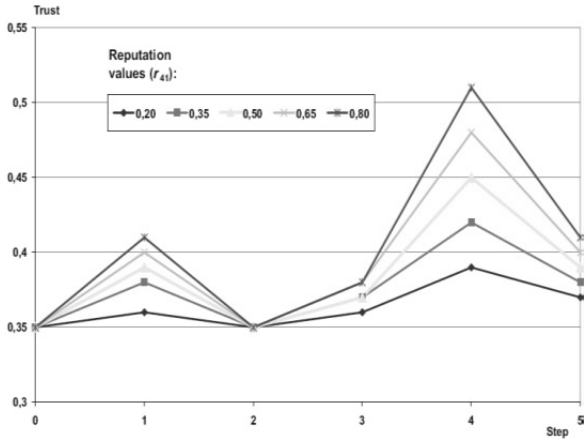

Figure 5. Study of size reputation – reputation values 0.20, 0.35, 0.50, 0.65, and 0.80, on horizontal axis are the steps (0 – 5), and on the vertical axis are trust values (example for reputation size study).

The reputation study results of relationship $s_1 \rightarrow s_4$ are shown in Figure 5. Trust increase and decrease followed the number of contacts and recommendations accordingly. The increasing value of reputation causes trust increase, which can be scaled using the weight coefficient w_{g_i}.

The study of contact influence and recommendation was performed for a mean value of reputation. While influence of contacts was examined, then number of recommendations was neglected and vice versa.

The results for six selected couples are presented in Figure 6 and Figure 7.

Results of recommendation influence indicated greatest change in relationship $s_1 \rightarrow s_2$ due to loss of recommendations, changes in relationship $s_3 \rightarrow s_2$,$s_1 \rightarrow s_4$, $s_2 \rightarrow s_5$, and $s_5 \rightarrow s_4$ were smaller, no trust change was in relationship $s_3 \rightarrow s_4$.

4 Conclusion and future work

We developed an interpersonal trust model integrating factors influencing trust evolution. The experiments proved that its behaviour to be in accordance with models considering a particular factor or a subset of factors in our model.

The model provides trust formation reasonably sensitive to parameters in the proposed formula. Hence, they can be tuned to reflect trust formation under various conditions.

Next, we intend to pursue the collaboration with sociologists to apply the model to real cases. The model itself will be deployed in an agent-based trust management model under development

Acknowledgements

This work was granted by the Ministry of Education, Youth and Sport of the Czech Republic – University spec. Research – 1311.

References

[1] Liu Y., Yau S., Peng D., Yin Y.: *A Flexible Trust Model for Distributed Service Infrastructures*. In Proc. 11th Symp. on Object Oriented Real-Time Distributed Computing, pp. 108 – 115, Orlando, USA, 2008.

[2] Zhang Z., Zhou M., Wang P.: *An Improved Trust in Agend-mediated e-commerce*. International Journal of Intelligent Systems Technologies and Applications, Vol. 4, pp. 271 – 284, 2008.

[3] Wu X., He J., Xu F.: *An Enhanced Trust Model Based on Reputation for P2P Networks*. IEEE Int. Conf. On Sensor Networks, Ubiquitous and Trustworthy Computing, pp. 67 – 73, Taichung, Taiwan, 2008.

[4] Wang X., Zhang F.: *A New Trust Model Based on Social Characteristic and Reputation Mechanism for the Semantic Web*. Int. Workshop on Knowledge Discovery and Data Mining, Univ. Of Adelaide, pp. 414 – 417 , Australia, 2008.

[5] Wang Y., Varadharajan V.: *Role-based Recommendation and Trust Evaluation*. In: Proc. 9th IEEE Int. Conf. on E-Commerce Technology and 4th IEEE Int. Conf. on Enterprise Computing, E-Commerce and E-Services, Tokyo, 2007.

[6] Camp L., Friedman A., Genkina A.: *Embedding Trust via Social Context in Virtual Spaces*. www.ljean.com/files/NetTrust.pdf, cit. 2008-09-12.

[7] Velloso P., Laufer R., Duarte O., Pujolle G.: HIT: *A Human-Inspired Trust Model*. In: IFIP International Federation for Information Processing, Volume 211 (2006), pp. 35 – 46, Boston Springer.

[8] *The World Book Dictionary*. World Book Inc. Scott Fetzer Company. The World Book Encyclopedia, Chicago, 1998.

[9] Gambetta D.: *Can We Trust Trust?* In D. Gambetta, ed.: Trust: Making and Breaking Cooperative Relations, electronic edition, Department of Sociology, Univ. of Oxford, chapter 13, pp. 213 237, www.sociology.ox.ac.uk/papers/gambetta 213- 237.pdf, accessed 2008-10-14.

[10] Lifen L. *Trust Derivation and Recommendation Management in a Trust Model*. In: Proc. Int. Conf. on Intelligent Information Hiding and Multimedia Signal Processing, pp. 219 – 222, Harbin, China, 2008.

[11] Ryutov T., Neuman C., Zhou L.: *Initial Trust Formation in Virtual Organizations*. Int. Journal of Internet Technology and Secured Transactions, Vol. 1 (2007), No. 1–2, pp. 81 – 94.

Corresponding author: A. Netrvalova
University of West Bohemia
Department of Computer Science and Engineering
Univerzitni 22, 30614 Plzen, Czech Republic
netrvalo@kiv.zcu.cz

Received & Accepted: MATHMOD 2009
Revised: September 12, 2009
Accepted: October 10, 2009

A Hybrid Model for Simulating Room Management Including Vacation Times

S. Tauböck[1], N. Popper[2], M. Bruckner[1,2], D. Wiegand[1], S. Emrich[1], S. Mesic[1]

[1] Vienna University of Technology, Vienna, Austria

[2] "die Drahtwarenhandlung" Simulation Services, Vienna, Austria

SNE Simulation Notes Europe SNE 19(3-4), 2009, 61-66, doi: 10.11128/sne.19.tn.09955

Aim of this project as a part of the simulation system <more space> is to simulate the movement of students between lecture rooms, attending their regular curriculum to implement dynamic vacation times. Major outcome is the calculated time which they need to move from a starting point (for example an auditorium) to another location (arrival point). The program is realized in the object-oriented programming language *Java* and connected to *Enterprise Dynamics*. Modeling approaches are *Cellular Automata* (CA) and discrete simulation because the literature of this approach is widely spread, and after analysis of the project, the cost-benefit calculation for this modeling was the best. One advantage especially shows that the CA can manage the dynamic behavior of the students finer and more efficient. This justifies the cost of planning and implementation of the corresponding interfaces. The goal of the project <*more-space*> is to develop software that shall support the planning phase of *University2015* - a project of the Vienna University of Technology (TU Vienna) to renovate all university buildings and to improve the existing infrastructure and the inherent processes – by determining and evaluating the (spatial) resources required and introducing a model for the room management that can simulate the usage of resources to optimize the planning of the rooms and the future "real-life" usage. The dynamic model implemented in *Enterprise Dynamics* is the main model and simulation system including the data model, process descriptions and dynamic behaviour as using of resources depending on different system or environmental dependencies.

Introduction

The project <*more-space*> was launched to develop software that shall support the planning phase of *University2015*. University2015 is a project of the Vienna University of Technology (TU Vienna) to renovate all university buildings and to improve the existing infrastructure and the inherent processes. This shall also be done by determining and evaluating the (spatial) resources required. In 2008 the working group consisting of the Research Group for Mathematical Modelling and Simulation and the Research Group for Real Estate Development and Management at the Vienna University of Technology were asked by GUT TU, co-responsible for Project Management of *Univercity 2015*, to introduce a model for the room management that can simulate the usage of resources to optimize the planning of the rooms and the future usage.

A classical discrete event simulator was chosen to develop the dynamic simulation including features like different possibilities of room selection, different management of the resources, variability of classes, class structures and number of students – only to mention a few of the features. This discrete dynamic simulator was combined with – and is guided by – methods and procedures of the real estate management like business process models. In the course of developing the first studies the working group identified two main problems that are different to tasks which are normally solved by classical discrete event models. On one hand the interfaces to data collection and booking system had to be improved and standardized. Booking features and also the representation of data was not sufficiently optimized neither to the needs of the simulation tool that has to be implemented nor to the needs of the future booking system that has to be simulated. On the other hand the buildings of the Vienna University of Technology – as the university will not move out of the city of Vienna – remain very scattered over a few districts of the city. Therefore a simulation of room booking and facility management has to implement different kinds of vacation times for students and teachers. Even more the problem of different structured buildings within the university had to be implemented and therefore event a big variety of vacation times even between classrooms within some buildings.

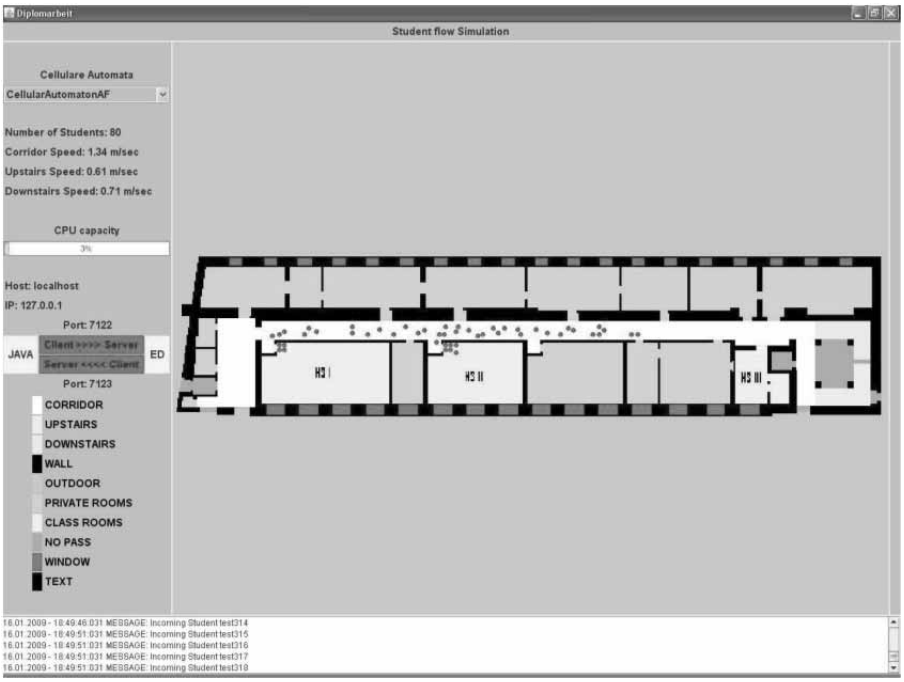

Figure 1. GUI in JAVA with CA of the

The idea was to combine the classical discrete simulation approach (because of its many advantages in questions of room booking, event queues, managing different numbers and kinds of servers) with a classical cellular automata to implement not only vacation times between buildings in different areas but also vacation times within the buildings itself.

This system is furthermore backuped with a dynamic computation of vacation and room clearance times in Taylor ED, as for static values (i.e. areas were the vacation times to not differ influenced by dynamic parameters) values can be computed in the discrete simulator itself. As a result using CAs an added value is given, as such models can – with some modifications – could be used for simulation of escape routes in emergency cases as well. [3]

Implementing the hybrid system different problems occur. For example questions of solving interface problems between Taylor ED and the CA implemented in JAVA had to be solved. Another question was to solve the problem of importing a huge amount of building data - that changes more or less often - into the Cellular Automata.

1 Hybrid model

Main elements of the hybrid model are "Students", these entities are moving through the existing structure of CA i.e. the “Building structure”. The building structure is processed on basis of CAD plans of the buildings. The students are forwarded from the simulation from ED, and processed as long as they do not reach their goal and then send back to ED. In order to make a smooth cooperation and for automation the capture of data, the following approaches have been chosen.

1.1 Representation of building structures

Building structures are based on plans and CAD Data of the University. At the moment those data is transformed manually to the needed structure described in the following part. As planned for future working processes those representation of different areas within the building should be integrated into the specifications for architects and planning offices to improve the speed of integrating different plans into the simulation system.

The building structure and related data are saved as an image file in the Portable Network graphics (.png) format and additional information is stored in two text files (.txt).

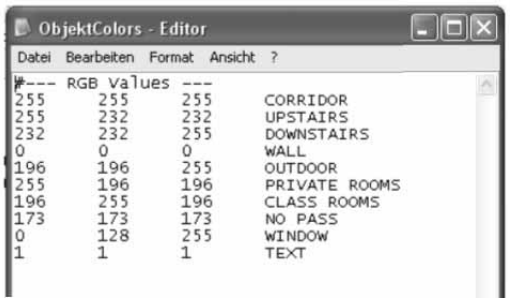

Figure 2. Text File describing the different colours for different areas within the Cellular Automata

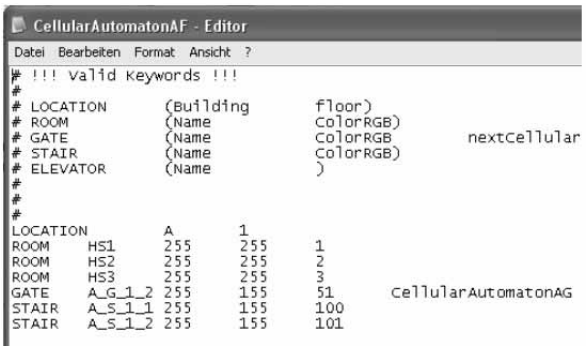

Figure 3. Text File describing special information for every instance of the Cellular Automata.

The image file includes the ground plan of the section that should be read and represents the structure of the Cellular Automata and the room arrangement (subdivision in private rooms and lecture halls) the staircases and the corridors (see Figure 1). Because elevators are not implemented in the simulation at the moment, they are inked in the colour code `NO PASS`, so as an area which is not accessible for students. Staircases are subdivided in `UPSTAIRS` and `DOWNSTAIRS`. The reason for this is because there is a difference between the average speeds a person can have upstairs or downstairs. While the upstairs velocity is approximately 0.61 m/sec you can move downstairs about 0.71 m/sec. With the colour code `CORRIDOR` in the image file the corridors are marked which you can cross with 1.34 m/sec. This is also the last of the three different speeds that are used in the simulation. Colour code `PRIVATE ROOM` are rooms such as offices, toilets, or similar marked which are not of direct benefit for students, while `CLASS ROOM` indicates space for the pure teaching (lecture rooms, laboratories, etc.).

Furthermore we have the area `WALL` which represents the walls, `OUTDOOR` represents the external areal and `TEXT`, indicates text in the graphic file that can give additional information. Plans of the buildings are at the moment separated into different areas; mostly one wing of one level is stored in one .png file. The corresponding levels or wings are connected via stairs (up- or down) or exits which are coded in a relatable way.

The first text file contains general information about the colours. Information is given for all ten different types of ground a particle can reach. Those colours have to be standard for all maps within the whole simulation and cannot be changed.

The second text file is especially for each image file and contains information about the colours that are used only in this image. This information is required to connect the single Cellular Automata, as a lot of different automata are processed on basis of one single plan. So we have to distinguish between exit of a particle between exit of a building or into a lecture room. In these cases the particle returns to the discrete Taylor ED model and leaves the CA model. The other possibility is - as mentioned - exiting one CA model via stairs or an exit to another level or wing of one building.

In this case exit IDs are used as shown in Figure 3 for identifying the following CA which the particle has to enter. For this reason a few “Key Words” are allowed. To mention `LOCATION`, `ROOM`, `GATE`, `STAIR` or `ELEVATOR`. These “key words” can have additional information about the change between the two different Cellular Automatas, for example information about the building number and the level where the CA is located or as well information about gates and stairs and which other CA they are connected to. Last but not least also information about the different lecture rooms is coded for every CA for additional information.

The whole structure of the systems is very simple. This simplification was a main goal in planning and structuring the whole simulation set. On one hand the data interface for getting information is complicated as plans change very often.

For this reason the interface should be very easy to use not only for members of the research group but also for architects or other persons working with the plans.

As mentioned above in future work processes even the producers of such plans should be able to more or less automatically implement a sufficient level of information for exporting data to the simulation system in their CAD software. In this case the best quality of information could be provided.

For this reason a mode was chosen, were data is defined not with classical matrices but with simple color codes, which are defined in one of the text files. On the other hand – as described above – the simulation has to handle a huge amount of data. Vienna University of Technology has to coordinate over 9.000 rooms in about 26 objects spread over the whole inner city of Vienna. A total floor area of about 276.000 square meters would result in a total matrix size for the CA of about 17.700.000 cells.

To handle those sizes two strategies were implemented. First of all the size of the matrices are not constant but variable to reduce the amount of cells. Second for this reason and for future parallelization reasons the plans were cut into a lot of different, small sub-planes to process them in an easy way. So the question of how to connect the different Cellular Automata instances is (and will be) of big importance.

1.2 Cellular automatas

The Cellular Automatas for different levels are connected at certain points, the gates or stairs. Superior structure of the cellular automata is a weighted undirected graph. Nodes are stairs, rooms and gates, Edges are the routes between the nodes with the distance as weight. In order to search for the shortest route across several CAs the Dijkstra algorithm is used.

So subdividing the CA with a size of about 18 Million cells into a number of “Sub-CAs” was described in the chapter above. The reason for this high amount of cells results as the size of a cell is assumed with 0.125×0.125 m – 64 cells per square meter, This assumptions had to be made to make the data connection to CAD possible on the one hand, and on the other hand to reach a sufficient grade of details for implementing the simulation system. Each student occupies 4×4 cells or 0.5×0.5 m value in normal transport areas, but the value is different for students in class rooms for example. In conclusion cell sizes are not constant, and especially the amount of cells a student needs. A reason for this can be found in the different ways the area a student needs is computed in the “real life” system.

As student space in lecture rooms is computed directly from the floor area in the specific lecture room, in laboratories the situation is of course totally different. A fixed number of working places are here to be used, no matter how big the room is on the plan or in “real life”. This is only a small example of how different the systems, measures and real situations are handled - and so have to be handled and computed within the simulation system.

For speed values of individuals in the system some information is described in Chapter 1.1 as the speed results of the different grounds particles can walk over. While on stairs the upstairs velocity is approximately 0.61 m/sec an individual can move downstairs with about 0.71 m/sec. On corridors particles can cross with 1.34 m/sec. But the ground is not the only influence on speed of individuals. Another influence is the density of particles in an area. This is well known from simulation tools for escape routes in emergency situations and was also taken and integrated in the model.

At the moment two additional points are examined. On one hand the question whether the areas between the different buildings should be implemented via CAs or not. As mentioned above in the outlines of the simulation structure this idea was integrated. At the moment results are not significant, whether the amount of computational time is reasonable. Results of tests have to be validated, at the moment the idea of combining an Agent Based simulation as it is used in [2] is examined. On the other hand interfaces to integrate clearance time for different types of lectures in different types of rooms have to be integrated into the system as well.

2 Interface between Java and TaylorED

Because the Java program for Cellular Automatas is of course only a part of the simulation system, it is necessary for data exchange to establish a connection between the two simulations. This interface was implemented with the aid of the Transmission Control Protocol and the Internet Protocol, or short TCP/IP.

2.1 Java cellular automata

Basically, the communication is divided into two different parts sending and the receiving data. Differences between these two states are the allocation of server and client functions.

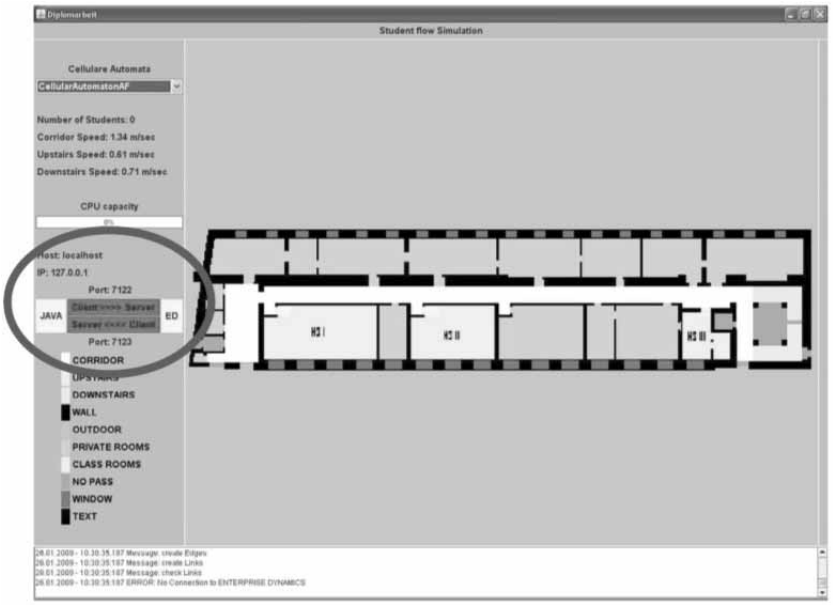

Figure 5. Representation of the Interface in JAVA GUI

In the implementation of this interface it is only a unidirectional traffic towards server possible, however, for this simulation bidirectional data traffic is required, so both Java and ED act as server and client at the same time.

The red area in the picture shows the most important information for communicating. From starting above the first three lines contains information about the Java client. In our case, both programs are running on the same computer so Java can send data to the ED server while it is sending to the host `localhost`, the loopback address `127.0.0.1` and the port 7122. Conversely Java acts as a server and receives data on port 7123. The underlying two yellow boxes with the content "JAVA" and "ED" represent the two programs, which are connected via a network. The status of the connection (red is a disturbed connection) will be symbolize by the two bars in the middle. Faultless connection is signaled with green color. The status check is realized with the aid of a well-defined message ("`PING`") by sending from Java in a parametric time interval to ED who must respond with the message ("`ALIVE`") in also a parametric time.

2.2 Discrete Event Simulation in Taylor ED

Taylor ED offers several Interfaces to communicate with external programs, for example DDE and ADO for communication with databases:

- *4d script commands* for execution of DDL functions
- Exchange of socket messages to allow communication via the *TCP/IP ports*
- *Sending and receiving emails* to communicate worldwide

For this particular simulation the communication using socket messages is used. It allows exchanging ASCII messages via a TCP/IP port. These messages are sent and received by a specified atom in ED; incoming messages trigger the so called `ONMESSAGE`-Event Handler of this atom, that contains the code sequence to be executed.

Enterprise Dynamics sends a message containing the students ID, the current position and the room the student has to move to, to the agent based model. A confirmation message ensures that the message was received; after processing this student the agent based model sends a return message that contains the ID of the student as well as the description of their movement: the current position as well as the time needed to cover the distance between former and current position.

So the interface is implemented with a few lines of code. As the system has to be called for every change for every student at the moment a kind of pulsing was integrated to collect requests.

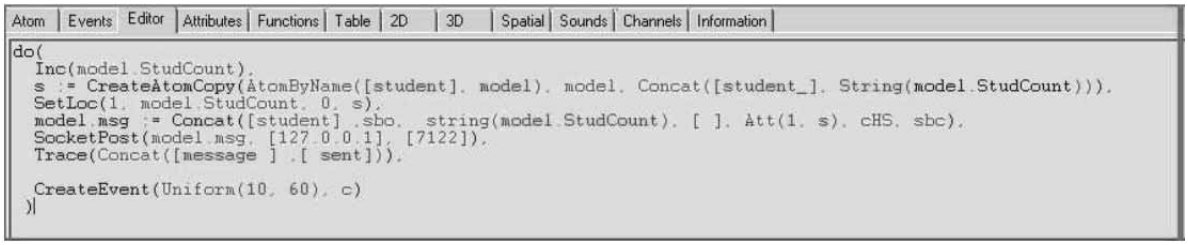

Figure 6. Screen Shot of Code sending a socket message at a student's (individuals) query for changing room

3 Conclusions

Combining different model types to implement hybrid simulation systems can solve some classical problems. On the other hand some other problems may occur. In this paper some aspects of possible advantages of such implementations were mentioned and combining positive characteristics of different model types like different possibilities of data identification, implementations of data interfaces or structural advantages were shown.

As Cellular Automatas were introduced in this simulation system to represent a model computing vacation times it was no choice in the setting of the whole project to re-implement the whole discrete system. A standard software for implementing parts like queuing, servers and so on would be a huge amount of work. So on the other handsome disadvantages like implementing interfaces for connecting the different "sub models" had to be accepted. As work on this project is in progress the quantitative results for the whole system with about 9.000 rooms and – in future – maybe about 30.000 students has to be validated.

References

[1] Breitenecker, F. and Solar, D. *Models, Methods, Experiments – Modern aspects of simulation languages*. In: Proc. 2nd European Simulation Conference, Antwerpen, 1986, SCS, San Diego, 1986, 195 - 199.

[2] Emrich S. et al., *Simulation of Influenza Epidemics with a Hybrid Model – Combining Cellular Automata and Agent Based Features*, In: Proc. ITI 2008 30th Int. Conf. on Information Technology Interfaces, 2008

[3] Tauböck S. and Breitenecker F. *Features of Discrete Event Simulation Systems for Spatial Pedestrian and Evacuation Dynamics*. In: Proc. PED 2005, 3rd Int. Conf. on Pedestrian and Evacuation Dynamics 2005, Vienna, Austria

Corresponding author: S. Tauböck,
Vienna University of Technology
Dept. for Analysis and Scientific Computing
Wiedner Hauptstrasse 8 - 10, 1040 Wien, Austria
shabnam.tauboeck+e101@tuwien.ac.at

Received & Accepted: MATHMOD 2009
Revised: September 21, 2009
Accepted: October 10, 2009

TN

A Simulation Model of the Interactions between Power Producers and Customers

Iana Vassileva, Cajsa Bartusch, Fredrik Wallin, Erik Dahlquist, Mälardalen Univ., Västerås, Sweden

SNE Simulation Notes Europe SNE 19(3-4), 2009, 67-74, doi: 10.11128/sne.19.tn.09957

We have had a strong mechanism for interaction between power production companies and the power trading/supplier companies for a number of years by now. In the future we can expect new types of more interactive communications between single customers and groups of customers towards the energy market companies. We can also expect a stronger demand-side from the customers, e.g. to buy only green energy, only nuclear etc. Power (kW) will be an important parameter aside of energy (kWh) and there will be new possibilities to buy energy when it is as cheap as possible. This may include new applications like charging batteries for your car when the electricity price is low. Differentiation of price may be not only as a direct function of time, but also energy availability like when it is windy, as wind power becomes a major part of many energy systems. Energy storage will be more important and perhaps we will get new possibilities to buy shares in central energy storages, in the same way as space is bought at servers for your applications, photos, webpages etc. Other type of functions may develop as a result of the introduction of individual metering of first electricity and later on hot water and temperature. By metering the individual consumption and billing the exact amount that has been consumed, there will also increase the driving force also to perform energy and load saving actions, e.g. turning off high demand functions like “infra-heating”, “large screen TV” and similar, when other usages are on, and the price is high. We expect displays with interaction possibilities in all homes, where you can see your consumption and pricing information. These new type of systems will put new demands on both hardware for supply and software to handle the services/functions. As part of developing this, mathematical modelling of the systems and tests with simulators will be an important tool. Also new soft ware functions will be developed to support the actual services, like simulators giving information on how different actions you make as a user will influence your energy consumption in the future, both short term and more long term. For the more long term case, new investments in new hardware and software may be proposed and evaluated for users in both technical and economic terms.
In this paper the system aspects including the costs is analysed through a simulation model. This includes the physical system as well as the user behaviour and possible effects of different price models, like a combination of kW and kWh. The effect on the users, the distributors and the power producers are evaluated.

1 Background

The total energy demand is approximately 400 Wh/y in Sweden. From this the total electricity demand is 146 TWh/y. 45 TWh/y of this is used to heat buildings. The electric power production is primarily made by Nuclear power 70 TWh/y and Hydro power 70 TWh/y. The maximum electric power is 27 500 MW, but this capacity is only needed when it is really cold outside, or large amounts of electricity is exported to other countries. Principally 9 000 MW is used for peak load when it is very low outdoor temperatures. It may also be possible to import power during peak load, but then the capacity of the transmission lines will be the limiting factor.

The settlements around the cities are expanding. This leads to a need for new cables and other equipment like transformers or to limit the maximum power, e.g. by differentiated prices.

In general, the potential for energy reduction can be promoted in three main sectors of energy users: in households, office buildings, and industry. This potential can be achieved by implementing various techniques and initiatives oriented at changing consumers’ behaviour in the direction of more efficient energy use.

There are economic incentives for limiting peak loads. Old hydro power plant operation cost is 20 – 30 SEK/MWh in Scandinavia. The cost for old nuclear power is approximately 160 – 200 SEK/MWh, while old combined heat and power plants (CHP) have a cost of approximately 180 – 250 SEK/MWh. New wind power will have a total cost of some 300-700 SEK/MWh while new coal condensing has an installed cost of 30 000 SEK/KW to be compared to 15000 SEK/KW just five years ago..

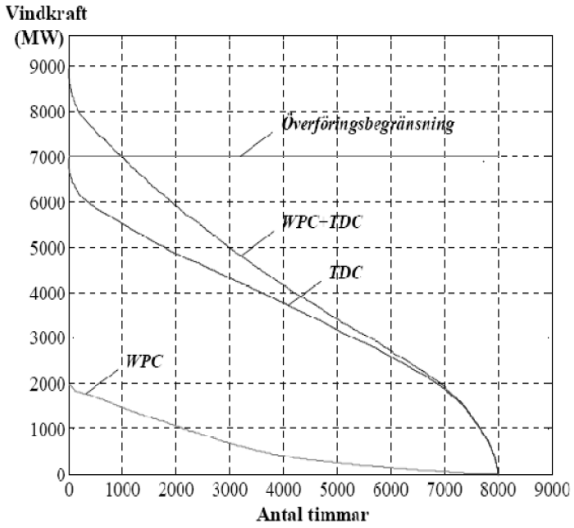

Figure 1. Number of hours per year at a certain power level for a maximum 2000 MW wind power park (WPC). TDC is the actual total power transmitted from northern Sweden to the Stockholm- Malardalen area. The WPC+TDC would be the total if 2000 MW wind power was installed. 7000 MW is the maximum transmission capacity today. The diagram is from the report by [2] Sveca and Söder [2002].

This means some 600- 800 SEK/MWh electric power. The new natural gas (NG)CHP with a combined cycle in Malmö costs approximately 50 000 SEK/MWel. The figures were recently calculated by [1] Swedenergy (2008).

What we can see from this is that wind power has a major interest from a cost point of view. A problem still is that the wind intensity is not correlated to the demand for electricity. In figure 1 we can see a diagram showing power output at different level as a function of the total number of hours at this production level per year.

The other end of the power chain is represented by the energy consumers. The consumption patterns vary very much between different users. In Figure 2 below it is possible to see variations in apartments in Vasteras during 2005-2006. What we can see from this is that the electricity consumption for apartments heated by in this case district heating, the electricity demand is not at all correlated to the size of the apartment. The number of people in each apartment is also roughly the same [3] Vassileva et al (2008).

If we look at single houses [4] Bartusch et al (2008) the situation is similar. The variation between different houses does not correlates to the number of persons living in them (figure 3).

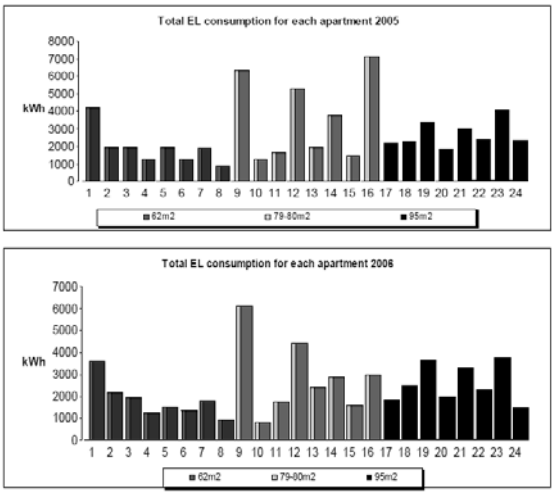

Figure 2. Electricity consumption patterns in apartments with district heating. The first 8 apartments are 62 m^2, next 8 79 – 80 m^2 and last 8 96 m^2

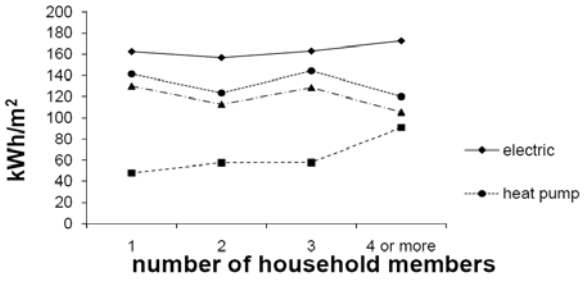

Figure 3. The energy consumption correlated to the number of inhabitants in single houses for households with different type of heating systems: direct electric, electric with heat pump, combined electric and biofuel stove and non-electric

It is also interesting to see that households with direct electric heating have almost the same energy consumption as those with a combined heating system. Only for houses with non-electric heating we see some correlation for very large families compared to those with fewer household members.

It is also interesting to see that the correlation to other factors like size of the house is low, as shown in figure 4.

If the correlation factor had been around 1.0, there would have been a clear correlation, while here it is almost 0 for combined systems, which shows absolutely no correlation, and as highest 0.367 for direct electric heating, which is a very weak correlation. In [5], [6] we can see other similar data presented.

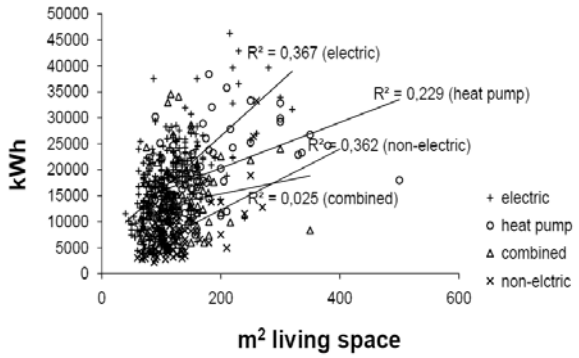

Figure 4. Correlation between electric power consumption as a function of the size of single houses with different heating systems: direct electric, electric with heat pump, combined electric and biofuel stove and nonelectric

The conclusion from this is that the individual behaviour is the most significant factor for the energy consumption. This leads to both advantages and disadvantages. The negative part is that it is difficult to perform direct predictions from data based on number of persons in a household, type of house, size etc. The positive part would be that behaviour can be changed. There are different incentives that can drive the behaviour in the correct direction, e.g. energy prices and environmental issues. Information and improvement of knowledge could also give positive effects.

We now will look at different energy systems and give a frame work on the correlation between different energy systems and how the effect of incentives could affect the systems.

2 Purpose with the simulations

The simulation model includes production facilities as sources, and sometimes also with storage capacity, transmission and distribution including loss calculations, and consumption by industry and households/offices.

Starting with the power production we include wind power plants, solar power, nuclear power, hydro power and thermal power plants. For the storage the focus is on hydro power, where pumps can be used to lift water back up to storages during low demand times. Also local small scale storages are assumed, e.g. cars and batteries. At the household side we assume different consumption patterns depending on time of the year, week, and day. Also individual differences are included.

The purpose of the model is to investigate how the losses will depend on different production conditions, especially the varying power supplies like wind and solar power. The simulations also considers how variations in the consumption pattern may influence the energy system, and what peak load cuttings would mean to the system.

2.1 Simulation model

The electric power in a power station is normally produced as a turbine drives a synchronous generator. A voltage is produced, as well as a current. If we have the new type of combined generator and transformer, the powerformer, we can produce a high voltage like 130 kV directly.

Otherwise, the produced voltage will be lower, and a transformer will bring it up to the wanted level before the transmission to the customers. Transmission lines are normally 130 kV, but can be also 400 kV, or even higher, in the national transmission lines. When the power reaches the customers, some industry or group of households or offices, the voltage is taken down to 380 V. We normally have three phases, with 220 V or 110 V single phase finally -220 V in Scandinavia.

In most transmission lines we use three phases. If we feed a symmetric three phase voltage, this can be seen as in figure 5.

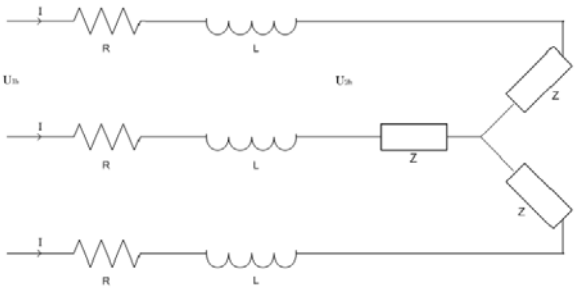

Figure 5. Three phase load with three phase feed, using a Y- connection

In the figure R is the resistance in each cable; L is the inductance and Z the impedance. U is the potential difference between the phases. The potential drop between two phases from feed to load is given by:

$$U_{1h} - U_{2h} = I \times \sqrt{3} \times (R \cos \varphi_2 + \omega L \sin \varphi_2) \qquad (1)$$

φ_2 is the shift between the phases. This is positive at inductive load, that is if U_2 is before I in the phase.

For a copper transmission cable, the resistance is 1,7Ω/km if the area of the conductor is 10 mm^2,while 0,17 Ω /km if the area of the conductor is 100 mm^2. The inductance L is almost independent of the conductor material for conductors up in the air, as long as the distance between the conductors is significantly larger than the diameter of the conductor.

At 50 Hz $X = \omega L$ = ca. 0.4 /km, phase. Normally L can be neglected compared to the resistance R. Then also the term $\omega L \sin \varphi_2$ can be neglected.

The loss in the conductor line due to the resistance is now given by:

$$P_f = R \times I^2 \times W$$

where P_f = resistive losses, R = resistance in one conductor, I = current and W = number of conductors. There are also other types of losses due to turbulence and hysteresis in metallic shields and losses in insulation materials, but these can normally be neglected.

A more important factor with respect to transmission losses is due to reactive power. The active power in AC-current is given by:

When $\cos \varphi = 1$, that is when the shift between the phases $\varphi = 0$, we have a maximum power transmission. When the phase shift increases, it will not be possible to transport as much current and power as before. We can compare to a beer bottle. If we have a lot of froth (=reactive power) we cannot fill the bottle with beer (= active power). Asynchronous motors or drives will produce reactive power. This can be counteracted by using a synchronous motor or capacitors. This is called reactive power compensation.

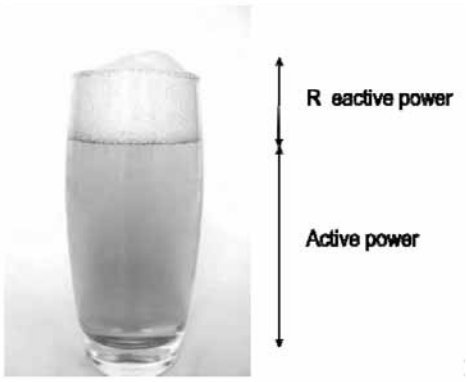

Figure 6. Illustration of reactive and active power by a glass of beer.

We do not include reactive power compensation in these calculations, typically this could improve the capacity by approximately 15 – 20%.

It can also be interesting to look at transmission and distribution losses in some different countries presented by [7] (World Bank 2002): World-wide 9%, Sweden, US, China 7%, Benin 71%, India and Iran 18%, Mexico 15% (The data is for the year 1998).

3 From the simulation and discussion

A simulation model has been made according to what has been described above. We now will use it for some system calculations. For Sweden hydro power is of major importance, and thus we start with a comparison of a system where we produce 300 MW electric power from a hydro power plant 1000 km away from where it will be utilized. We then compare this system to a system with a maximum 300 MW wind power plant at the same site.

A system where as much as possible is produced is compared to one where we maximize the production from the wind power plant and then use the hydro power plant as a buffer system. In the first system we also look at the possibility to use the wind energy to pump water back to the hydro power dam when the demand for power is low.

First we look at the transmission line. For a 300 MW transmission line we assume a cable with **2000 mm area** of copper. This corresponds to a 50 mm diameter cable. The resistance is approximately 0.0085 Ω/km. For a 1000 km line then the resistance will be 8.5 Ω. The current I = 300 000 KW /($\sqrt{3}$× 400kV) = **433 A.**

The power losses $P_f = 8.5\ \Omega \times 433\text{A}^2 \times 3 = 4.8\text{MW}$ or **1.6%** losses. For a 500 mm area copper cable the losses would be $P_f = 34\ \Omega \times 433^2 \times 3 = 19\text{MW}$ or **6,3%.** If we used the transmission line for a constant load of only 75 MW instead, the following losses would occur:

The current is I = 75 000KW / ($\sqrt{3}$× 400 kV) = **108A** and the power losses $P_f = 8.5\ \Omega \times 108^2 \times 3 = 0.3\text{MW}$ which gives **0.4%** losses using the 50 mm diameter cable (2 000 mm^2). If we instead used a smaller cable with 25 mm diameter (500 mm^2) the losses would be $P_f = 34\ \Omega \times 108^2 \times 3 = 1.2$ MW which gives **1.6 % losses.**

With a 18 mm diameter (250 mm^2) the losses would be $P_f =$ 68 Ω ×108^2×3 = 2.4MW which gives **3.2%** losses. For an 11 mm diameter cable, the losses would be 8%.

It can also be interesting to see how the cost for cables of different dimensions relate to reduced losses during the transmission. If we just look at the copper cost for the cable the price per kg was 49 SEK/kg May 2008. For the 50 mm diameter cable and 1000 km the investment cost will be for the copper in the cable 1000000m×($0{,}025^2$×π)×8900kg/m3 = 17470ton × 49000SEK/ton = 856MSEK. For a 25 mm diameter cable it will be 214 MSEK and for the 18 mm 111 MSEK.

If we now look at the cost for the losses, 0.4% losses corresponds to 0.004 × 75MW × 8700h/y × 250SEK/MWh = 0.65MSEK/y if we assume the price per MWh to be 250 SEK, while 8% losses corresponds to 13 MSEK/y. If we capitalize the investment cost to an annual cost with annuity 0.125 respectively summarize this cost over 10 years, and compare to the annual cost for the losses.

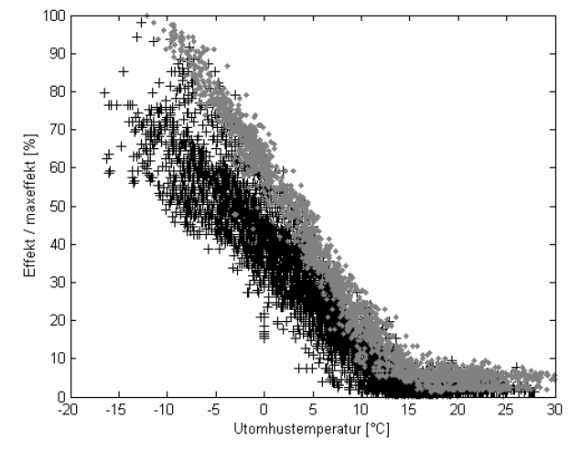

Figure 7. Heat power as a function of out-door temperature in Stockhom for offices during working days (red) compared to Saturday/Sundays (black) [9] [Kvarnstrom et al 2007].

A three phase transformer costs approximately 150 SEK/kVA. For 75 MW the investment cost will be = 75000kVA × 150 = 11MSEK and for 300MW = 45MSEK.

For reactive power compensation capacitors can be used. According to [8] Hume et al [2007] the cost for capacitors are $16,480 / MVAR for a dual bus connected capacitor at 220 kV or 110 kV (based on 2006 ODV information published by Transpower with a CPI of 3%) while a distribution power factor correction capacitor will cost about $34700 per MVAR for switched 11 kV zone substation capacitors.

For 75 MVAR (MW) that means in case of distribution power correction 34690$/MVAR × 6.3 SEK/$ × 75MVAR = 16.4MSEK. In relation to the other costs this is quite small. These cost have not been included in our calculations below, but can be added if reactive power compensation is to be included.

For a complete transmission line the cost is around 5000 SEK/kVA according to estimates done for an 800 MW transmission line at 400 kV. If we extrapolate from this we get 300 MW 1500 MSEK, and for 75 MW 375 MSEK.

Lately the electricity price has passed 650 SEK/MWh and it is predicted to pass 1000SEK/MWh perhaps already during the summer 2008 due to a strong demand on coal from China driving the price, and problems with transmission lines from Norway.

With these figures the incentive to reduce losses is increased even further. If the price does not pass 1 000 SEK/MWh now, it probably will do so within a foreseeable time horizon.

If we now look at a system where we have a combination of 300 MW hydro power and maximum 300 MW wind power, a maximum capacity of 600 MW would be needed. If we instead make a transmission line with the maximum capacity of 400 MW, the investment cost is reduced significantly. When there is a surplus capacity of wind power compared to the demand this may be used to pump water backwards up to the dam.

The investment cost for the transmission line with respect to copper will be reduced from 866 to 577 or by 290 MSEK, and if we take the total cost for the transmission line from 3 000 to 2 000 MSEK, or 1 000 MSEK. With an annuity of 0.125 this gives an annual cost reduction by 125 MSEK/y for the investment cost.

At the same time the transmission losses are reduced during the maximum load conditions, but increased to some extent when there is no wind at all. In the mountain areas the winds are quite good, and we assume that we can have maximum capacity 300 MW 20% of the year and 75 MW 60% of the year. If we operate at maximum capacity all the time, the transmission losses for this then become 300 × 8760 × 0.2 × 0.016 = 8410MWh respectively 75 × 8760 × 0.6 × 0.003 = 2365 MWh. The total losses will sum up to 10 775 MWh, to a value of 7 MSEK/y at the electricity price 650 SEK/MWh.

If we run at maximum load, 100 MW, we instead get 100 × 8760 × 0.2 × 0.0053 = 929MWh, respectively, 75 × 8760 × 0.6 × 0.003 = 2365MWh. The total losses then becomes 3 294 MWh to a value of 2.1 MSEK/y.

On the other hand, we will lose some of the electricity due to losses during the pumping in the pump plant. The pump will have an efficiency of 65%, which means a loss of 200MW × 8760 × 0.2 × 0.35 = 122640MWh or a value of 80 MSEK/y.

This shows that building a smaller transmission capacity gives a saving of 125 MSEK/y but losses in the pump power plant gives losses (80 – (7 – 2)) = 75MSEK/y. Still it can be a feasible solution to utilize the excess wind for pumping water instead of sending it directly to the transmission line. This solution also will make it possible to balance huge amount of wind power as otherwise we will run into problems with transmission of the electric power long distance.

Today the total power transmission capacity from northern Sweden is 7 000 MW, but with large amount of installed wind power the capacity will be too low. If we go back to figure 1, we can see that there is a problem already with the ongoing expansion with some 2 000 MW wind when there are strong winds, and high demand, during approximately 1 000 hours per year.

The energy used in households and offices is significantly higher during working days due to an increased ventilation, although the heat demand principally should be lower when you have many people, computers and other heat sources ”on”. This also gives an increased electric power demand for the ventilation.

We have already shown how the reduction of the peak loads is reducing the capital cost on the transmission lines, but also how the reduction of losses gives additional earnings, when the total transfer of power is reduced in an existing line. If we reduce the total peak power from 600 to 400 MW the transmission capacity can be reduced as shown, with annual savings of 125 MSEK for capital costs. If we also reduce the time when the maximum capacity is utilized, additional reductions in losses are gained in the range of 1 – 10 MSEK/year, as shown earlier.

An alternative approach is to keep the transmission of power from the north at as constant level as possible, and then compensate the variations in the demand locally. In this case we can have both local storages like batteries as well as local production of electric power and/or heat. If we produce as much wind power and solar power as possible, when available, batteries in plug in cars can be interesting as the energy storage media. If we assume that the battery is a lead battery like the common ones in cars, the capacity we can store is 30-40 Wh/kg and the efficiency 70 – 92%.

The number of cycles for a battery is for this type some 500 – 1 000 cycles, and the life time 3 – 20 years, depending on the operating conditions. For a Litium-ion battery the capacity may be 160 Wh/kg and the efficiency is 99.9%, and the number of charging cycles may be around 1 200 cycles during a life time of 2 – 3 years. There are also some new alternatives that may prove to be very interesting in the future.

The company EEstor claim that they can charge their double layer capacitor system in five minutes with 52 kWh in a 152 kg heavy (33 liter) unit. This operates at 3500 V, which makes this possible. This means 200 – 300 Wh/kg, and the efficiency is 95% in the experiments performed. The car they have tested on can travel 480 km with one charging (52 kWh), which means 1.3 kWh/10 km. The target price for such battery is $2 100 (12 600 SEK), but right now it is $3 200 (19 200 SEK). If we assume the life time will be five years and we travel distance of 10 000 km/y, the cost per 10 km would be with an annuity factor 0.2 only 3.8 SEK. If we add the cost for the electricity 1.3 × (1 / 0.95) × 1SEK/kWh = 1.4 SEK the total cost would be 5.2 SEK/10 km, which is about half the cost that we pay for gasoline.

If we just use existing lead batteries, the cost for a battery with the capacity 2,6 kWh is 2 000 SEK with the volume 30 liters, and the weight 65 kg. If we want a transportation distance of at least 150 km, it means 15 × 1.3 = 19.5kWh, with a price of some 19.5 × 2000 / 2.6 = 15000SEK. This would mean with an annuity of 0.2 and 10 000 km/y only 3 SEK/10 km. This means that even the batteries of today could be economic, although the weight would be some 450 kg. With a Litium –Ion battery the battery weight may be only 100 kg for the same capacity, but the life time probably shorter.

From this we can make a simulation where we charge the batteries while the price of electricity is low, that is when the demand is lower than the available capacity normally. If you have your own photo voltaic solar panel this would be when there is day-light. If you buy power from the grid, this will be the case when it is windy and wind power production is high, or when the general demand is low. The first case with your own production when it is day-light will reduce the demand from the grid during the summer half of the year, while the demand will be higher during the winter months.

If you have electric heating, this can be compensated by using a pellet burner or wood stove for heating instead, at least when the electricity price is high. For a house that changes the electric heating system with full load to one with reduced electric load including e.g. pellet boiler goes from approximately 9 kW to 3 kW maximum electric load. How far the new maximum load will last depends of various conditions. For a house with electrical heating it will be during very cold winter time problems occurs. During the last 20 years, this has been very rare in south and mid Sweden, but normally at least 2 – 3 days per winter, when it is significantly below –10 °C.

The power consumption as well as the wind energy production is seen in the figure 8 below. Here we can see that the normal summer load is around 10 000 MW, while approximately 20 000 MW during the winter. There are few peak loads up to 27 000 MW during very cold days. We can see that it is more wind power produced during the winter, but there are also periods with almost no wind even winter time. Still, there should be a possibility to reduce the power consumption by 30 – 50% by introducing better incentives to bring down peak loads.

If we look at the short term variations we can see that these are within 2 500 – 5 000 MW year around, and this variation can be handled with short term storages. This would reduce the need for transmission and thus also reduce the losses.

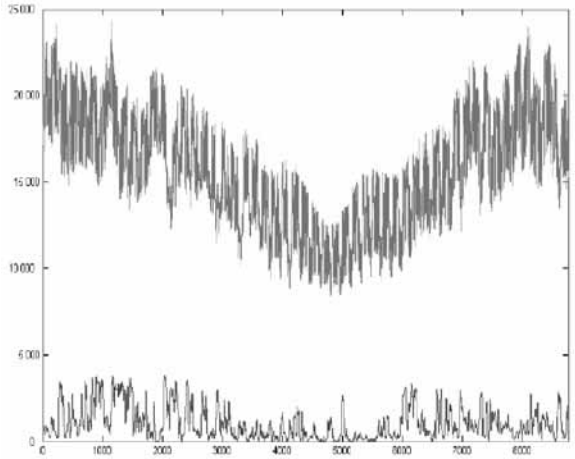

Figure 8. Consumption of electric power(upper) respectively production of power from wind during 2007.

4 Conclusions

In this paper we have shown how the existing electric power consumption pattern looks like and what the consequences would be if we could change the consumption pattern through good incentives. The peak load can be reduced by some 30 – 50% and the short term variation by some 10 – 20% over the year. For the calculation a simulator model has been used. Here we can see how the optimal system could look like under different assumptions.

This paper presents existing electric energy consumption patterns and discuss consequences if these patterns could be changed through different initiatives. The peak load can be reduced in two different perspectives, long term and short term with approximately 30 – 50% and 10 – 20%, respectively.

The calculation steps for a simulator model are presented together with a discussion of optimal energy system design choices. This proposed simulator will form a powerful tool to optimize processes and use of resources.

References

[1] Swedenergy. Statistics. 2008.

[2] Sveca J., Söder L.*: Wind power integration in power systems with bottleneck problems.* VIND-2002 conference in Malmö, November 6-7, 2002.

[3] Vassileva I., Bartusch C., Dahlquist E.: *Differences in electricity and hot water consumption in apartments of different sizes.* International Conference on Green Energy with energy management and IT, Stockholm, Sweden, March 12-13 2008.

[4] Bartusch C., Odlare M., Wallin F., Dahlquist E.: Electricity consumption and load demand in single-family houses. International Conference on Green Energy with energy management and IT, Stockholm, Sweden, March 12-13 2008.

[5] Widén J., Lundh M., Vassileva I., Dahlquist E., Ellegård K., Wäckelgård E.: *Constructing load profiles for household electricity and hot water from time-use data – modelling approach and validation.* Submitted to Energy and Buildings Journal. 2008.

[6] Lundh M., Vassileva I., Dahlquist E., Wäckelgård E.: Comparison between hot water measurements and modelled profiles for Swedish households. Eurosun October 2008, Portugal, 2008.

[7] UN, World Bank Development Indicators 2002.

[8] Hume D., de Silva R.: System Studies Group NZ Ltd: Relative Power Factor Correction costs. October 2007. Transmission Electricity Commission. 2007.

[9] Kvarnstrom J., Dotzauer E., Gollvik L., Andersson C.: *Lastprognoser för fjärrvärme* (Load forecasts for district heating). Värmeforsk Report (in Swedish) 2007.

Corresponding author: Erik Dahlquist,
Mälardalen University, Västerås, Sweden
erik.dahlquist@mdh.se.at

Received & Accepted: SIMS 2008
Revised: Juli 7, 2009
Accepted: September 10, 2009

Towards Dynamic Structure Hybrid DEVS for Scientific and Technical Computing Environments

C. Deatcu, T. Pawletta, Hochschule Wismar – Univ. of Technology, Business & Design, Germany

SNE Simulation Notes Europe SNE 19(3-4), 2009, 75-78, doi: 10.11128/sne.19.sn.09959

The established Discrete Event System Specification (DEVS) offers opportunities to comprehensively describe discrete event systems. In this paper the classic DEVS approach is extended with specifications and methods for continuous and variable structure modelling to hybrid models with a variable modular, hierarchical structure. To let engineers benefit from these powerful modelling instruments, they are integrated into the well-accepted and popular scientific and technical computing environment (SCE) Matlab. Furthermore, integration with other computing methods provided by the chosen SCE is obvious and can be accomplished. We appreciate DEVS based algorithms for modelling and simulation in SCEs as a complement and addition to existing tools as Simulink, Stateflow and SimEvents for engineering tasks such as e. g. discrete eventbased control design. Moreover, a SCE provides a prototyping environment for the evolution of the DEVS approach itself.

Introduction

Since Zeigler et al. introduced the Discrete Event System Specification (DEVS) in the seventies [8], many extensions of the DEVS formalism where designed. This paper presents an approach for dynamic structure hybrid DEVS, the DSDEVS-hybrid formalism, depicts its formal modelling and simulation concepts and gives an overview on the implementation of the DSDEVS-hybrid toolbox for Matlab.

Our modelling approach for modular hierarchical hybrid systems with structural variability at the coupled system level is based on the work in [6, 1, 4] and classic DEVS theory [9]. A dynamic structure system in DEVS context is a modular hierarchical system whose structure changes during simulation time. Hierarchical models are composed of two system types, atomic and coupled models. Coupled models consist of other coupled models and/or atomic models. The dynamic behaviour of a system is reflected in atomic models, while dynamic structure is defined at the coupled system level. Dynamic structure changes are e.g. creation, deletion and exchange of models. Hybrid means that besides discrete model fractions, continuous model parts are contained, as well.

There are two ways to approach those kinds of systems, resulting from the two general worldviews. One approach starts from the continuous modelling and simulation worldview and therefore extends a continuous model to a hybrid one. Discrete events are expressed as root-finding problems. The model is then simulated by a continuous simulation engine, i.e. it is processed by an ODE solver with discontinuity detection and localisation.

Usually, in modular hierarchical modelling and simulation environments, the model structure is flattened before execution. Hence, hierarchical structure information is partly not available during simulation time and dynamic structure behaviour needs to be elaborately modelled at atomic system level. It seems to be more promising to gain access to the problem through the second worldview, the discrete event worldview. In that case a discrete simulator rules the simulation engine and calls an ODE solver to compute continuous model fractions. Among descriptions for discrete event system models and their simulators, we have chosen and enhanced the Discrete Event System Specification (DEVS). In contrast to other ongoing research, e.g. integration of DEVS into the Modelica language [7] that employs DEVS for the description of only the discrete part of hybrid models, the described approach takes DEVS as the basis. DEVS itself and particularly its related simulator concepts are extended with hybrid and at the same time dynamic structure features.

1 Formal modelling concept

An overview of the formalisms that underpin and extend DEVS theory is given by Zeigler et al. in [9]. One of several extensions of the basic DEVS formalism is the hybrid DEVS formalism presented by Praehofer [6]. Another approach for hybrid DEVS modelling was introduced by Kofman [3, 2], who proposes quantisation of the state variables instead of time discretisation to approximate differential equations. The suitability for dynamic structure modelling of this approach is not followed up in this paper.

1.1 Atomic model specification

Praehofer [6] defined a hybrid atomic system by the tuple

$$A_{\text{hybrid}} = (X, Y, S, f, c_{\text{se}}, \lambda_c, \delta_{\text{x\&s}}, \delta_{\text{int}}, \lambda_{\text{d}}, ta) \quad (1)$$

where X, Y, and S specify the set of inputs, outputs and states which may be continuous or discrete. Continuous dynamics are mapped by the rate of change function f and the continuous output function λ_{c}. Discrete events are internal, external and state events. State event conditions are defined using the state event condition function c_{se}. External events and state events induce state transitions using the function $\delta_{\text{x\&s}}$. Internal events activate the discrete output function λ_{d} and also the internal state transition function δ int . After each discrete state transition internal events are rescheduled by the time advance function ta. Local structural changes of the continuous dynamics can be modelled by structuring the dynamic description using logic variables inside the rate of change function f, the state event condition function c_{se} and the continuous output function λ_{c} . This definition for hybrid atomic DEVS fits for being combined with a coupled system definition for dynamic structure models. Hybrid behaviour is defined on atomic system level, while dynamic structure is modelled at coupled system level.

1.2 Coupled model specification

In order to allow dynamic structure behaviour, e.g. the creation, deletion and exchange of submodels, additional data structures to represent this dynamic need to be established. Barros [1] proposes to add a special atomic model called network executive to each coupled model which holds the structure information and describes the structure dynamics. In contrast to this approach we favour the extension of the classic DEVS coupled model definition in way that allows to hold structure information directly in the coupled model. The specification of a classic DEVS coupled model [6, 9] is as follows:

$$N = (X_N, Y_N, D, \{M_d | d \in D\}, EIC, EOC, IC, Select) \quad (2)$$

where X_N is the set of input values and Y_N is the set of output values. The index N stands for network model as synonym for coupled model. D is the set of the component names, while M_d represents a dynamic subsystem. The property of closure under coupling, which is ensured for classic coupled DEVS, enables the representation of every coupled DEVS as an atomic DEVS. Thus, dynamic subsystems may be other coupled DEVS models or atomic DEVS models. EIC, EOC and IC define the coupling relations. The external coupling relation EIC connects external inputs to component inputs, the external output coupling EOC connects component outputs to external outputs and the internal coupling IC defines connections among components, i.e. component outputs are connected to component inputs. For couplings no direct feedback loops are allowed. Finally, $Select$ acts as a special function to prioritise one subsystem in case of simultaneous internal events in subsystems.

To allow structure variability, some extensions of this coupled system's definition have to be introduced. In the context of this work, possible structural changes at the coupled system level are

- Creation, Cloning, Deletion and
- Replacement of atomic or coupled subsystems,
- Their movement between coupled systems and
- Changes of couplings between system components.

We call the actual composition of a subsystem set and its coupling relations the structure state. A dynamic structure DEVS can have different structure states $s_0, s_1, \ldots, s_n \in S_N$. Furthermore, structure dynamics information, e.g. the number and kind of structure changes already achieved, needs to be stored. The set of structural variables H_N holds this information. For a dynamic structure coupled DEVS the $Select$ function can depend on the structure state and structure dynamics information. Consequently, we define the set of sequential structure states S_N of a dynamic structure coupled DEVS as:

$$S_N = H_N \times D \times \{M_d | d \in D\} \times \times EOC \times EIC \times IC \times Select \quad (3)$$

This set of sequential structure states extends the formal definition of classic coupled DEVS without structure variability to the dynamic structure DEVS definition. We define a dynamic structure DEVS as follows:

$$N_{\text{dyn}} = (X_N, Y_N, \{d_N\}, S_N, \delta N_{\text{x\&s}}, \delta N_{\text{int}}, \lambda N_d, taN) \quad (4)$$

Note that coupling information as well as $Select$ rules are now capsuled in the set of structure states S_N. The name of the coupled system is stored in d_N. Furthermore, a dynamic structure hybrid DEVS implies the functions $\delta N_{\text{x\&s}}$, δN_{int}, λN_d and taN. The transition, output and time advance functions until now were defined for atomic hybrid DEVS only. These functions provide operations similar but not identical to those for atomic systems.

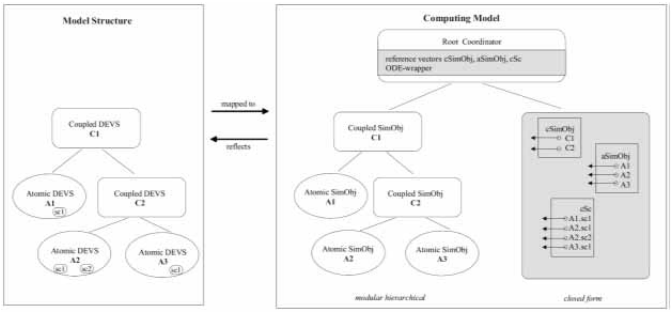

Figure 1. Mapping elements of a model structure to simulation objects of a computing model

In analogy to event-oriented dynamic behaviour of classic atomic DEVS systems, dynamic structure changes in coupled DEVS are induced by events. Relevant events are external, internal or state events. If an external event occurs, it will be sent to the affected subsystems, as known from classic DEVS. If it influences the structure dynamics of the coupled system, its state transition function $\delta N_{\text{x\&s}}$ is executed. After that the time advance function taN is called to recalculate the time until the next internal event. State events that affect structure can be caused by output events of subsystems or threshold events of (i) continuous outputs of subsystems, (ii) continuous inputs of the coupled system or (iii) structure related states of the set H_N.

For state events first $\delta N_{\text{x\&s}}$ is executed, and then taN is called. The time advance function taN for coupled DEVS also schedules events triggered by the internal structure of a coupled DEVS. The structure changes to be accomplished are specified with the structure state transition function δN_{int}. For the generation of structure related output events caused by internal events, the discrete output function λN_d is introduced. Presented specifications for atomic and coupled DEVS models together with a new simulation concept form the DSDEVS-hybrid formalism. The formal approach and its application on a real engineering system are described in detail in [5].

2 Simulation concept

In dynamic structure as well as static structure hybrid DEVS formalisms and associated simulator concepts the continuous part of the model causes events to occur in the DEVS part. The model is simulated by a modified discrete event simulation engine which calls an ODE solver during simulation cycles. Structure information of the hybrid modular hierarchical model remains available during simulation time. Thus, the design and simulation of dynamic structure hybrid models becomes imaginable. Computation algorithms for modular hierarchical DEVS models including dynamic structure and hybrid system extensions were established in [9, 6, 1, 5]. The key idea is to map a model specification to interacting program objects to reflect the system components and their coupling relations. This means for each part of the hierarchical model a program object exists which exclusively handles the dynamics, i.e. the simulation of this model part. These program objects are referred to as simulation objects of the computing model. On top of the hierarchically organised computing model the root coordinator initiates and controls the simulation cycles. Figure 1 illustrates the relations between the specified model and resulting program objects. The regions highlighted in grey are not part of classic DEVS formalisms, but extensions introduced with the DSDEVS-hybrid formalism.

Until now, problems arised for the effective calculation of continuous model parts if they are distributed over different program objects. Current approaches work with the Euler method and do not support the use of other ODE solvers. However, engineers ask for advanced ODE solvers with implicit integration methods, predictor/ corrector integration methods and automatic step width control to solve e.g. stiff systems. The proposed DSDEVS-hybrid formalism based on [5] comprises new data structures and methods which automatically generate the description of the continuous model equations and continuous state vectors of all model components in a closed form. This closed description is prerequisite for the efficient use of advanced ODE solver methods. To achieve a closed description we make use of wrapper concepts. On top of the simulation engine the root coordinator is extended by the ODE-wrapper method. The ODE-wrapper method allows the closed model representation by using additional data structures. These data structures hold by the root coordinator are the vector of references to all continuous state variables *cSc* and the vectors *cSimObj* and *aSimObj* filled with references to all atomic and coupled models. These references provide a dynamic representation of the modular hierarchical model in the required closed form. In Figure 1 data structures and newly introduced methods are highlighted in grey. Taking benefit of the wrapper concept leads to possibilities for defining interfaces to advanced ODE solvers which are e.g. provided by programmable scientific and technical computing environments (SCEs).

3 Implementation of the DSDEVS-Hybrid Toolbox for Matlab

Unlike other modelling methodologies for discrete event systems such as Petri nets or state charts, DEVS formalisms have not been widely accepted by engineers, although they are to be seen as powerful tools to solve engineering problems. To help eliminating this lack of acceptance we propose the employment of SCEs. Since engineers, unlike scientists, are rather familiar with the use of SCEs such as Matlab than of high level programming language simulation libraries, the integration of DEVS algorithms into those environments is overdue. Furthermore, SCEs provide a large number of predefined advanced ODE solvers which can be involved to compute the continuous parts of hybrid models. Our research aims to integrate advanced DEVS algorithms into SCEs and to take benefit of combination with other computing methods and toolboxes, e.g. for distributed and parallel computing, HLA modelling and for simulation based reactive control of discrete event systems. Moreover, a SCE provides a prototyping environment for the evolution of the DEVS approach itself.

For Matlab a prototype implementation of dynamic structure hybrid DEVS modelling and simulation exists which is named *DSDEVS-hybrid toolbox*. Practicability of the formal approach is therewith proofed and verified. Major class definitions for the Matlab DSDEVS-hybrid toolbox reflecting the formal definitions for dynamic structure hybrid atomic and coupled DEVS models can be found in [4].

4 Conclusions

The described modelling and simulation approach extends and brings together DEVS-based formalisms for dynamic structure and hybrid modelling. The improvements of the simulation engine by employing the ODEwrapper method avoids from the need to flatten the model before execution. Hence, structure information remains available and dynamic structure modifications are possible. Nevertheless, the closed form required to take benefit of advanced ODE solvers can be provided. Thus, the proposed formalism is applicable to complex engineering problems. To enlarge application field, further research will add ports and parallel extensions to DSDEVS-hybrid. By integrating DSDEVS-hybrid into SCEs, engineers are encouraged to break new ground in modelling and simulation while staying in their familiar software environment.

Current toolbox implementation is done with previous Matlab releases, where supplied object oriented programming features were rather poor and leaded to a complex file hierarchy. To define a new class, the programmer needed to establish a directory for the class, where all M-files which included the methods for the class were collected. For each class method a separate M-file had to be created so that class definitions became complicated and hard to follow up. Since 2008, Matlab offers enhanced features for object oriented programming. So, reimplementation with taking benefit of these features is obvious.

References

[1] Barros, F. J.: *The Dynamic Structure Discrete Event System Specification Formalism.* Transactions of the SCS International, 1996, 13(1), 35 – 46.

[2] Cellier, F. E. and Kofman, E.: *Continuous System Simulation.* Springer Pub., 2006

[3] Kofman, E.: *Discrete Event Simulation of Hybrid Systems.* SIAM Journal on Scientific Computing, 2004, 25(5), 1771-1797

[4] Pawletta, T., Deatcu, C., Pawletta, S., Hagendorf, O. and Colquhoun, G.: *DEVS-Based Modeling and Simulation in Scientific and Technical Computing Environments*. In: Proceedings of SpringSim 2006 (DEVS Symposium), Huntsville, AL, USA, 2006, 151 - 158

[5] Pawletta, T., Lampe, B., Pawletta, S. and Drewelow, W.: *A DEVS Based Approach for Modeling and Simulation of Hybrid Variable Structure Systems.* Lecture Notes in Control and Information Science (Eds.:S. Engel et.al.), Springer Pub., 2002, Vol. 279, 107 – 130

[6] Praehofer, H.: *System Theoretic Foundations for Combined Discrete-Continuous System Simulation.* PhD thesis, VWGÖ, Vienna, 1992

[7] Sanz, V., Urquia, A. and Dormido, S.: *Introducing Messages in Modelica for Facilitating Discrete-Event System Modeling.* In: Proc. 2nd Int. Workshop on Equation-Based Object-Oriented Languages and Tools, Paphos, Cyprus, 2008, 83 – 93

[8] Zeigler, B. P., Kim, T. G. and Praehofer, H.: *Theory of Modeling and Simulation, 1st Edition.* Academic Press, 1976.

[9] Zeigler, B. P., Kim, T. G. and Praehofer, H.: *Theory of Modeling and Simulation, 2nd Edition.* Academic Press, 2000.

Corresponding author: Christina Deatcu,
Univ. Applied Sciences Wismar
RG Computational Engineering & Automation
PF 1210, D-23952 Wismar, Germany
christina.deatcu@hs-wismar.de

Received & Accepted: MATHMOD 2009
Revised: September 15, 2009
Accepted: November 3, 2009

SNE News Section

EUROSIM Data & Quick Info

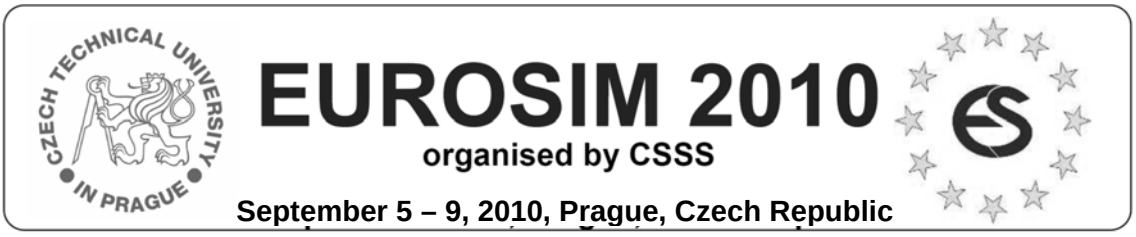

Contents

Simulation News Europe is the official journal of EUROSIM and sent to most members of the EUROSIM Societies as part of the membership benefits. Furthermore **SNE** is distributed to other societies and to individuals active in the area of modelling and simulation. SNE is registered with ISSN 1015-8685. Circulation of printed version is 3000 copies.

eSNE − SNE at Web SNE issues are also available at `www.argesim.org` as eSNE – *Electronic SNE* . Web-resolution eSNEs are free for download. Subscribers, e.g. members of EUROSIM Societies have access to SNE Archive with high-resolution eSNE copies and and with sources of ARGESIM Benchmarks.

This *EUROSIM Data & Quick Info* compiles data from EUROSIM and EUROSIM societies: addresses, weblinks, officers of societies with function and email, to be published regularly in SNE issues – independent of individual reports of the societies.

SNE Reports Editorial Board

EUROSIM

Mikuláš Alexík, alexik@frtk.utc.sk
Borut Zupančič, borut.zupancic@fe.uni-lj.si
Felix Breitenecker, Felix.Breitenecker@tuwien.ac.at

ASIM: Thorsten Pawletta, pawel@mb.hs-wismar.de
CROSSIM: Vesna Dušak, *vdusak@foi.hr*
CSSS: Mikuláš Alexík, alexik@frtk.utc.sk
DBSS: A. Heemink, a.w.heemink@its.tudelft.nl
FRANCOSIM: Y. Hamam, y.hamam@esiee.fr
HSS: András Jávor, javor@eik.bme.hu
ISCS: M. Savastano, mario.savastano@unina.it
PSCS: Zenon Sosnowski, zenon@ii.pb.bialystok.pl
SIMS: Esko Juuso, esko.juuso@oulu.fi
SLOSIM: Borut Zupančič, zupancic@fe.uni-lj.si
UKSIM: Richard Zobel, r.zobel@ntlworld.com
CAE-SMSG: Emilio Jiminez, *emilio.jiminez@unirioja.es*
LSS: Yuri Merkuryev, merkur@itl.rtu.lv
ROMSIM: Florin Stanciulescu, sflorin@ici.ro

ARGESIM

Felix Breitenecker, Felix.Breitenecker@tuwien.ac.at
Anna Mathe, Anna.Mathe@tuwien.ac.at
Nikolas Popper, Niki.Popper@drahtwarenhandlung.at

→ `www.sne-journal.org`
✉ `office@sne-journal.org`
→ `www.eurosim.info`

If you have any information, announcement, etc. you want to see published, please contact a member of the editorial board in your country or to office@sne-journal.org.

Editorial Information/Impressum - see front cover

Information EUROSIM

EUROSIM Federation of European Simulation Societies

General Information. *EUROSIM*, the Federation of European Simulation Societies, was set up in 1989. The purpose of EUROSIM is to provide a European forum for regional and national simulation societies to promote the advancement of modelling and simulation in industry, research, and development.

→ www.eurosim.info

Member Societies. EUROSIM members may be national simulation societies and regional or international societies and groups dealing with modelling and simulation. At present EUROSIM has thirteen full members and one observer member:

ASIM	Arbeitsgemeinschaft Simulation *Austria, Germany, Switzerland*
CEA-SMSG	Spanish Modelling and Simulation Group *Spain*
CROSSIM	Croatian Society for Simulation Modeling *Croatia*
CSSS	Czech and Slovak Simulation Society *Czech Republic, Slovak Republic*
DBSS	Dutch Benelux Simulation Society *Belgium, Netherlands*
FRANCOSIM	Société Francophone de Simulation *Belgium, France*
HSS	Hungarian Simulation Society *Hungary*
ISCS	Italian Society for Computer Simulation *Italy*
LSS	Latvian Simulation Society *Latvia*
PSCS	Polish Society for Computer Simulation *Poland*
SIMS	Simulation Society of Scandinavia *Denmark, Finland, Norway, Sweden*
SLOSIM	Slovenian Simulation Society *Slovenia*
UKSIM	United Kingdom Simulation Society *UK, Ireland*
ROMSIM	Romanian Society for Modelling and Simulation, *Romania, Observer Member*

Contact addresses, weblinks and officers of the societies may be found in the information part of the societies.

EUROSIM board/EUROSIM officers. EUROSIM is governed by a board consisting of one representative of each member society, president and past president, and representatives for SNE and SIMPRA. The President is nominated by the society organising the next EUROSIM Congress. Secretary and Treasurer are elected out of members of the Board.

President	Mikuláš Alexík (CSSS), *alexik@frtk.fri.utc.sk*
Past president	Borut Zupančič (SLOSIM) *borut.zupancic@fe.uni-lj.si*
Secretary	Peter Fritzson (SIMS) *petfr@ida.liu.se*
Treasurer	Felix Breitenecker (ASIM) *felix.breitenecker@tuwien.ac.at*
SIMPRA Repres.	Jürgen Halin *halin@iet.mavt.ethz.ch*
SNE Repres.	Felix Breitenecker *felix.breitenecker@tuwien.ac.at*

SNE – Simulation News Europe. EUROSIM societies are offered to distribute to their members the journal *Simulation News Europe* (SNE) as official membership journal. SNE is a scientific journal with reviewed contributions in the *Notes Section* as well as a membership newsletter for EUROSIM with information from the societies in the *News Section*. Publisher are EUROSIM, ARGESIM and ASIM.

Editor-in-chief	Felix Breitenecker *felix.breitenecker@tuwien.ac.at*

→ www.sne-journal.org, menu SNE

✉ office@sne-journal.org

EUROSIM Congress. EUROSIM is running the triennial conference series EUROSIM Congress. The congress is organised by one of the EUROSIM societies. EUROSIM 2010 will be organised by CSSS in Prague, September 5-10, 2010.

Organisation EUROSIM 2010	Miroslav Šnorek *snorek@fel.cvut.cz*
Information CSSS	Mikulas Alexik (CSSS) *alexik@frtk.utc.sk*

→ www.eurosim2010.org

ASIM
German Simulation Society
Arbeitsgemeinschaft Simulation

ASIM (Arbeitsgemeinschaft Simulation) is the association for simulation in the German speaking area, servicing mainly Germany, Switzerland and Austria. ASIM was founded in 1981 and has now about 700 individual members, and 30 institutional or industrial members. Furthermore, ASIM counts about 300 affiliated members.

→ www.asim-gi.org with members' area

info@asim-gi.org, admin@asim-gi.org

ASIM – Inst. f. Analysis and Scientific Computing
Vienna University of Technology
Wiedner Hauptstraße 8-10, 1040 Vienna, Austria

ASIM Officers

President	Felix Breitenecker *felix.breitenecker@tuwien.ac.at*
Vice presidents	Sigrid Wenzel *s.wenzel@uni-kassel.de*
	Thorsten Pawletta, *pawel@mb.hs-wismar.de*
Secretary	Anna Mathe, *anna.mathe@tuwien.ac.at*
Treasurer	Ingrid Bausch-Gall, *Ingrid@Bausch-Gall.de*
Membership affairs	S. Wenzel, *s.wenzel@uni-kassel.de*
	W. Maurer, *werner.maurer@zhwin.ch*
	I. Bausch-Gall, *Ingrid@Bausch-Gall.de*
	F. Breitenecker (*mail address above*)
Universities	W. Wiechert *wiechert@simtec.mb.uni-siegen.de*
Industry	S. Wenzel, *s.wenzel@uni-kassel.de*
	K. Panreck, *Klaus.Panreck@hella.com*
Conferences	Klaus Panreck *Klaus.Panreck@hella.com* Albrecht Gnauck *albrecht.gnauck@tu-cottbus.de*
Publications	Th. Pawletta, *pawel@mb.hs-wismar.de*
	F. Breitenecker (*mail address above*)
Repr. EUROSIM	F. Breitenecker (*mail address above*)
Deputy	W. Wiechert *wiechert@simtec.mb.uni-siegen.de*
Edit. Board SNE	Thorsten Pawletta, *pawel@mb.hs-wismar.de*
Web EUROSIM	Anna Mathe, *anna.mathe@tuwien.ac.at*

Last data update March 2009

ASIM Working Groups. ASIM, part of GI - Gesellschaft für Informatik, is organised in Working Groups, dealing with applications and comprehensive subjects:

ASIM Working Groups

GMMS	Methods in Modelling and Simulation Peter Schwarz, *schwarz@eas.iis.fhg.de*
SUG	Simulation in Environmental Systems Wittmann, *wittmann@informatik.uni-hamburg.de*
STS	Simulation of Technical Systems H.T.Mammen, *Heinz-Theo.Mammen@hella.com*
SPL	Simulation in Production and Logistics Sigrid Wenzel, *s.wenzel@uni-kassel.de*
SVS	Simulation of Transport Systems U. Brannolte, *Brannolte@bauing.uni-weimar.de*
SBW	Simulation in OR C. Böhnlein, *boehnlein@wiinf.uni-wuerzburg.de*
EDU	Simulation in Education/Education in Simulation W. Wiechert, *wiechert@simtec.mb.uni-siegen.de*

CROSSIM – Croatian Society for Simulation Modelling

CROSSIM-*Croatian Society for Simulation Modelling* was founded in 1992 as a non-profit society with the goal to promote knowledge and use of simulation methods and techniques and development of education. CROSSIM is a full member of EUROSIM since 1997.

→ www.eurosim.info

vdusak@foi.hr

CROSSIM / Vesna Dušak
Faculty of Organization and
Informatics Varaždin, University of Zagreb
Pavlinska 2, HR-42000 Varaždin, Croatia

CROSSIM Officers

President	Vesna Dušak, *vdusak@foi.hr*
Vice president	Jadranka Božikov, *jbozikov@snz.hr*
Secretary	Vesna Bosilj-Vukšić, *vbosilj@efzg.hr*
Executive board members	Vlatko Čerić, *vceric@efzg.hr*
	Tarzan Legović, *legovic@irb.hr*
Repr. EUROSIM	Vesna Dušak, *vdusak@foi.hr*
Edit. Board SNE	Vesna Dušak, *vdusak@foi.hr*
Web EUROSIM	Jadranka Bozikov, *jbozikov@snz.hr*

Last data update March 2009

CSSS – Czech and Slovak Simulation Society

CSSS -The *Czech and Slovak Simulation Society* has about 150 members working in Czech and Slovak national scientific and technical societies (*Czech Society for Applied Cybernetics and Informatics, Slovak Society for Applied Cybernetics and Informatics*). The main objectives of the society are: development of education and training in the field of modelling and simulation, organising professional workshops and conferences, disseminating information about modelling and simulation activities in Europe. Since 1992, CSSS is full member of EUROSIM.

→ www.fit.vutbr.cz/CSSS

snorek@fel.cvut.cz

CSSS / Miroslav Šnorek, CTU Prague
FEE, Dept. Computer Science and Engineering,
Karlovo nam. 13, 121 35 Praha 2, Czech Republic

CSSS Officers

President	Miroslav Šnorek, *snorek@fel.cvut.cz*
Vice president	Mikuláš Alexík, *alexik@frtk.fri.utc.sk*
Treasurer	Evžen Kindler, *ekindler@centrum.cz*
Scientific Secr.	A. Kavička, *Antonin.Kavicka@upce.cz*
Repr. EUROSIM	Miroslav Šnorek, *snorek@fel.cvut.cz*
Deputy	Mikuláš Alexík, *alexik@frtk.fri.utc.sk*
Edit. Board SNE	Mikuláš Alexík, *alexik@frtk.fri.utc.sk*
Web EUROSIM	Petr Peringer, *peringer@fit.vutbr.cz*

Last data update December 2008

FRANCOSIM – Société Francophone de Simulation

FRANCOSIM was founded in 1991 and aims to the promotion of simulation and research, in industry and academic fields. Francosim operates two poles.

- Pole Modelling and simulation of discrete event systems. Pole Contact: *Henri Pierreval, pierreva@imfa.fr*
- Pole Modelling and simulation of continuous systems. Pole Contact: *Yskandar Hamam, y.hamam@esiee.fr*

→ www.eurosim.info

y.hamam@esiee.fr

FRANCOSIM / Yskandar Hamam
Groupe ESIEE, Cité Descartes,
BP 99, 2 Bd. Blaise Pascal,
93162 Noisy le Grand CEDEX, France

FRANCOSIM Officers

President	Yskandar Hamam, *y.hamam@esiee.fr*
Treasurer	François Rocaries, *f.rocaries@esiee.fr*
Repr. EUROSIM	Yskandar Hamam, *y.hamam@esiee.fr*
Edit. Board SNE	Yskandar Hamam, *y.hamam@esiee.fr*

Last data update April 2006

DBSS – Dutch Benelux Simulation Society

The Dutch Benelux Simulation Society (DBSS) was founded in July 1986 in order to create an organisation of simulation professionals within the Dutch language area. DBSS has actively promoted creation of similar organisations in other language areas. DBSS is a member of EUROSIM and works in close cooperation with its members and with affiliated societies.

→ www.eurosim.info

a.w.heemink@its.tudelft.nl

DBSS / A. W. Heemink
Delft University of Technology, ITS - twi,
Mekelweg 4, 2628 CD Delft, The Netherlands

DBSS Officers

President	A. Heemink, *a.w.heemink@its.tudelft.nl*
Vice president	W. Smit, *smitnet@wxs.nl*
Treasurer	W. Smit, *smitnet@wxs.nl*
Secretary	W. Smit, *smitnet@wxs.nl*
Repr. EUROSIM	A. Heemink, *a.w.heemink@its.tudelft.nl*
Deputy	W. Smit, *smitnet@wxs.nl*
Edit. Board SNE	A. Heemink, *a.w.heemink@its.tudelft.nl*

Last data update April 2006

HSS – Hungarian Simulation Society

The Hungarian Member Society of EUROSIM was established in 1981 as an association promoting the exchange of information within the community of people involved in research, development, application and education of simulation in Hungary and also contributing to the enhancement of exchanging information between the Hungarian simulation community and the simulation communities abroad. HSS deals with the organization of lectures, exhibitions, demonstrations, and conferences.

→ www.eurosim.info

javor@eik.bme.hu

HSS / András Jávor,
Budapest Univ. of Technology and Economics,
Sztoczek u. 4, 1111 Budapest, Hungary

HSS Officers

President	András Jávor, *javor@eik.bme.hu*
Vice president	Gábor Szűcs, *szucs@itm.bme.hu*
Secretary	Ágnes Vigh, *vigh@itm.bme.hu*
Repr. EUROSIM	András Jávor, *javor@eik.bme.hu*
Deputy	Gábor Szűcs, *szucs@itm.bme.hu*
Edit. Board SNE	András Jávor, *javor@eik.bme.hu*
Web EUROSIM	Gábor Szűcs, *szucs@itm.bme.hu*

Last data update March 2008

PSCS – Polish Society for Computer Simulation - update

PSCS was founded in 1993 in Warsaw. PSCS is a scientific, non-profit association of members from universities, research institutes and industry in Poland with common interests in variety of methods of computer simulations and its applications. At present PSCS counts 257 members.

→ www.ptsk.man.bialystok.pl

leon@ibib.waw.pl

✉ PSCS / Leon Bobrowski, c/o IBIB PAN, ul. Trojdena 4 (p.416), 02-109 Warszawa, Poland

PSCS Officers

President	Leon Bobrowski, *leon@ibib.waw.pl*
Vice president	Andrzej Grzyb, Tadeusz Nowicki
Treasurer	Z. Sosnowski, *zenon@ii.pb.bialystok.pl*
Secretary	Zdzislaw Galkowski, *Zdzislaw.Galkowski@simr.pw.edu.pl*
Repr. EUROSIM	Leon Bobrowski, *leon@ibib.waw.pl*
Deputy	A.Chudzikiewicz, *ach@it.pw.edu.pl*
Edit. Board SNE	Z.Sosnowski, *zenon@ii.pb.bialystok.pl*
PSCS Board Members	R. Bogacz , Z. Strzyzakowski Andrzej Tylikowski

Last data update March 2009

ISCS – Italian Society for Computer Simulation

The Italian Society for Computer Simulation (ISCS) is a scientific non-profit association of members from industry, university, education and several public and research institutions with common interest in all fields of computer simulation.

→ www.eurosim.info

Mario.savastano@uniina.at

✉ ISCS / Mario Savastano, c/o CNR - IRSIP, Via Claudio 21, 80125 Napoli, Italy

ISCS Officers

President	MarioSavastano, *mario.savastano@unina.it*
Vice president	F. Maceri, *Franco.Maceri@uniroma2.it*
Repr. EUROSIM	F. Maceri, *Franco.Maceri@uniroma2.it*
Edit. Board SNE	Mario Savastano, *mario.savastano@unina.it*

Last data update April 2005

SIMS – Scandinavian Simulation Society

SIMS is the *Scandinavian Simulation Society* with members from the four Nordic countries Denmark, Finland, Norway and Sweden. The SIMS history goes back to 1959. SIMS practical matters are taken care of by the SIMS board consisting of two representatives from each Nordic country. Iceland will be represented by one board member.

SIMS Structure. SIMS is organised as federation of regional societies. There are FinSim (Finnish Simulation Forum), DKSIM (Dansk Simuleringsforening) and NFA (Norsk Forening for Automatisering).

→ www.scansims.org

petfr@ida.liu.se

✉ SIMS/Peter Fritzson, IDA, Linköping University, 58183, Linköping, Sweden

SIMS Officers

President	Peter Fritzson, *petfr@ida.liu.se*
Treasurer	Vadim Engelson, *vaden@ida.liu.se*
Repr. EUROSIM	Peter Fritzson, *petfr@ida.liu.se*
Edit. Board SNE	Esko Juuso, *esko.juuso@oulu.fi*
Web EUROSIM	Vadim Engelson, *vaden@ida.liu.se*

Last data update December 2008

SLOSIM – Slovenian Society for Simulation and Modelling

SLOSIM - Slovenian Society for Simulation and Modelling was established in 1994 and became the full member of EUROSIM in 1996. Currently it has 69 members from both slovenian universities, institutes, and industry. It promotes modelling and simulation approaches to problem solving in industrial as well as in academic environments by establishing communication and cooperation among corresponding teams.

→ msc.fe.uni-lj.si/SLOSIM

slosim@fe.uni-lj.si

✉ SLOSIM / Rihard Karba, Faculty of Electrical Engineering, University of Ljubljana, Tržaška 25, 1000 Ljubljana, Slovenia

SLOSIM Officers

President	Rihard Karba, *rihard.karba@fe.uni-lj.si*
Vice president	Leon Žlajpah, *leon.zlajpah@ijs.si*
Secretary	Aleš Belič, *ales.belic@fe.uni-lj.si*
Treasurer	Milan Simčič, *milan.simcic@fe.uni-lj.si*
Repr. EUROSIM	Rihard Karba, *rihard.karba@fe.uni-lj.si*
Deputy	B. Zupančič, *borut.zupancic@fe.uni-lj.si*
Edit. Board SNE	Rihard Karba, *rihard.karba@fe.uni-lj.si*
Web EUROSIM	Aleš Belič, *ales.belic@fe.uni-lj.si*

Last data update March 2009

UKSIM – United Kingdom Simulation Society

UKSIM has more than 100 members throughout the UK from universities and industry. It is active in all areas of simulation and it holds a biennial conference as well as regular meetings and workshops.

→ www.uksim.org.uk

david.al-dabass@ntu.ac.uk

✉ UKSIM / Prof. David Al-Dabass
Computing & Informatics,
Nottingham Trent University
Clifton lane, Nottingham, NG11 8NS
United Kingdom

UKSIM Officers

President	David Al-Dabass, *david.al-dabass@ntu.ac.uk*
Secretary	A. Orsoni, *A.Orsoni@kingston.ac.uk*
Treasurer	B. Thompson, *barry@bjtcon.ndo.co.uk*
Membership chair	K. Al-Begain, *kbegain@glam.ac.uk*
Univ. liaison chair	R. Cheng, *rchc@maths.soton.ac.uk*
Repr. EUROSIM	Richard Zobel, *r.zobel@ntlworld.com*
Edit. Board SNE	Richard Zobel, *r.zobel@ntlworld.com*

Last data update March 2009 (partially)

CEA-SMSG – Spanish Modelling and Simulation Group

CEA is the Spanish Society on Automation and Control In order to improve the efficiency and to deep into the different fields of automation, the association is divided into thematic groups, one of them is named 'Modelling and Simulation', constituting the group.

→ www.cea-ifac.es/wwwgrupos/simulacion

simulacion@cea-ifac.es

✉ CEA-SMSG / María Jesús de la Fuente,
System Engineering and AutomaticControl department,
University of Valladolid,
Real de Burgos s/n., 47011 Valladolid, SPAIN

CAE - SMSG Officers

President	María J. la Fuente, *maria@autom.uva.es*
Repr. EUROSIM	Emilio Jiminez, *emilio.jiminez@unirioja.es*
Edit. Board SNE	Emilio Jiminez, *emilio.jiminez@unirioja.es*

Last data update March 2009

LSS – Latvian Simulation Society

The Latvian Simulation Society (LSS) has been founded in 1990 as the first professional simulation organisation in the field of Modelling and simulation in the post-Soviet area. Its members represent the main simulation centres in Latvia, including both academic and industrial sectors.

→ briedis.itl.rtu.lv/imb/

merkur@itl.rtu.lv

✉ LSS / Yuri Merkuryev, Dept. of Modelling
and Simulation Riga Technical University
Kalku street 1, Riga, LV-1658, LATVIA

LSS Officers

President	Yuri Merkuryev, *merkur@itl.rtu.lv*
Repr. EUROSIM	Yuri Merkuryev, *merkur@itl.rtu.lv*
Edit. Board SNE	Yuri Merkuryev, *merkur@itl.rtu.lv*

Last data update December 2008

ROMSIM – Romanian Modelling and Simulation Society

ROMSIM has been founded in 1990 as a non-profit society, devoted to both theoretical and applied aspects of modelling and simulation of systems. ROMSIM currently has about 100 members from both Romania and Republic of Moldavia.

→ www.ici.ro/romsim/

sflorin@ici.ro

✉ ROMSIM / Florin Stanciulescu,
National Institute for Research in Informatics, Averescu Av. 8 – 10, 71316 Bucharest, Romania

ROMSIM Officers

President	Florin Stanciulescu, *sflorin@ici.ro*
Vice president	Florin Hartescu, flory@ici.ro Marius Radulescu, *mradulescu@ici.ro*
Secretary	Zoe Radulescu, *radulescu@ici.ro*
Repr. EUROSIM	Florin Stanciulescu, *sflorin@ici.ro*
Deputy	Florin Hartescu, *flory@ici.ro*
Edit. Board SNE	Florin Stanciulescu, *sflorin@ici.ro*

Last data update March 2009


515.000.000 KM, 380.000 SIMULATIONEN
UND KEIN EINZIGER TESTFLUG.
DAS IST MODEL-BASED DESIGN.
Nachdem der Endabstieg der beiden Mars Rover unter Tausenden von atmosphärischen Bedingungen simuliert wurde, entwickelte und testete das Ingenieur-Team ein ausfallsicheres Bremsraketen-System, um eine zuverlässige Landung zu garantieren. Das Resultat – zwei erfolgreiche autonome Landungen, die exakt gemäß der Simulation erfolgten.
Mehr hierzu erfahren Sie unter:
www. mathworks.de/mbd
MATLAB®
&SIMULINK®
The MathWorks
Accelerating the pace of engineering and science

EUROSIM 2010

organised by CSSS

September 2010, Prague, Czech Republic

EUROSIM 2010

7th EUROSIM Congress on Modelling and Simulation

Eurosim Congress the most important modelling and simulation event in Europe

September 5-10, 2010, Prague, Czech Republic

Congress Venue
The Congress will take place in Prague, the capital city of Czech Republic, at the Congress Center of Masaryk College, part of Czech Technical University, in cooperation with the Faculty of Electrical Engineering of CTU.

About Czech Technical University in Prague
Czech Technical University celebrates 300 years of its history in 2007. Under the name Estate Engineering Teaching Institute in Prague was founded by the rescript of the Emperor Josef I of 18 January 1707 on the basis of a petition of Christian Josef Willenberg (1676-1731). This school was reorganized in 1806 as the Prague Polytechnic, and, after the disintegration of the former AustroHungarian Empire in 1918, transformed in to the Czech Technical University in Prague.

About EUROSIM
EUROSIM, the federation of European simulation societies, was set up in 1989. Its purpose is to promote, especially through local simulation societies, the idea of modelling and simulation in different fields, industry, research and development. At present, EUROSIM has 14 full members and 4 observer members.

Congress Scope and Topics
The Congress scope includes all aspects of continuous, discrete (event) and hybrid modelling, simulation, identification and optimisation approaches. Contributions from both technical and non-technical areas are welcome. Two basic tracks will be organized: M&S Methods and Technologies and M&S Applications.

Czech Republic - EUROSIM 2010 Host Country
The Czech Republic is a country in the centre of Europe. It is interesting for its 1,000-year-long history, rich culture and diverse nature. The country is open to new influences and opportunities thanks to a high level of industrial infrastructure, safety measures and plural media. The location of the Czech Republic in the very heart of Europe contributes to the fact that one can get there easily and fast. Usually all it takes to enter the country is a valid passport. The Czech Republic belongs to the Schengen zone. The need for a visas to enter the Czech Republic is very exceptional.

Prague - EUROSIM 2010 Host City
Prague is a magical city of bridges, cathedrals, gold-tipped towers and church spires, whose image has been mirrored in the surface of the Vltava River for more than a millennium.Walking through the city, you will quickly discover that the entire history of European architecture has left splendid representatives of various periods and styles. There are Romanesque, Gothic, Renaissance, Baroque and Classicist buildings, as well as more modern styles, such as Art Nouveau and Cubist. A poet once characterized Prague as a symphony of stones.

About CSSS
CSSS (The Czech and Slovak Simulation Society) has about 150 members in 2 groups connected to the Czech and Slovak national scientific and technical societies (Czech Society for Applied Cybernetics and Informatics, Slovak Society for Applied Cybernetics and Informatics). Since 1992 CSSS is a full member of EUROSIM.

Invitation
Czech and Slovak Simulation Society is greatly honored with the congress organisation and will do the best to organise an event with a high quality scientific programme with some other acompanied actions but also with some unforgettable social events.

Mikuláš Alexík, EUROSIM president,
Miroslav Šnorek, president of CSSS, EUROSIM 2010 Chair